UNIVERSITY OF CALIFORNIA SAN DIEGO

Thermal Improvement of Normally Consolidated Clay

A dissertation submitted in partial satisfaction of the requirements for the degree Doctor of Philosophy

in

Structural Engineering

by

Radhavi Abeysiridara Samarakoon

Committee in charge:

Professor John Scott McCartney, Chair
Professor Ahmed-Waeil Elgamal
Professor Veronica Eliasson
Professor Jeffrey Gee
Professor Ingrid Tomac

2022

The Dissertation of Radhavi Abeysiridara Samarakoon is approved, and it is acceptable in quality and form for publication on microfilm and electronically.

University of California San Diego

2022

DEDICATION

To my family

TABLE OF CONTENTS

LIST OF FIGURES

LIST OF TABLES

LIST OF SYMBOLS

a	Material parameter
b	Material parameter
d	diameter
e	Void ratio
e_0	Initial void ratio
e_f	Final void ratio
f	Yield function
g	Coefficient of gravity
Δe_v^{Tp}	Thermo-plastic change in void ratio
e^p	Plastic change in void ratio due to mechanical loading
h	Height
n	Porosity
p	Total stress
p'	Mean effective stress
p_0'	Initial mean effective stress
p_c'	Preconsolidation stress
p_c' (T)	Apparent preconsolidation stress at temperature T
p_v'	Effective vertical stress
q	Undrained shear strength
q_f	Undrained shear strength at failure
r	radius

t	Time
v	Velocity
B	Skempton's pore pressure parameter
C	Specific heat capacity of the soil
G_{max}	Small strain shear modulus
K	Intrinsic permeability
T	Temperature
T_0	Reference temperature
u,U	Pore water pressure
V_p	P-wave velocity
V_s	Shear wave velocity
α	Drained volumetric thermal expansion coefficient of clay
α_0	Material parameter (Cui et al. 2000)
α_w	Volumetric thermal expansion coefficient of water
ε	Strain
$d\varepsilon_v^{Te}$	Thermo-elastic strain
$d\varepsilon_v^{e}$	Elastic strain due to mechanical loading
$d\varepsilon_v^{Te}$	Thermo-plastic strain
γ	Material parameter (Laloui and Cekerevac 2003)
η_w	Dynamic viscosity of the fluid
κ	Slope of RCL
λ	Slope of VCL
λ_f	Thermal conductivity of pore water

λ_s	Thermal conductivity of the soil particles
λ_T	Thermal conductivity of the soil
ν	Specific volume
$\Delta\nu_T^p$	Thermo-plastic change in volume
$\Delta\nu_T^e$	Thermo-elastic change in volume
ρ	Bulk density of soil
ρ_t	Total density of soil
ρ_w	Fluid density
σ_1	Major principal stress
σ_3	Minor principal stress

ACKNOWLEDGEMENTS

I would like to extend my sincerest gratitude to my PhD advisor and mentor Prof. John S. McCartney for his continuous support and guidance throughout my PhD journey. I truly appreciate the time he spent in the lab where I learnt so much from fixing equipment to designing new experimental set-ups. I would like to thank him for always being there to provide advice, whether it was about research challenges, future career advice or offering feedback on my application material amidst his busy schedule. It has been a great privilege and an inspiring experience to work with him and has made me a better researcher at the end of this journey.

I would like to thank my committee members, Professor Ahmed Elgamal, Professor Veronica Eliasson, Professor Jeffrey Gee and Professor Ingrid Tomac for their valuable suggestions which helped improve my research. A special thank you also goes to Prof. Lelli Van Den Einde for her mentorship, encouragement and giving me the opportunity to improve my teaching skills by being a part of the COSMOS program. Furthermore, I am thankful to Dr. LianGe Zheng of the Energy Geosciences Division at Lawrence Berkeley National Lab for the collaboration to host me as an intern under the NSF INTERN program.

I also want to express my gratitude to the staff at UCSD Powell Structural Laboratory, Noah Aldrich, Andrew Sander and Abdulla Hamid for always being helpful whenever I needed assistance with modifications to my experimental set-ups. I would like to thank, Hardik Mehta of Trautwein - GEOTAC for the technical support provided to me during my experimental studies.

My sincere thanks go to my colleagues in my research group Dr. Ismaail Ghaaowd, Kaitlin Hall, Jeffrey Newgard, Isaac Kreitzer, Dr. Fatemah Behbehani, Dr. Wenyong Rong, Dr. Leticia Nocko, Dr. Yewei Zheng and Axel Yarahuaman for their friendship and support with laboratory work.

I would like to thank all my friends, especially, Dr. Long Wang, Dr. Chaiane Wiggers de Souza, Dr. Gloria Faraone, Dr. Giorgio Quer, Dr. Supun Nakandala, Thanya De Silva, Rusiru Gambheera, Thejani Gamage, Dr. Raghavendra Sivapuram, Ben Katko, Dr. Rodrigo Chavez Morales, Lingzhi Zheng, Dr. Manuel Vega Loo, Javier Buenrosto and Dr. Muhammad Zayed for their research inputs, encouragement and the good times we shared. In addition, I appreciate the assistance from the staff of Department of Structural Engineering including Yvonne Wollman, Julie Storing, Joana Halnez, Kyung Brown and Lindsay Walton.

I gratefully acknowledge the financial support for this work provided by the National Science Foundation Grant CMMI 1941571 and the Department of Structural Engineering at UC San Diego. I also wish to thank the Charles Lee Powell Foundation, the Sho Funai Educational Foundation and CalGeo for their fellowship recognition and generous financial support during the course of my PhD.

A sincere thank you goes to Dr. Nuwan Nanayakkara, Dr. Chamu Sundaramurthy and Priyanka Nanayakkara for always welcoming me like a member of their family and offering me a home away from home. Last but not least, I owe a deep sense of gratitude to my parents Jayantha Samarakoon and Dr. Paba Palihawadana and my brother Lasura Samarakoon for their unconditional love and support.

This dissertation contains a combination of published and unpublished materials, as described below.

Chapter 2 of this dissertation is based on a manuscript submitted to the Journal Geomechanics for Energy and the Environment titled “Impact of initial effective stress on the thermo-mechanical behavior of normally consolidated clay”, with authors, Radhavi Abeysiridara

Samarakoon, Isaac L. Kreitzer and John S. McCartney. The dissertation author is the first author of this paper.

Chapter 3 of this dissertation is based on material published by GeoCongress 2020 in Minneapolis, MN titled “Effect of drained heating and cooling on the preconsolidation stress of saturated normally consolidated clays”, with authors, Radhavi Abeysiridara Samarakoon and John S. McCartney. The dissertation author is the first author of this paper.

Chapter 4 of this dissertation is based on a manuscript submitted to the Journal Computers and Geotechnics titled “Simulation of thermal drains using a new constitutive model for thermal volume change of normally consolidated clays”, with authors, Radhavi Abeysiridara Samarakoon and John S. McCartney. The dissertation author is the first author of this paper.

Chapter 5 of this dissertation is based on material published in 2nd International Conference on Energy Geotechnics (ICEGT-2020) by E3S Web of Conferences titled “Role of initial effective stress on the thermal consolidation of normally consolidated clays”, with authors, Radhavi Abeysiridara Samarakoon and John S. McCartney. The dissertation author is the first author of this paper.

Chapter 6 of this dissertation is based on material from a manuscript in preparation for publication, tentatively titled “Use of bender elements to evaluate linkages between thermal volume changes and shear modulus hardening in drained and undrained thermal triaxial tests”, with authors, Radhavi Abeysiridara Samarakoon, Isaac L. Kreitzer and John S. McCartney. The dissertation author is the first author of this paper.

VITA

2014	Bachelor of Science in Civil Engineering University of Moratuwa, Moratuwa Sri Lanka
2014	Civil Engineer Maga Engineering (pvt) ltd, Sri Lanka
2016	Master of Science in Civil Engineering University of South Florida, Tampa, United States
2022	Doctor of Philosophy in Structural Engineering University of California San Diego, La Jolla, United States

PUBLICATIONS

Samarakoon, R.A., Kreitzer, I.L., McCartney, J.S. "Impact of initial effective stress on the thermo-mechanical behavior of normally consolidated clay." Geomechanics for Energy and the Environment. [In Review]

Samarakoon, R.A., McCartney, J.S. "Simulation of thermal drains using a new constitutive model for thermal volume change of normally consolidated clays." Computers and Geotechnics. [In Review]

Vahedifard, F., Thota, S.K., Cao, T.D., Samarakoon, R.A., McCartney, J.S. (2020). "Temperature-dependent model for small-strain shear modulus of unsaturated soils." ASCE Journal of Geotechnical and Geoenvironmental Engineering. 146(12), 04018038.

Samarakoon, R.A., and McCartney, J. S. (2019). "Simplified model for heat transfer in unsaturated soils considering a nonisothermal thermal conductivity function." Geotechnical Engineering Journal of the SEAGS & AGSSEA. 50(1), 16-22.

Samarakoon, R.A., and McCartney, J.S. (2021). "Performance of prefabricated thermal drains in soft clays." Geosynthetics Conference. Kansas City, MO, USA. Feb. 21-24. Nicks, J. and Beauregard, M., eds. IFAI, Roseville, MI.1-12.

Samarakoon, R.A., and McCartney, J.S. (2020). “Role of initial effective stress on the thermal consolidation of normally consolidated clays.” Proceedings of the 2nd International Conference on Energy Geotechnics (ICEGT-2020). La Jolla, CA. April. 10-13, 2022. E3S Web Conferences, Les Ulis, France. 1-6.

Samarakoon, R.A., and McCartney, J.S. (2020). “Analysis of thermal drains in soft clays.” GeoAmericas 2020, 4th Pan American Conference on Geosynthetics. Rio de Janeiro, Brazil. Oct. 26-29. 1-9.

Samarakoon, R.A., and McCartney, J.S. (2020). “Effect of drained heating and cooling on the preconsolidation stress of saturated normally consolidated clays.” GeoCongress 2020. GSP 315. Minneapolis, MN. ASCE. Feb. 25-28. 620-629.

Samarakoon, R. A., Ghaaowd, I., McCartney, J.S. (2018). "Impact of drained heating and cooling on undrained shear strength of normally consolidated clay." Energy Geotechnics: SEG-2018. Proceedings of the 2nd International Symposium on Energy Geotechnics. Lausanne, Switzerland. Sep 26-28. A. Ferrari, L. Laloui, eds. Springer, Vienna. 243-249.

Samarakoon, R. A., McCartney, J.S., Dong, Y. and Lu, N. (2018). “Nonisothermal apparent thermal conductivity function for heat transfer in unsaturated soils.” 7th International Conference on Unsaturated Soils, Hong Kong. Aug 3-5.

ABSTRACT OF THE DISSERTATION

Thermal Improvement of Normally Consolidated Clay

by

Radhavi Abeysiridara Samarakoon

Doctor of Philosophy in Structural Engineering

University of California San Diego, 2022

Professor John Scott McCartney, Chair

Construction on soft clay deposits poses challenges to geotechnical engineers due to low shear strength, high compressibility, and complex dynamic response. The main soil improvement technique used in practice requires the placement of a surcharge load in conjunction with vertical drains, which is time consuming, requires transporting significant amount of surcharge material, and can only be used in onshore applications. As an alternative, this study investigates the improvement of soft clays using in-situ heating with geothermal heat exchangers. Heating of soft clays leads to differential expansion of the pore water and soil solids, causing pressurization and drainage of the pore water resulting in permanent volumetric contraction.

While the impact of temperature on soft soils has been widely investigated, a key missing piece of information is the effect of initial mean effective stress of the soft clay on thermal volume change and corresponding increase in undrained shear strength. To address this limitation, the overall objective of this study is to understand the effects of subjecting saturated normally consolidated clays with different initial mean effective stresses to drained heating. Innovative testing approaches include glass thermal triaxial tests which permits use of image analysis to track thermal volume changes, and a thermal triaxial cell with embedded bender elements to measure the shear wave velocity of clay specimens. The magnitude of thermal volumetric strain increased with increasing initial mean effective stress, which is a departure from expected trends in established constitutive models. A corresponding increase in undrained shear strength with both temperature and initial mean effective stress was observed. Further, an increase in the shear wave velocity was observed during heating and no significant change was observed during cooling, indicating permanent hardening of the clay.

Experimental results were useful in calibrating a new constitutive model for the thermal volume change of normally consolidated clays, which was implemented into numerical simulations of heat transfer and water flow around a vertical drain containing a geothermal heat exchanger. Overall, this study provides the technology behind an exciting new thermal soil improvement technique that can have positive long-term energy savings for civil infrastructure in soft soil regions.

1 Introduction

1.1 Research Motivation

The use of in-situ heating for improving mechanical properties of soil is an area which has been investigated in proof-of-concept field scale testing. This process combines geothermal heat exchangers with vertical drains, where they can transmit heat to the surrounding clay once embedded in a soft clay deposit. In addition to thermal improvement of soft clay, the geothermal heat exchangers can be used for thermal energy storage after soil improvement is complete making it cost-effective and sustainable. Although geothermal heat exchanger systems have been in use for more than 50 years, experience has been restricted to relatively rigid soil and rock deposits, meaning that there is significant potential for new advancements in this area.

One of the challenges when implementing this technology is the knowledge gap of thermal effects on soil mechanical properties. While the thermo-mechanical behavior of clay has gained interest in recent years related to geotechnical applications including high level radioactive waste disposal, energy foundations and other thermally active geostructures (i.e., walls, embankments), these applications focused primarily on stiff, overconsolidated clays. Accordingly, there is a lack of experimental data on the thermo-mechanical behavior of soft, normally consolidated clays. Furthermore, there are limitations on the existing hypotheses and constitutive models explaining the physical phenomena responsible for thermally induced irreversible volume change and increased undrained shear strength in soft soil. For instance, the existing models predict the same amount of thermal volume change for normally consolidated clays, irrespective of its mean effective stress. On the other hand, field and laboratory tests as well as poromechanics theories suggest different thermal pressurization effects can be obtained at different mean effective stresses during undrained heating of normally consolidated clays (Bergenstahl et al. 1994;

Abuel-Naga et al. 2007b; Ghaaowd et al. 2017; Campanella and Mitchell 1968). Therefore, it can be reasoned that the thermal volume change of normally consolidated clays, which occurs as a result of thermal pressurization and thermal yielding of soil, may also be dependent on the initial effective stress state of the clay prior to heating.

Based on these observations of stress-dependent thermal pressurization, the hypothesis tested in this study is that normally consolidated clays with different initial mean effective stresses will experience different levels of improvement in their mechanical properties due to stress-dependent thermal hardening. More specifically, the effect on thermal volume change and undrained shear strength is considered. If this hypothesis is valid, thermal soil improvement can be applied strategically where it can be targeted with depth. Furthermore, the experimental observations will be useful in the development of a new constitutive model which will enable improved prediction of thermal volume change of normally consolidated clays.

1.2 Research Objectives

The overall objective of this study is to understand the thermo-mechanical behavior of saturated normally consolidated clay subjected to heating and cooling as part of a thermal soil improvement technique. The specific objectives are:

- Experimentally investigate the impact of initial mean effective stress on the thermal volume change of normally consolidated clay,
- Experimentally investigate the impact of initial mean effective stress on the undrained shear strength of normally consolidated clay,
- Investigating the effect of anisotropy on the thermal volume change of normally consolidated clay,

- Develop a constitutive model to predict thermal volume change of normally consolidated soils at different initial mean effective stress states,
- Understanding linkages between thermal volume change and shear modulus hardening during drained and undrained heating cooling cycles,
- Implementing the developed constitutive model into numerical simulations of heat transfer and water flow around a vertical drain containing a geothermal heat exchanger, and
- Investigate the effect of temperature and surcharge on the performance of a thermal vertical drain.

1.3 Research Approach

The impact of initial effective stress on the thermo-mechanical behavior of normally consolidated clay was investigated experimentally using a thermal triaxial set-up developed by (Alsherif and McCartney 2015). A novel approach using digital images was adopted to measure the thermal volume change during drained heating in a non-contact manner. A second thermal triaxial cell with embedded bender elements was used to investigate the linkages between thermal volume change and shear modulus hardening. A new constitutive model was developed based on the observations from thermal triaxial testing where the effect of mean effective stress was factored in when predicting the thermal volume change of normally consolidated clay.

The performance of a thermal drain was investigated numerically. A numerical model was developed considering the coupled effects of heat transfer, fluid flow and thermal volume change in saturated clay. The proposed constitutive model was incorporated into the numerical model to predict thermal volume change. Based on the numerical simulations, recommendations

were made with respect to the amount of surcharge and maximum temperature required for thermal consolidation of a normally consolidated clay at a given stress state.

1.4 Dissertation Organization

The dissertation is prepared as a paper-based dissertation, with the different chapters presenting excerpts of publications submitted or published in international peer-reviewed journals and conference proceedings. This dissertation is organized as follows:

Chapter 2 presents an experimental study on the thermo-mechanical behavior of saturated normally consolidated clay that focuses on the impact of initial mean effective stress. Specifically, the impact of initial mean effective stress on the drained thermal volume change response and undrained shear strength before and after drained heating was investigated. Chapter 3 presents an experimental study conducted using a thermal triaxial set-up on the effect of a heating cooling cycle on the preconsolidation stress of a saturated normally consolidated clay. Chapter 4 presents a thermo-mechanical constitutive model for saturated normally consolidated clay. The model captures the increase in thermal volume change with increasing mean effective stress in normally consolidated clays. Chapter 5 presents experimental results and analysis from thermal triaxial tests conducted on saturated normally consolidated clay subjected to a heating cooling cycle. The impact of initial effective stress during drained heating and cooling was investigated. Chapter 6 presents experimental results and analysis from thermal triaxial tests conducted on saturated normally consolidated clay subjected to drained and undrained heating cooling cycles. Linkages between thermal volume change and shear modulus hardening were investigated.

2 Impact of Initial Effective Stress on the Thermo-mechanical Behavior of Normally Consolidated Clay

2.1 Introduction

The thermo-mechanical behavior of clay has become an important topic of research because of increased interest in geomechanical problems involving thermal effects. As most of these geomechanical problems studied in the literature involved overconsolidated or compacted clays (i.e., cast-in-place energy piles, buffer systems for nuclear waste repositories, backfill for buried electrical cables), there has not been a significant amount of attention on investigating the thermo-mechanical behavior of soft, normally consolidated clays. Recently, there has been interest in using in-situ heating to improve the engineering properties of soft clay (Abuel-Naga et al. 2006; Pothiraksanon et al. 2010; Samarakoon and McCartney 2020a, 2021; Ghaaowd and McCartney 2021; Ghaaowd et al. 2022). In-situ thermal soil improvement combines geothermal heat exchangers with vertical drains, which will be embedded in a soft clay deposit transferring heat to the surrounding soil. In addition to being used during the preconsolidation stage to expedite consolidation, the ground heat exchangers can also be used as an underground heat storage system for the building after soil improvement has been completed. When assessing thermal soil improvement methods, it is important to understand the thermo-mechanical behavior of soft clays at different initial mean effective stresses indicative of different depths in a clay layer. Within the domain of soil improvement, this study aims to investigate the role of initial effective stress on the thermo-mechanical behavior of normally consolidated clay subjected to drained heating. Specifically, the effect on undrained shear strength and volume change is considered.

Several researchers have investigated the thermo-mechanical response of clay (Campanella and Mitchell 1968; Hueckel and Baldi 1990; Cekerevac and Laloui 2004; Abuel-Naga et al. 2007a). Undrained heating of saturated clays leads to an increase in excess pore water pressure whereas drained heating of saturated clays results in thermal volume changes depending on the stress history of the clay. The thermal volume change of highly overconsolidated clays was observed to be expansive, elastic, and recoverable, whereas the thermal volume change of normally consolidated clays was contractive, plastic, and partly irrecoverable. Although thermal volumetric strains are much smaller in comparison to volumetric strains obtained by mechanical loading, the reduction in void ratio obtained during drained heating leads to an increase in undrained shear strength for normally consolidated clays (Houston et al. 1985). The undrained shear strength of clay was observed to be dependent on temperature and different trends were seen based on the drainage conditions during heating (Houston et al. 1985; Kuntiwattanakul et al. 1995; Tanaka 1997; Abuel-Naga 2006). In general, normally consolidated clay specimens subjected to shear after undrained heating showed a decrease in undrained shear strength with temperature whereas specimens subjected to drained heating resulted in an increase in undrained shear strength with increasing temperature.

Constitutive models describing the thermo-mechanical behavior of clays have been developed by several researchers (Hueckel and Borsetto 1990; Cui et al. 2000; Laloui and Cekerevac 2003; Abuel-Naga et al. 2007a; Abuel-Naga et al. 2009). The thermal volume changes in these models are typically driven by changes in the apparent preconsolidation or yield stress with changes in temperature. As an artifact of this approach to predict thermal volume changes, these models predict the same amount of thermal volume change for normally consolidated clays, irrespective of the initial stress state or initial void ratio. The constitutive

models were generally validated using tests conducted on initially overconsolidated clay specimens which were mechanical loaded to a normally consolidated state after drained heating to different elevated temperatures in order to define a relationship between the yield stress and temperature. Compression curves obtained from isothermal tests carried out at elevated temperatures showed compression curves with slopes similar to that of a compression curve at room temperature but with a shift to the left. The constitutive models developed based on these observations predict that normally consolidated clays will have the same thermal hardening response and the same amount of volume change regardless of its initial mean effective stress. While many of the models included successful validation of the volume change of a single normally consolidated clay specimen, they did not validate the model for normally consolidated clay specimens having different initial stresses.

On the other hand, field tests (Bergenstahl et al. 1994), laboratory tests (Abuel-Naga et al. 2007b; Uchaipichat and Khalili 2009; Ghaaowd et al. 2017) and poromechanics theories (Campanella and Mitchell 1968) show that normally consolidated, saturated clay having different initial mean effectives stresses and void ratios lead to different thermal pressurization effects during undrained heating. The effect of the initial effective stress state on the thermal pressurization process leads to the hypothesis that the thermal volume change of normally consolidated clays will also be dependent on the initial mean effective stress for normally consolidated clays. However, there are limited studies in the literature where the thermal behavior of normally consolidated clays at different initial mean effectives stress states were carefully investigated. In previous studies conducted by the authors on normally consolidated kaolinite specimens, it was observed that the thermal volume change and undrained shear strength was dependent on the initial mean effective stress (Samarakoon et al. 2018; Samarakoon

and McCartney 2020b). Based on the observations of excess pore water pressure behavior under undrained conditions and limited experimental data on thermal volume change of normally consolidated clays, there is a need to further investigate the effect of initial mean effective stress on the thermo-mechanical behavior of normally consolidated clays. To that end, this study presents the results from an experimental investigation involving drained heating of saturated normally consolidated kaolinite specimens at different initial mean effectives stresses representative of different depths in a clay deposit.

2.2 Material and Methods

2.2.1 Material

Commercial kaolinite clay obtained from M&M Clays Inc. of McIntyre, GA was used in this study. The properties of the Georgia kaolinite clay are summarized in Table 2.1, including the compression indices obtained from an isotropic compression test at room temperature. The Georgia kaolinite clay is classified as CL according to the Unified Soil Classification System (USCS). The compression curve for Georgia kaolinite clay is shown in Figure 2.1 along with the slopes of the virgin compression line (VCL) and the recompression line (RCL).

Table 2.1. Properties of Georgia kaolinite clay

Parameter	**Value**
Liquid Limit	47
Plasticity Index	19
Specific Gravity	2.6
Slope of VCL (λ)	0.09
Slope of RCL (κ)	0.02
USCS Classification	CL

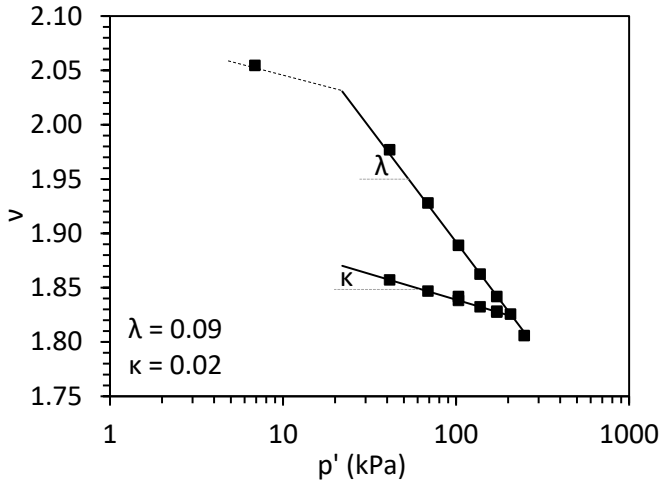

Figure 2.1. Compression curve for Georgia kaolinite clay

2.2.2 Experimental Set-up

The laboratory tests were conducted using a modified triaxial system developed by (Alsherif and McCartney 2015). A schematic of the experimental set-up is shown in Figure 2.2. The triaxial system comprised of a Pyrex cell capable of withstanding high temperatures and pressures applied during testing. Heat was applied to the cell by circulating heated water from a temperature-controlled circulating bath through a stainless-steel U-shaped pipe placed inside the cell. A circulation pump able to accommodate high temperatures and pressures was used to ensure uniform mixing of cell water. Two thermocouples were placed to measure the temperature of the cell fluid and at the bottom of the specimen respectively. The temperature recorders were accurate to 0.5 °C. The cell pressure was applied using a flow pump whereas the back-pressure was controlled using a pressure panel. Drainage was allowed only from the top of the specimen. Changes in the pore water pressure were monitored at the bottom of the specimen using a pore water pressure transducer.

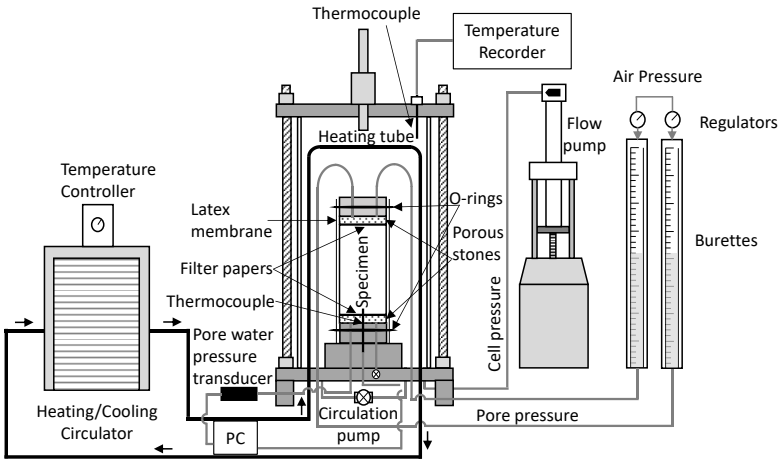

Figure 2.2. Schematic of the thermal triaxial set-up

Obtaining volume change measurements using outflow pipettes is challenging at elevated temperatures due to the thermal expansion of the system. Therefore, the volume change was measured using an image analysis technique in a non-contact manner. Two high resolution cameras (Nikon D7500, AF-P DX NIKKOR 70-300mm f/4.5-6.3G ED lens) were used to capture the images of the specimen at specified time intervals throughout the duration of the test. The camera lens selected has minimal distortion effects on the images. For a given time, images were captured from two planes of the specimen which are perpendicular to each other. Images were converted to a binary form and the total volume of the specimen was obtained from the summation of discrete volumes associated with a series of stacked disks where the height of a single disk (Δh) was one vertical pixel, and the diameter (d) was the number of horizontal pixels (Uchaipichat et al. 2011). 2D to 3D mapping for a single disk is shown in Equation (2.1) and the total volume of the specimen is obtained as shown in Equation (2.2) where n is the number of vertical pixels for Δh = 1 pixel.

$$Volume\ of\ a\ single\ disk = \pi d^2 \Delta h/4 \tag{2.1}$$

$$Total\ volume\ of\ specimen = \sum_{i=1}^{n} \pi {d_i}^2 \Delta h_i/4 \tag{2.2}$$

An average of the volumes calculated from the two image planes was taken as the total volume of the specimen at a given time. The volume obtained from Equation (2.2) is expressed in units of cubic pixel. The true volume of the specimen was obtained by calibrating the calculated pixel volumes against the actual volume of the specimen measured at the beginning of the test. The relationship between the pixel diameter and the true diameter of the specimen was found to be linear for a limited range of diameters, based on tests conducted on specimens with different diameters (Macari et al. 1997; Hormdee et al. 2014). The range of diameters considered are applicable to the specimen dimensions used in this study.

Examples of images from the stages of processing and typical results during different stages of triaxial testing are shown in Figure 2.3. Void ratios obtained from image analysis during consolidation are shown in Figure 2.4, along with a comparison of void ratios obtained from pipette readings. Good agreement (Root-mean-square deviation (RMSD) = 0.05) is seen in the trends of void ratio changes during consolidation between the measurements obtained from image analysis and pipette readings. In addition to directly calculating changes in volume using Equation (2.2), the results from these image analyses can be used to interpret the axial and radial thermal strains, which may be useful in interpreting the thermal volume change response.

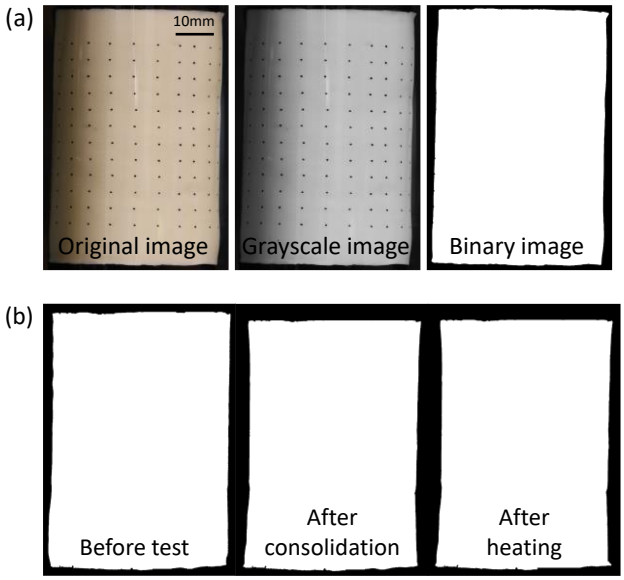

Figure 2.3. Image processing: (a) Examples of images from the three stages of processing; (b) Typical results from processed images for different stages of triaxial testing

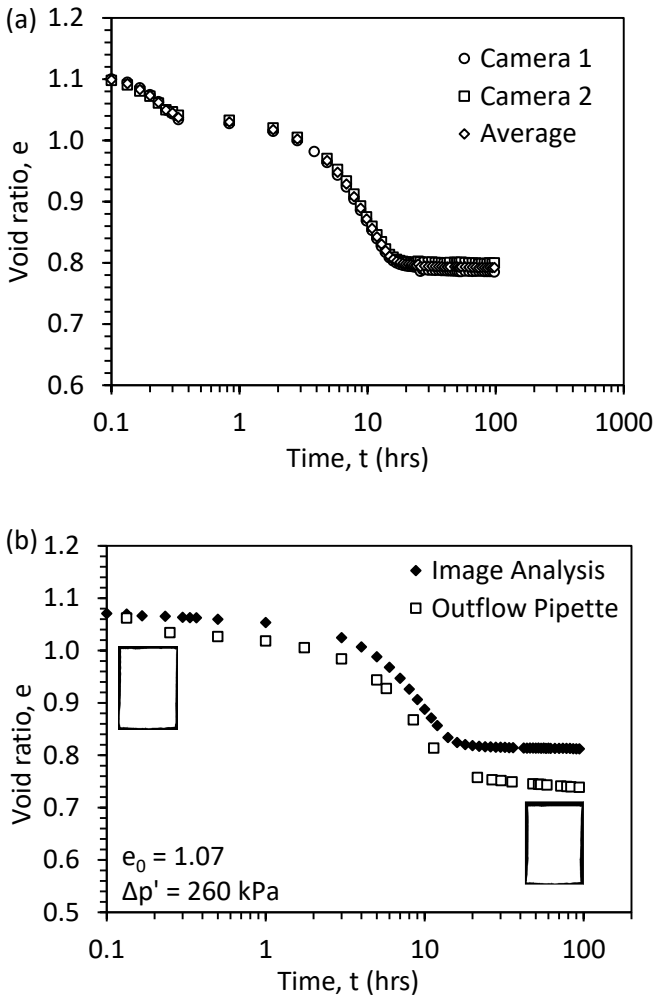

Figure 2.4. Typical void ratio measurements: (a) Void ratio variations measured using image analysis during consolidation; (b) Comparison of void ratios measured using images analysis and outflow pipette readings

2.3 Procedure

The clay specimens were prepared by forming a slurry from clay and deionized water at a gravimetric water content of 130% in a commercial planetary mixer. The slurry was then poured into a hollow steel cylinder of diameter 88.9 mm with porous stones and filter paper placed on both top and bottom. The slurry was first consolidated using a compression frame at a constant rate of 0.04 mm/min for 48 hours. Then constant vertical stresses of 26, 52, 103 and 181 kPa

were applied in 24 hour-long increments. At the end of load application, the sedimented clay layer was extracted and trimmed into a cylindrical specimen with a diameter of 72.4 mm and height of 145 mm, making it suitable for testing in the thermal triaxial cell. The specimen was back-pressure saturated by applying cell pressure and back-pressure in stages until the Skempton's pore water pressure parameter B was at least 0.95. Then the specimen was isotropically consolidated by applying a specified mean effective stress. Four different mean effective stresses were considered in this study as 230, 260, 290 and 320 kPa respectively. The specimens were at normally consolidated conditions at these stress states considered. A total of 8 tests were conducted in this study. The first set of tests were at room temperature where 4 specimens were first isotropically consolidated to the 4 different mean effective stresses mentioned above respectively. The cell pressure was increased using ramp loading and the back pressure was maintained constant to subject the specimen to the specified effective stress. The applied isotropic stress state was maintained until the volume change of the specimen reached a steady state. Once primary consolidation was complete, the specimens were sheared under undrained conditions. The second set of tests were heated tests conducted at the same mean effective stresses considered. For the heated tests, once the primary consolidation was completed, the specimens were subjected to drained heating where the temperature was increased from room temperature to about 60 °C. After the specimen reached equilibrium, it was subjected to undrained shear at the elevated temperature. A summary of the thermo-mechanical stress paths for the thermal triaxial tests are shown in Figure 2.5.

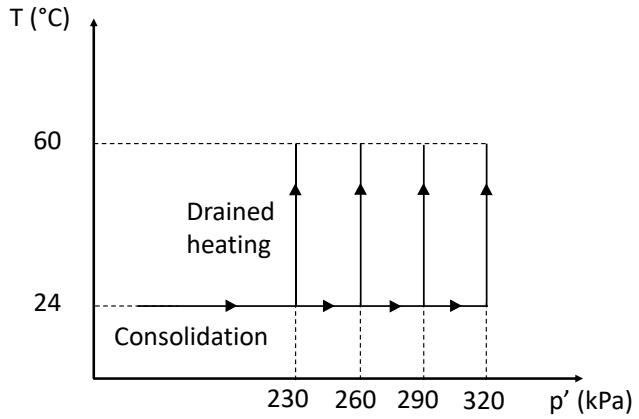

Figure 2.5. Summary of the thermo-mechanical paths for the triaxial testing program

2.4 Results

2.4.1 Typical Time Series Results

The change in mean effective stress, excess pore water pressure and temperature for a typical thermal triaxial test (target mean effective stress at heating = 290 kPa) is shown in Figure 2.6. The mean effective stress increases during isotropic consolidation and remains constant throughout the test apart from the slight decrease observed at the onset of heating. Correspondingly, an increase in pore water pressure is also observed at the onset of heating. This is due to the relatively high rate of heating at the beginning of the heating stage. With the sudden increase in temperature and the low permeability of the clay specimen, partially drained conditions prevail during the initial stage of heating. As the temperature stabilizes with time and the pore water pressures dissipate, the mean effective stress regains its equilibrium value. The temperature is measured at the top of the cell as well as the bottom of the specimen. Although both measurements of temperature follow similar trends, a difference of 8.6 °C is observed between the two locations during heating.

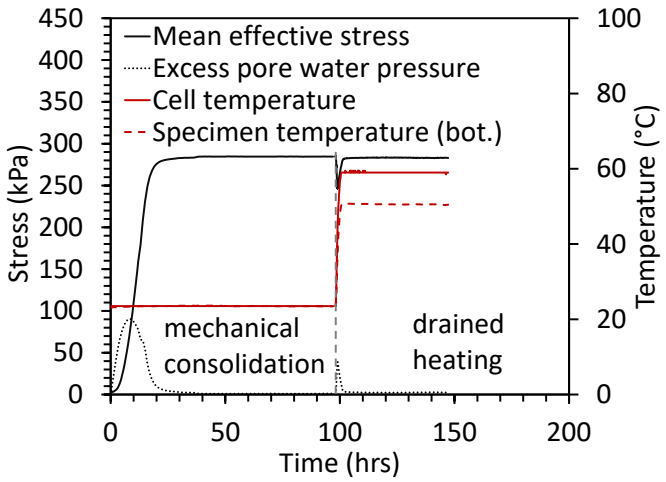

Figure 2.6. Changes in mean effective stress and temperature for a typical thermal triaxial test (target mean effective stress at heating = 290 kPa)

As described in section 2.3, the kaolinite specimens in this study were prepared using a sedimentation process. The kaolinite slurry was sedimented in a cylindrical mold in an oedometric stress state. The slurry was first consolidated by applying a constant strain rate and then subjected to vertical stress incrementally. As no strain was allowed in the radial direction, K_0 conditions can be assumed during the specimen preparation stage. During triaxial testing however, the specimens were consolidated to a normally consolidated state under isotropic stress conditions. As a result of the specimen preparation process under K_0 conditions, there may exist some stress-induced anisotropy in the specimens prior to consolidation. Most studies evaluating thermal volume change behavior were conducted using oedometers or triaxial cells and the results are typically reported as volumetric strains. However, the presence of stress-induced anisotropy may impact the deformation of the specimen when subjected to mechanical and thermal loading. Coccia and McCartney (2012) developed a new thermo-hydro-mechanical true triaxial cell which had the ability to subject soil specimens to different anisotropic stress states. Tests were conducted on cubicle specimens of saturated overconsolidated Bonny silt and plastic

contraction in the major stress direction and elastic expansion in the minor stress direction was observed as the initial stress anisotropy increased during heating. Similar observations were made by Shanina and McCartney (2017) for cubical specimens of unsaturated silt. To assess this, radial and axial strain trends during isotropic consolidation and drained heating were investigated. The reason for reporting thermal deformations in the literature only in terms of void ratio or volumetric strain may be the difficulty of measuring both radial and axial strains in conventional triaxial and oedometric tests. This issue was resolved in this study through the use of image analysis.

As described in section 2.2.2, the specimen was divided into a series of stacked disks where the height of a disk was one pixel. The diameter at a given height was the number of horizontal pixels. The diameter of the specimen at a given time was obtained using an average of diameter values obtained along the height of the specimen. The height of the specimen was obtained in a similar manner by discretizing the specimen into vertical disks. Using the diameter and height values obtained for a given time, axial and radial strains were calculated. Figure 2.7(a) shows the variation of axial and radial strains during isotropic consolidation and drained heating for a typical thermal triaxial test (target mean effective stress at heating = 290 kPa). As seen in the figure, the radial strain obtained during isotropic consolidation is higher in comparison to the axial strain. Furthermore, the rate of strain increase at the beginning of consolidation is higher in the radial direction. During drained heating, the thermal strains obtained also show a similar behavior where more deformation is observed in the radial direction and a small increase in axial strain. Similar behavior was observed for the specimens at other initial mean effective stresses.

Based on these observations, although the specimen was subjected to isotropic loading, the strain response of the specimen was anisotropic with radial strain being more dominant compared to axial strain. This may be due to the specimen preparation process where the specimen was consolidated under axial loading in the vertical direction with no allowance for radial deformation. As the specimen continues to contract during drained heating, similar behavior is observed. Although the thermal strains are smaller in comparison, radial strain during drained heating is still observed to be larger than the axial strain. Hueckel and Pellegrini (1996) obtained similar results for Boom clay where plastic contractive strain was larger in the horizontal direction than in the vertical direction during heating under isotropic stress conditions. The component of horizontal stress during isotropic loading is higher than that during K_0 consolidation. It was speculated that the arrangement of clay microstructure during K_0 compression may mainly leave space between horizontal neighboring clusters and their closure during heating will results in larger lateral thermal strains.

Figure 2.7(b) shows the variation in void ratio and temperature for a typical test (target mean effective stress at heating = 290 kPa) during mechanical consolidation and drained heating. As expected, the void ratio decreases during mechanical consolidation and a further decrease is observed during drained heating. In comparison, the change in void ratio during drained heating for a temperature increase of 35.5 °C is smaller than that obtained during mechanical consolidation. As seen from the figure, care was taken to ensure that primary consolidation was completed prior to starting the heating stage. The compression curve for the same test is shown in Figure 2.8. During drained heating, the specimen is subjected to contractive volume change at the given target mean effective stress.

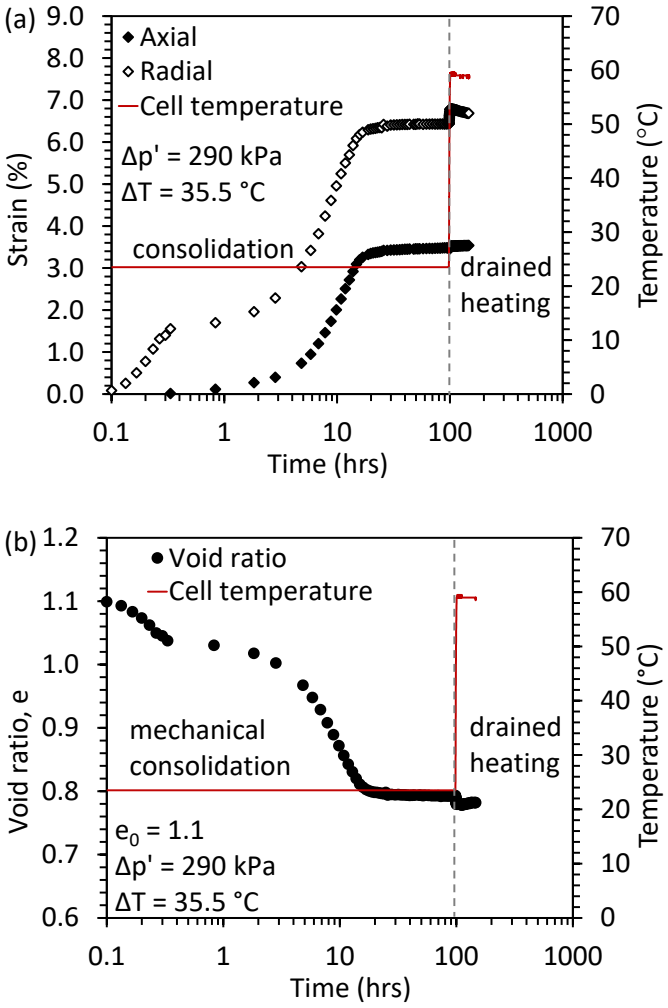

Figure 2.7. Thermo-mechanical volume changes during different stages of a typical thermal triaxial test (target mean effective stress at heating = 290 kPa): (a) Variation in axial and radial strains; (b) Variation in void ratio

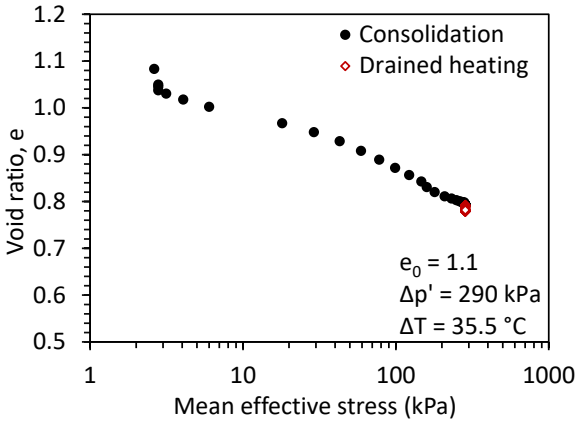

Figure 2.8. Compression curve during thermo-mechanical loading from a typical thermal triaxial test (target mean effective stress at heating = 290 kPa)

2.4.2 Consolidated Undrained Shearing Results

For the heated tests, once the specimens reached equilibrium during the drained heating stage, they were subjected to shear under undrained conditions. The specimens tested at room temperature were sheared under undrained conditions after primary consolidation was completed. The consolidated undrained triaxial compression test results for specimens at room temperature and after heating are shown in Figure 2.9. The principal stress ratio versus axial strain, maximum principal stress difference versus axial strain and excess pore water pressure versus axial strain are shown in Figures 2.9(a) – 2.9(c) respectively. As seen from the principal stress ratio trends, friction is observed to be mobilizing throughout the test for both heated and not heated specimens. This trend is typical for consolidated undrained tests on normally consolidated clays. In comparison to the room temperature tests, an increase in the maximum principal stress difference can be observed for the specimens sheared at 59 °C for all the initial effective stress states considered. The shapes of the stress-strain curves for all 8 tests were relatively similar despite different peak values. Correspondingly, the excess pore water pressure

during shear was seen to be decreasing at elevated temperature for the four different initial effective stresses considered.

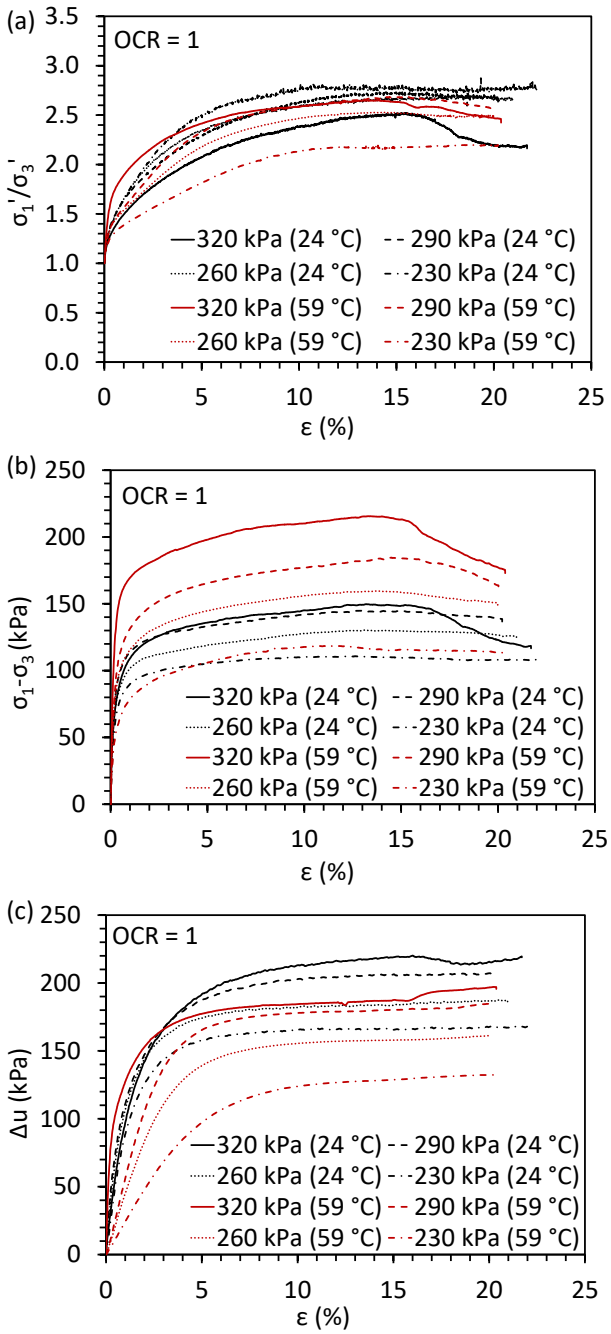

Figure 2.9. Consolidated Undrained (CU) triaxial compression test results for unheated and heated normally consolidated kaolinite: (a) Principal stress ratio vs. axial strain; (b) Maximum principal stress difference vs. axial strain; (c) Excess pore water pressure vs. axial strain

The effective stress paths for the normally consolidated specimens sheared at room temperature and after heating is shown in Figure 2.10. It can be observed that the maximum principal stress difference values fall onto the same peak failure envelope irrespective of their heating path. A similar observation was made in a previous study conducted by the authors where different heating paths at different initial mean effective stresses were considered (Samarakoon et al. 2018). Figure 2.11 shows the relationship between the maximum principal stress difference and the mean effective stress at failure for the 8 clay specimens considered. The markers represent the peaks of the maximum principal stress difference and the corresponding mean effective stress. The slope corresponds to the slope of the peak failure envelope and is not that of the critical state line.

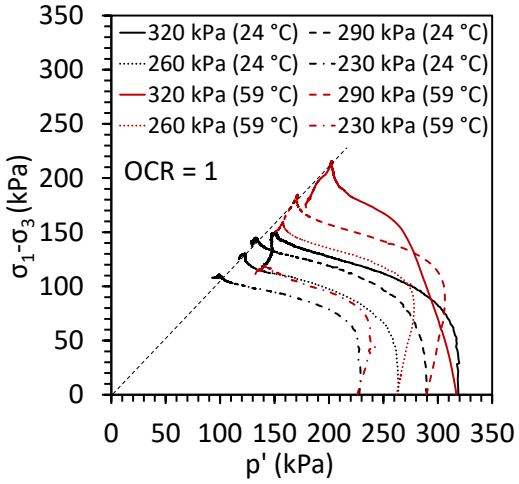

Figure 2.10. Effective stress paths for unheated and heated normally consolidated kaolinite

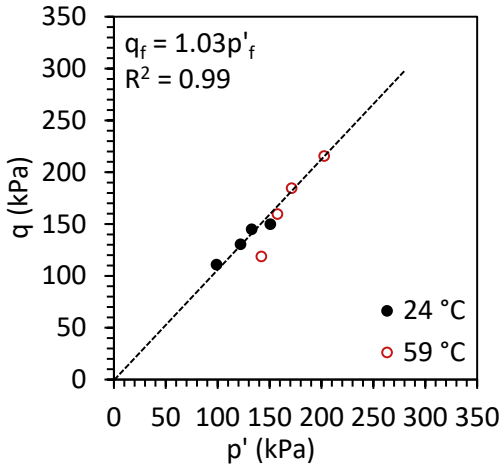

Figure 2.11. Relationship between maximum principal stress difference and mean effective stress at failure for normally consolidated kaolinite specimens sheared at room temperature and after heating

2.5 Analysis

2.5.1 Thermal Volume Change

Figure 2.12 shows a comparison of the results obtained for thermal volumetric strains at different initial mean effective stresses. Thermal volumetric strain obtained during drained heating at different initial mean effective stresses considered was compressive and is represented as a positive value. The thermal volumetric strain values obtained range from 0.4% - 0.94% which agrees with the typical strain values observed in literature for normally consolidated clays during drained heating (Hueckel and Baldi, 1990; Baldi et al. 1988; Delage et al. 2004; Cekerevac and Laloui 2004). The contractive volumetric strain observed during heating was observed to increase with increasing initial mean effective stress. As hypothesized, this observation confirms that thermal volume change of normally consolidated clay is dependent on the initial mean effective stress. It is also in accordance with the excess pore water trends reported by (Abuel-Naga et al. 2007b; Ghaaowd et al. 2017) where higher excess pore water pressures were generated as the initial mean effective stress increased. The authors made similar

observations in kaolinite specimens subjected to a drained heating cooling cycle in a previous study (Samarakoon and McCartney 2020b). During drained heating, the thermal volumetric strain was observed to increase as the initial mean effective stress increased.

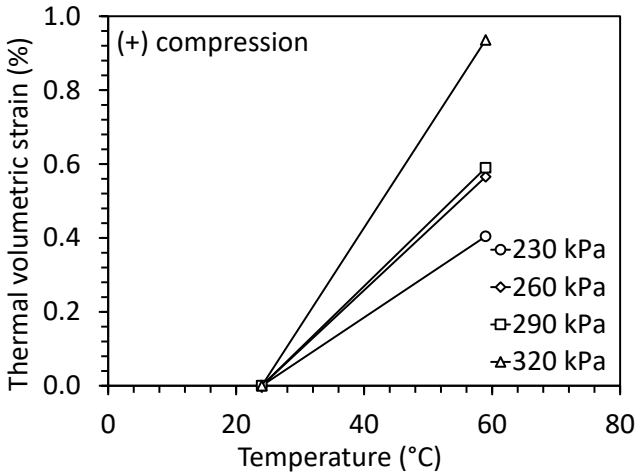

Figure 2.12. Thermal volumetric strain for unheated and heated normally consolidated kaolinite at different initial mean effective stresses

2.5.2 Undrained Shear Strength

Undrained shear strength values obtained for the normally consolidated specimens tested at different initial mean effective stresses are summarized in Figure 2.13. Results for the specimens sheared at both room temperature as well as 59 °C are shown. It is assumed that the maximum principal stress difference corresponds to the undrained shear strength of the soil. A clear increase in undrained shear strength can be seen for the specimens sheared after heating. This increase in undrained shear strength can be attributed to the plastic volumetric contraction which occurred during drained heating. Like the results obtained for thermal volume change, the increase in undrained shear strength after heating is observed to increase with increasing initial mean effective stress. As described in the previous section, a higher degree of thermal volume

change was observed as the initial mean effective stress increased. As a result of this plastic decrease in volume, the undrained shear strength after heating is also observed to increase with increasing initial mean effective stress. The final void ratios versus the undrained shear strength values are plotted in Figure 2.14. The best fit relationship between the undrained shear strength and the void ratio is observed to be linear where the undrained shear strength increases as the void ratio decreases.

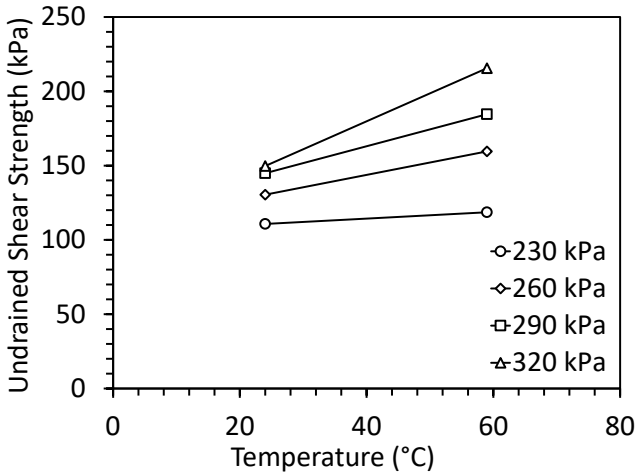

Figure 2.13. Undrained shear strength values for unheated and heated normally consolidated kaolinite at different initial mean effective stresses

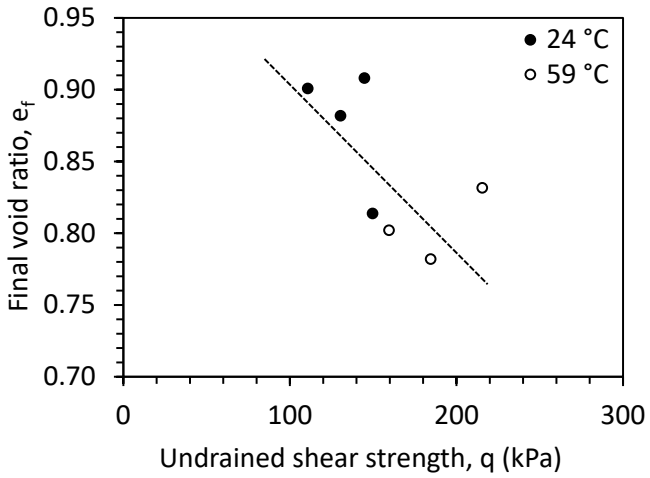

Figure 2.14. Relationship between the void ratio at failure and undrained shear strength for unheated and heated normally consolidated kaolinite

These results are in contrast with a previous observation made by the authors (Samarakoon et al. 2018) where the amount of increase in undrained shear strength after drained heating was smaller for specimens with greater initial mean effective stresses. However, this observation from the previous study was counterintuitive as greater thermally induced excess pore water pressures are expected for clay with greater initial mean effective stresses (Ghaaowd et al. 2017). The authors attribute these inconsistencies to the differences in specimen preparation and the experimental procedures followed. For instance, the clay specimens in Samarakoon et al. (2018) were consolidated in a larger diameter mold during the sedimentation stage and quartered at the end of the sedimentation process to obtain four separate triaxial test specimens. In the current study, each triaxial specimen was sedimented individually in a single mold. During testing in Samarakoon et al. (2018), drainage was allowed from both top and bottom with Bishop's pajamas whereas only top drainage was allowed in the current study without the use of Bishop's pajamas. Due to the long duration of testing required for clay specimens, the observed trends are based on only 8 tests where a limited range of stress states

and temperature was considered. Further testing conducted at different stresses and temperatures considering different soil types will assist in confirming the established trends. The possible sources of error include differences in initial conditions arising from the specimen preparation process, specimens being slightly nonhomogeneous and potential leakage from cell into the specimen during saturation.

The results for thermal volumetric strain and the increase in undrained shear strength at different initial mean effective stresses are synthesized in Figure 2.15. Based on these findings, it is clear that the thermal volumetric strain and the undrained shear strength of normally consolidated kaolinite specimens is dependent on the initial mean effective stress. The trends observed show that the thermal volumetric strain and the corresponding increase in undrained shear strength increases with increasing initial mean effective stress. This is contrary to the existing thermo-elasto-plastic models where the same magnitude of volumetric strain is predicted for normally consolidated clays subjected to an increase in temperature irrespective of its initial mean effective stress. However, in applications involving normally consolidated clays such as improvement of soft clay deposits using in-situ heating, it is important to account for the effect of initial mean effective stress on the thermal behavior of clay. The findings from this study will enable users to strategically apply thermal soil improvement over different depths of a clay layer thus increasing the efficiency of the thermal soil improvement process.

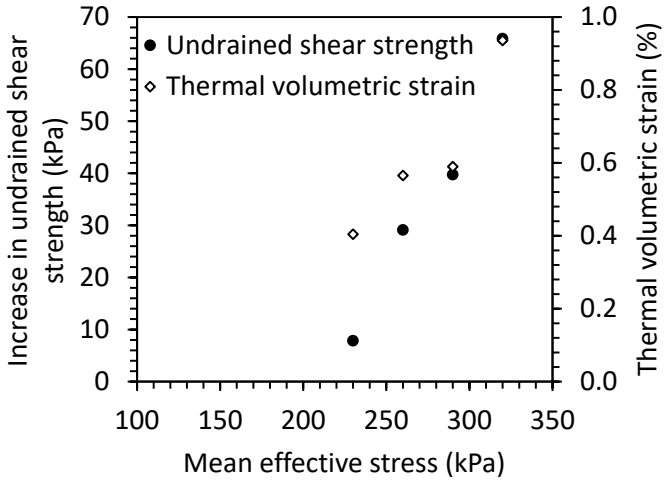

Figure 2.15. Summary of thermal volumetric strain and increase in undrained shear strength after heating of normally consolidated kaolinite at different initial mean effective stresses

2.5.3 Effect of Anisotropy on Thermal Deformation

A summary of the results for the ratio between axial strain and radial strain for normally consolidated specimens at different initial mean effective stresses are shown in Figure 2.16. The ratios are less than 1 because the radial strain observed was higher than the axial strain. As expected, strain observed during isotropic consolidation is higher than the strain during drained heating. An interesting observation is that the ratio between axial strain and radial strain increases as the initial mean effective stress increases. This indicates that as the initial mean effective stress increases, the strain response of the specimen is less anisotropic. The anisotropic strain response observed during drained heating may not be a result of thermal behavior of the clay but rather due to the inherent anisotropy in the specimen caused by the sedimentation process during specimen preparation. Although the specimen is mechanically loaded to a normally consolidated state prior to heating, there may still exist some degree of anisotropy in the specimen. As a result, we may continue to observe an anisotropic strain response as the specimen is subjected to thermal loading. Based on observations by both Coccia and McCartney

(2012) and Shanina and McCartney (2017) the inherent anisotropy from soil preparation (static compaction in their case) did not have a significant impact on the overall thermal volumetric strains but only on the strain response in different directions. However as seen in Figure 2.16, the impact of the specimen anisotropy will be less significant as the initial mean effective stress increases. Although the stress-induced anisotropy in the test specimens considered in this study was a result of the preparation process, the anisotropic stress state is representative of natural soil deposits in at rest conditions. Characterizing the thermal deformation of clays with inherent anisotropy can be useful in geotechnical applications involving thermal effects.

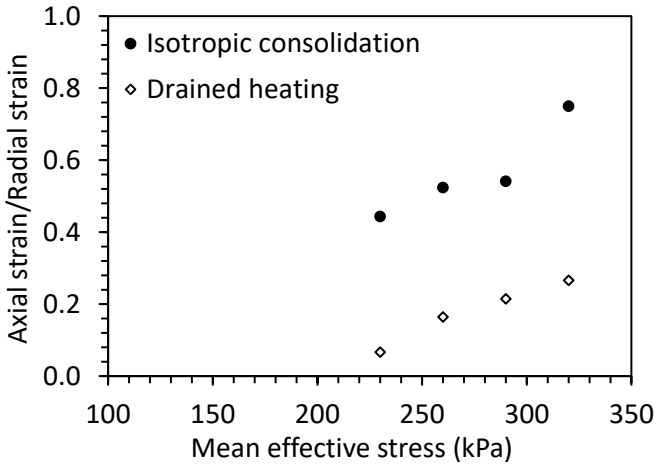

Figure 2.16. Axial strain and radial strain ratio for normally consolidated kaolinite specimens at different initial mean effective stresses

2.6 Conclusion

This paper presents the results of an experimental study investigating the impact of initial mean effective stress on the thermo-mechanical behavior of saturated normally consolidated clay. Contrary to the existing thermo-elasto-plastic models, the thermal volumetric strain was observed to be dependent on the initial mean effective stress of the specimen. Thermal

volumetric strain during drained heating was contractive and increased as the initial mean effective stress increased. Correspondingly, the undrained shear strength also increased with increasing initial mean effective stress. These findings are useful when configuring geothermal heat exchangers for soil improvement via in-situ heating where thermal soil improvement can be strategically applied over different depths of a clay layer. The specimen preparation process of sedimentation under vertical loading was found to affect the strain response of the clay specimen where more deformation was observed in the radial direction during isotropic consolidation as well as drained heating. Further studies can be conducted on a broader range of soil types and stress states to better understand the trends of thermal behavior of normally consolidated clay and to incorporate the effect of initial mean effective stress into thermo-elasto-plastic constitutive models.

ACKNOWLEDGEMENTS

Chapter 2 of this dissertation is based on a manuscript submitted to the Journal Geomechanics for Energy and the Environment titled "Impact of initial effective stress on the thermo-mechanical behavior of normally consolidated clay", with authors, Radhavi Abeysiridara Samarakoon, Isaac L. Kreitzer and John S. McCartney. The dissertation author is the first author of this paper.

3 Effect of Drained Heating and Cooling on the Preconsolidation Stress of Saturated Normally Consolidated Clays

3.1 Introduction

Soft clay deposits pose challenges to geotechnical engineers due to their low shear strength, high compressibility and complex dynamic response. Preconsolidation with surcharge loading and use of vertical drains are widely used methods to enhance the performance of soft clays. A more recent approach to soft soil improvement is in-situ heating by using geothermal heat exchangers embedded in the soft soil deposit.

The effect of temperature on preconsolidation stress of saturated clays has been studied by several researchers (Plum and Esrig 1969; Tidfors and Sallfors 1989; Eriksson 1989; Hueckel and Baldi 1990; Towhata et al. 1993; Boudali et al. 1994; Cui et al. 2000; Sultan et al. 2002; Laloui and Cekerevac 2003; Abuel-Naga et al. 2006, 2007). These studies conclusively show an apparent reduction in preconsolidation stress with increasing temperature for initially over consolidated soil specimens heated to different temperatures and subjected to subsequent loading. Tidfors and Sallfors (1989) observed a linear decrease in preconsolidation stress with increasing temperature based on thermal oedometer tests conducted on 5 different clays at temperatures up to 55 °C. On the other hand, Eriksson (1989) observed a nonlinear decrease in preconsolidation stress with temperature for sulphide clay. Laloui and Cekerevac (2003) expressed this apparent decrease in preconsolidation stress using a logarithmic function and a soil specific material parameter. A typical schematic of how the thermal softening relationship was obtained from heating tests on initially overconsolidated clays is shown in Figure 3.1(a), and the typical shape of the thermal yield (TY) curve defined from the preconsolidation stress values is shown in Figure 3.1(b).

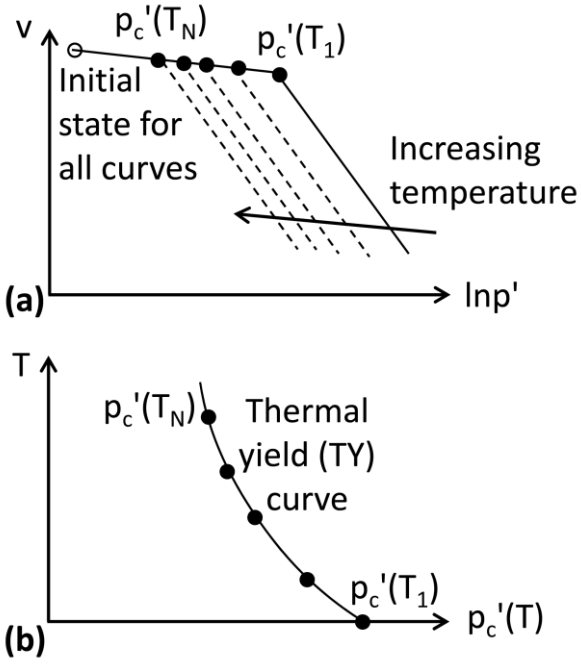

Figure 3.1. (a) Compression curves on initially overconsolidated soils under different temperatures; (b) TY curve definition

The change in apparent preconsolidation stress with temperature is particularly important in predicting the behavior of normally consolidated soils using thermo-elasto-plastic models. For normally-consolidated soils, the current mean effective stress is equal to the yield stress, so heating will lead to a shift of the TY curve to the right as shown in Figures 3.2(a) and 3.2(b). The shape of the TY curve in Figure 3.2(b) is from Laloui and Cekerevac (2003), but other empirical relationships have been proposed in the literature (e.g., Hueckel and Borsetto 1990; Cui et al. 2000). Heating will also cause the virgin compression line (VCL) to shift to the left by the difference between $p_c'(T_1)$ and $p_c'(T_2)$ on the initial TY curve as shown in Figure 3.2(c). The shift in the VCL corresponds to plastic contraction expressed in Figure 3.2(c) as a change in specific volume $\Delta v_T{}^p$. Cooling is expected to lead to elastic contraction $\Delta v_T{}^e$, and mechanical loading after a heating-cooling cycle will result in a hardening effect with yielding when reaching the

VCL corresponding to the initial state before heating and cooling. If the soil had been compressed under elevated temperatures (without cooling), the clay is expected to behave in normally consolidated conditions and follow the lower VCL in Figure 3.2(c).

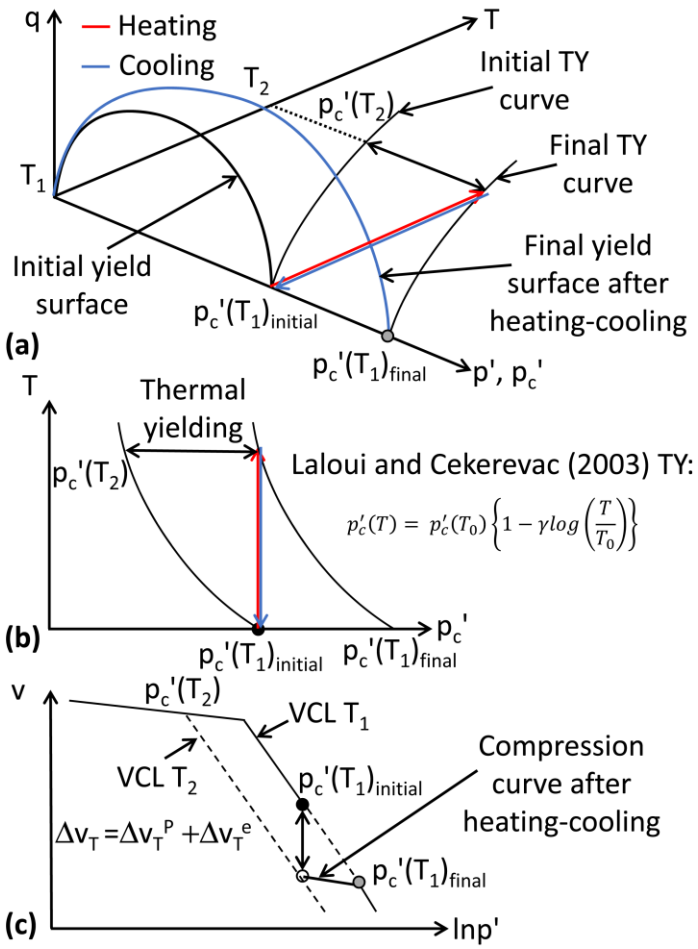

Figure 3.2. Thermal yielding of normally consolidated clays during heating and cooling: (a) q-p'-T space; (b) Rightward shift in TY curve during heating; (c) Thermal volume change and subsequent compression curve after heating-cooling

An issue is that thermo-elasto-plastic models like that shown schematically in Figure 3.2 may not capture the behavior of normally consolidated soils after a drained heating-cooling

cycle. Upon further loading of a saturated normally consolidated clay subjected to a drained heating-cooling cycle, an apparent overconsolidation state has been observed (Plum and Esrig 1969; Laloui and Cekerevac 2003; Abuel-Naga et al. 2007). Based on the model in Figure 3.2, it would be expected that the preconsolidation stress would be the value corresponding to the intersection with the virgin compression curve before heating. However, this is not always observed in the literature. The overconsolidated behavior and the shift in the virgin compression line observed by Plum and Esrig (1969) is shown in Figure 3.3 for illitic clay heated to 50 °C then cooled to 24 °C. Another example is that Sultan et al. (2002) observed that a higher increase in preconsolidation stress was obtained upon further loading for a heating cooling cycle with a higher change in temperature.

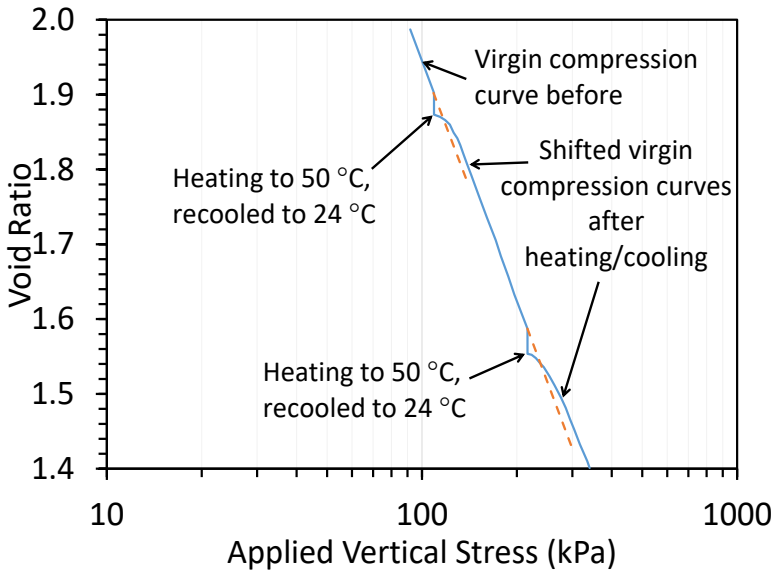

Figure 3.3. Change in preconsolidation stress after a heating cooling cycle observed by Plum and Esrig (1969)

For illite and Newfield clay samples which were only heated to 50 °C, Plum and Esrig (1969) observed normally consolidated behavior upon further loading. Hueckel and Baldi (1990) and Abuel-Naga et al. (2007) also observed similar behaviour for Pontida clay, Boom clay and Bangkok clay respectively. On the contrary, Towhata et al. (1993) and Sultan et al. (2002) observed an apparent overconsolidation effect upon further loading of a sample only subjected to heating for remolded kaolinite and boom clay respectively.

Several studies in literature found the slope of the virgin compression line to be unaffected by temperature (Finn 1951; Campanella and Mitchell 1968; Plum and Esrig 1969; Laloui and Cekerevac 2003). In contrast, Tanaka et al. (1997) and Sultan et al. (2002) observed a change in the slope of the virgin compression line at different temperatures. These contradicting observations in literature indicated the need for further investigation of the effect of temperature on the preconsolidation stress and compression curve on normally consolidated clays. This study focuses on the results obtained from a triaxial test conducted on a saturated normally consolidated clay subjected to a heating cooling cycle.

3.2 Material and Test Methods

3.2.1 Material

Commercial kaolinite clay obtained from M&M Clays Inc. of McIntyre, GA was used in this study. This clay was also tested by Ghaaowd et al. (2017), Takai et al. (2016) and Samarakoon et al. (2018). Properties of the clay are given in Table 2.1.

3.2.2 Experimental Set-up

The laboratory test was performed using a modified triaxial system developed by Alsherif and McCartney (2015). A schematic of the system is shown in Figure 3.4. The system comprised of a Pyrex pressure vessel having low thermal creep behavior. A stainless steel, U-shaped pipe was placed inside the cell and heated water was circulated using a heated water bath to control the temperature inside the cell. To ensure uniform mixing, a pump capable of withstanding high fluid pressures and temperatures was used to circulate the cell water. A pore water pressure transducer was used to measure the changes in pore water pressure during heating and cooling. The cell fluid temperature was measured using a thermocouple and a temperature recorder to a 0.5 °C accuracy. The cell pressure was applied using a flow pump and the back-pressure was controlled using a pressure panel.

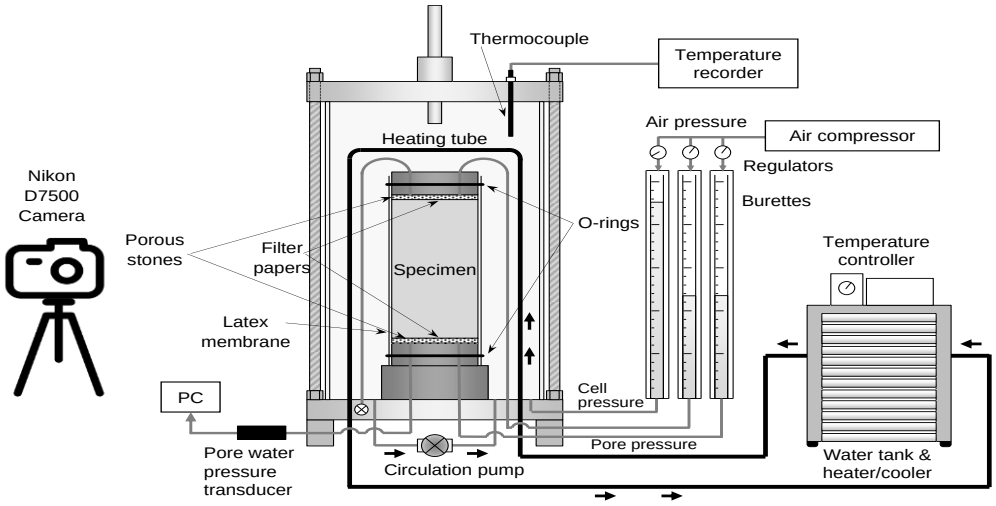

Figure 3.4. Thermal triaxial set-up

In addition to monitoring the drainage from the specimen during consolidation, heating and cooling, images of the specimen were taken using a high-resolution camera (Nikon D7500,

AF-P DX NIKKOR 70-300mm f/4.5-6.3G ED lens) during the test to measure changes in volume using an approach similar to Uchaipichat et al. (2011). The sample volume was considered to be made up of a series of stacked disks where the height of a single disk was one vertical pixel and the diameter was the number of horizontal pixels. Macari et al. (1997) found the relationship between the observed and true radius to be linear using a simplified two dimensional model which maps the specimen to the image plane. This approximation is more applicable when the distance between the camera and the specimen is large compared to the specimen height. Based on this approximation, the magnification effects due to the cell and cell fluid were accounted for by using the actual specimen volume measured at the beginning of the test.

3.2.3 Procedure

For preparation of the specimen, clay powder was first mixed with deionized water in a mixer to form a slurry with a water content of 130%. The slurry was then poured into a steel hollow cylinder having a diameter of 88.9 mm. Porous stones and filter paper were placed on the top and bottom of the slurry. The slurry was consolidated using a compression frame at a constant rate of 0.04mm/min for 48 hours. Then it was subjected to constant vertical stresses of 26, 52, 103 and 181 kPa in 24 hour-long increments.

The sedimented clay layer was then extracted and trimmed to a smaller cylindrical specimen with diameter of 72.4 mm suitable for testing in the thermal triaxial cell. The specimen was back-pressure saturated until the Skempton's pore water pressure parameter B value was at least 0.95. The initial void ratio of the specimen was 1.05. It was then isotropically consolidated following loading, unloading and reloading paths to a final mean effective stress of 248 kPa. The

specimen is at normally consolidated conditions at this stress state. While maintaining the normally consolidated stress state, the specimen was subjected to drained heating where the temperature was increased from 23 °C to 59.5 °C in 5 increments (about 7 °C per increment). Each increment was maintained for about 4-5 hours until the volume change stabilized. Then the specimen was cooled back to room temperature in a similar manner. Following a heating cooling cycle, the specimen was isotropically loaded in increments up to a mean effective stress of 310 kPa. The thermo-mechanical path for the test procedure is shown in Figure 3.5.

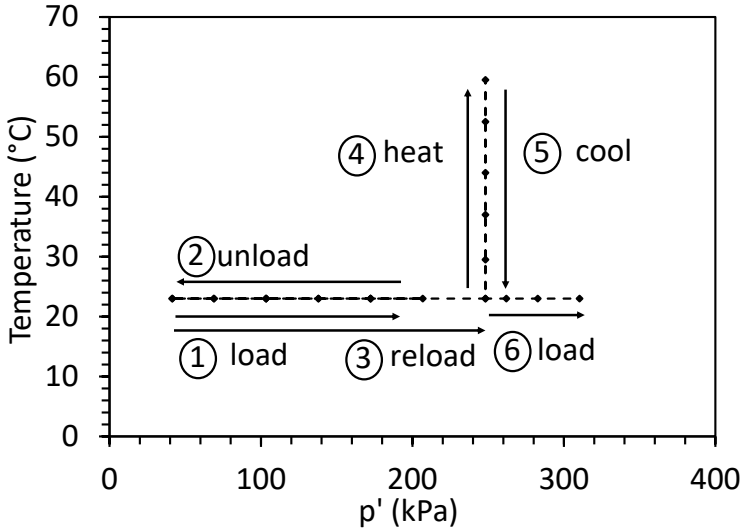

Figure 3.5. Thermo-mechanical path evaluated in the thermal triaxial test

3.3 Experimental Results and Discussion

The change in void ratio of the specimen during heating and cooling is shown in Figure 3.6(a) along with the corresponding temperature profile. A decrease in void ratio is observed during heating whereas an increase in void ratio is observed during subsequent cooling. However, the net effect on the specimen was a reduction in void ratio after a heating cooling cycle. The change in volumetric strain with temperature is shown in Figure 3.6(b). The increase

in void ratio during cooling is not in agreement with the general trend observed in literature where elastic contraction is observed during cooling. (Baldi et al. 1991; Sultan et al. 2002; Abuel-Naga et al. 2006) However, Plum and Esrig (1969) and Hueckel and Baldi (1990) observed a slight expansion during drained cooling for illitic clay and Pontida clay respectively.

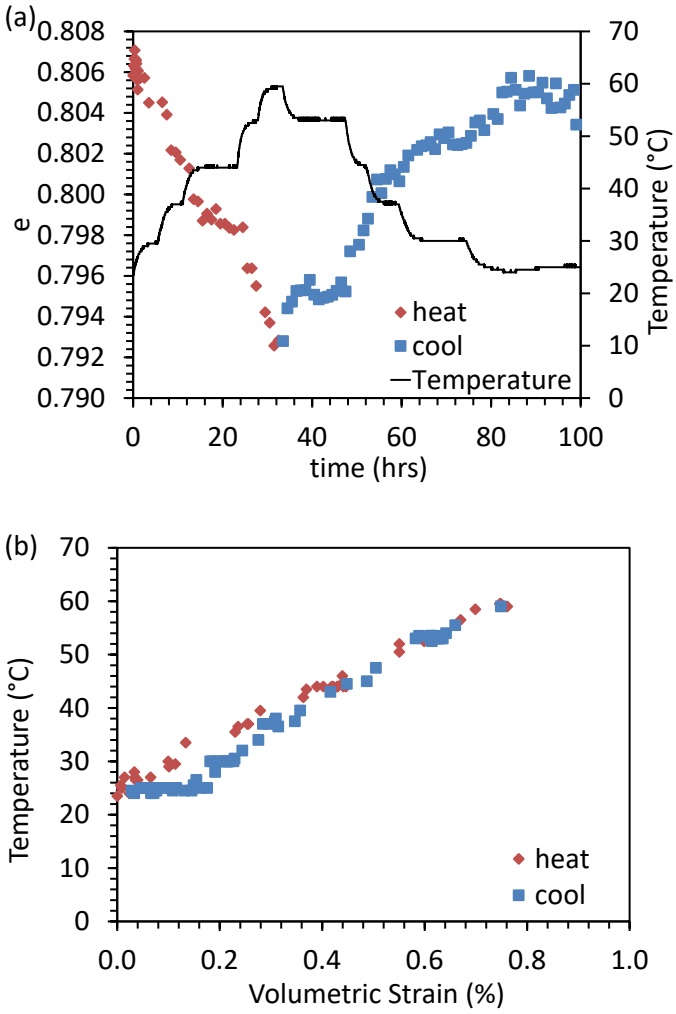

Figure 3.6. (a) Volume change of the specimen during drained heating and cooling; (b) Change in thermal volumetric strain with temperature

The change in excess pore water pressure during the heating-cooling cycle is shown in Figure 3.7. The change in excess pore water pressure is observed to be between ±4.5 kPa. Based on the observations, the change in excess pore water pressure generated during incremental heating and cooling under drained conditions can be considered negligible. This indicates that the thermal volume change process can be assumed to be drained during the entire heating and cooling process.

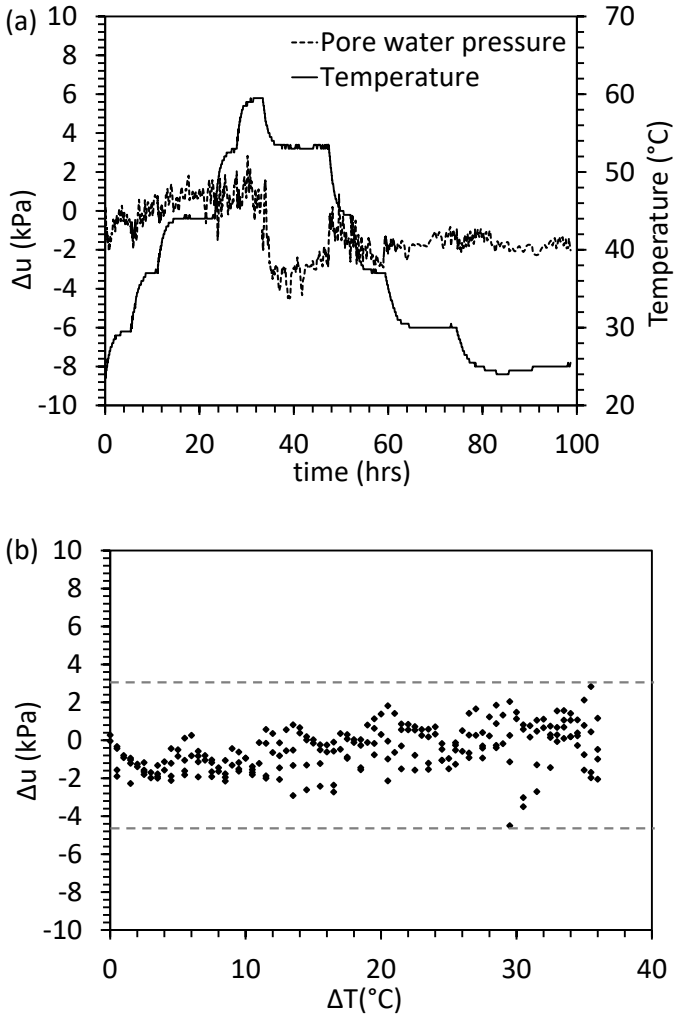

Figure 3.7. (a) Excess pore water pressure during heating and cooling; (b) Variation of excess pore water pressure with temperature

The compression curve for the specimen is shown in Figure 3.8 in the *e* vs ln(*p'*) plane. It can be observed that the specimen which was initially at a normally consolidated state showed overconsolidated behavior after being subjected to a heating cooling cycle. The slope in the compression curve immediately after a heating cooling cycle is similar to that of the recompression index (κ) of the clay. Upon further loading the specimen regains a normally consolidated state at a higher mean effective stress than before. The slope in this section is similar to that of the virgin compression index (λ) with a shift in the curve to the right. The new preconsolidation stress was estimated to be around 290 kPa which results in an increase of 42 kPa due to a heating cooling cycle. This conforms to the thermal hardening phenomenon described in literature where a soil specimen experiences a hardening effect merely due to a temperature change without any additional mechanical loading.

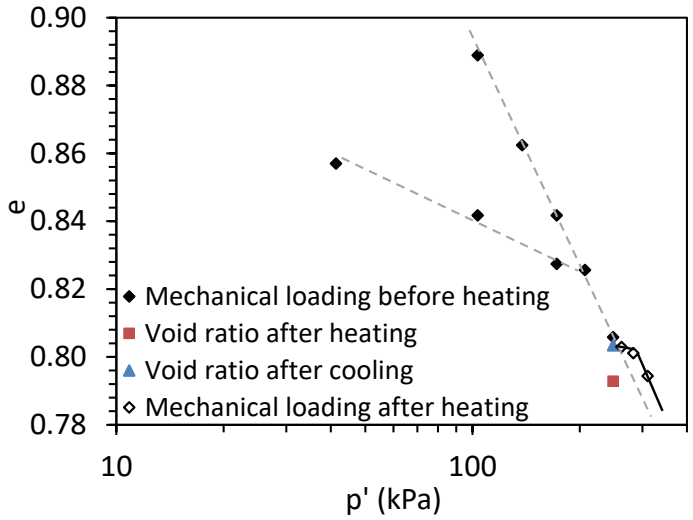

Figure 3.8. Compression curve for thermo-mechanical loading showing the shift in the virgin compression curve after the heating-cooling cycle

3.4 Conclusion

The results presented in this study indicate a normally consolidated clay subjected to a heating cooling cycle will observe an increase in its preconsolidation stress upon further loading. This increase is attributed to the thermal hardening phenomenon that the soil undergoes due to a heating cooling cycle. A displacement of the virgin compression line was observed where it shifted to the right with a similar slope after a heating cooling cycle. The clay specimen which was at a normally consolidated state prior to being subjected to a heating cooling cycle, behaved as an overconsolidated clay during subsequent loading with a slope similar to that of the recompression index. After reaching its new preconsolidation stress, a normally consolidated behavior could be observed again. The results indicate the possibility of using in-situ heating with geothermal heat exchangers as a means of improving soft soils to induce a hardening effect.

ACKNOWLEDGEMENTS

Chapter 3 of this dissertation is based on material published by GeoCongress 2020 in Minneapolis, MN titled “Effect of drained heating and cooling on the preconsolidation stress of saturated normally consolidated clays”, with authors, Radhavi Abeysiridara Samarakoon and John S. McCartney. The dissertation author is the first author of this paper.

4 Simulation of Thermal Drains using a New Constitutive Model for Thermal Volume Change of Normally Consolidated Clays

4.1 Introduction

The use of thermal drains has been proposed as an approach to improve the mechanical properties of normally consolidated soft clays (Abuel-Naga et al. 2006; Pothiraksanon et al. 2010; Samarakoon and McCartney 2020a, 2021). A thermal drain combines a vertical drain used for radial consolidation of soft clay layers with a geothermal heat exchanger. The geothermal heat exchanger consists of a closed-loop, "U"-shaped pipe that transfers heat to the ground by circulating heated fluid through the pipe with a heat pump at the ground surface. The thermal drain itself can either be a prefabricated thermal drain consisting of a plastic strip with internal channels to support vertical water flow encased within a geotextile filter that is pushed into the clay, or a cylindrical borehole installed with a casing and backfilled with sand. The motivation for using thermal drains is twofold. First, the heating of the soft clay will lead to an increase in excess pore water pressure due to differential expansion of the pore water and soil solids (Mitchell and Campanella 1968; Ghabezloo and Sulem 2009; Ghaaowd et al. 2017). The thermal drain provides a drainage path for the pressurized water, and the consolidation process will result in contraction of the clay layer. Second, the increase in temperature will cause a reduction in water viscosity, which will result in an increase in hydraulic conductivity of the clay and an increase in the rate of consolidation (Houston et al. 1985). Thermal drains are best suited for normally consolidated and lightly consolidated clays, as heavily overconsolidated clays are expected to expand and contract elastically during heating and cooling, respectively (e.g., Baldi et al. 1988, Laloui and Cekerevac 2003; Abuel-Naga et al. 2007a, 2007b), although an increase

in hydraulic conductivity would still be encountered in all clays. A typical deployment of thermal drains with a surface surcharge is shown in the schematic in Figure 4.1.

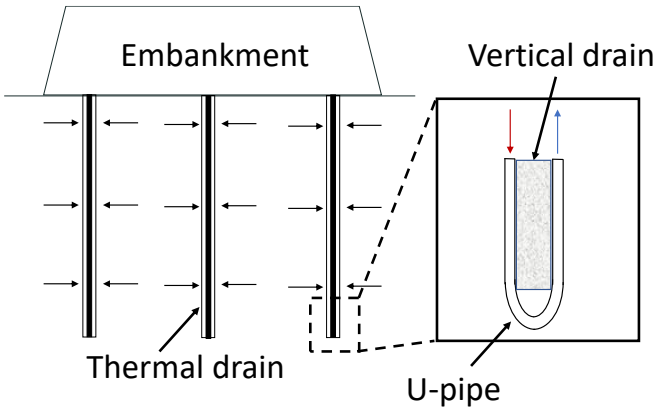

Figure 4.1. Schematic of thermal drains embedded in a soil layer with a detail showing fluid flow in a closed-loop heat exchanger

An increase in the rate of consolidation as well as the magnitude of the ultimate surface settlement have been confirmed in calibration chamber experiments on thermal drains in soft clay layers that included comparisons with conventional drains (Abuel-Naga et al. 2006; Artidteang et al. 2011; Salager et al. 2012). The performance of thermal drains used in combination with a surficial surcharge load as part of the preconsolidation of a soft clay site was also investigated by Pothiraksanon et al. (2010). They applied a change in temperature of approximately 60 °C over the course of 200 days to a clay layer having a thickness of 8 m with a sand surcharge of 6 m and observed a total settlement of approximately 400 mm for a thermal drain and 240 mm for a prefabricated vertical drain. An advantage of thermal drains over conventional vertical drains is that a surficial surcharge may not be necessary due to the thermal pressurization of the soft clay associated with heating of the drain. Bergenstahl et al. (1994)

applied a change in temperature of approximately 60 °C to a 10 m-thick layer of clay over the course of 8.5 months using geothermal heat exchangers without vertical drains or the use of a surcharge and observed a thermally-induced settlement of 37 mm which was linked to the generation and dissipation of thermally-induced excess pore water pressures.

An issue that is critical to consider in the simulation of thermal drains in the field is the variation in expected thermal volume change as a function of depth in the clay layer. There is a growing set of data indicating that the thermal volume change in normally consolidated clays will change with its effective stress state (Samarakoon et al. 2018; Samarakoon and McCartney 2020b; Samarakoon et al. 2022). Furthermore, field-scale and laboratory studies (Bergenstahl et al. 1994; Abuel-Naga et al. 2007b; Uchaipichat and Khalili 2009; Ghaaowd et al. 2017) as well as poroelastic theories (Campanella and Mitchell 1968, Ghabezloo and Sulem 2009) show different thermal pressurization effects at different effectives stresses and void ratios during undrained heating of normally consolidated clays. The magnitude of thermal volumetric strains observed in the literature is relatively small, with an average of 1% volumetric strain occurring during a change in temperature of 60 °C. However, even a slight increase in thermo-plastic volumetric strain at a given depth will result in a significant improvement in clay mechanical properties as shown by Ghaaowd and McCartney (2021) and Ghaaowd et al. (2022) for pile pullout capacity and Samarakoon et al. (2022) for undrained shear strength of kaolinite specimens. Therefore, it is evident that the effect of effective stress state plays a critical role when simulating thermal drains in normally consolidated clays. To that end, the goal of this study is to develop a new constitutive model to predict the thermal volume change of normally consolidated clays which can be applied to studying the behavior of thermal drains. The model

will be calibrated using data from thermal triaxial tests and used to simulate tank tests with thermal drains.

4.2 Background on Thermo-Mechanical Modeling of Saturated Clays

Several thermo-mechanical models have been developed by researchers to predict the thermal volume change of clay (Hueckel and Borsetto 1990; Cui et al. 2000; Laloui and Cekerevac 2003; Abeul-Naga et al. 2007a, Abuel-Naga et al. 2009). In general, the thermal volume change is dependent on the stress history. For overconsolidated clays, elastic expansion is expected upon heating with a tendency for contraction at higher temperatures, whereas for normally consolidated clays, plastic contraction can be observed. In some instances, lightly overconsolidated clays may also show contractive behavior (Baldi et al. 1988, Abuel-Naga et al. 2007b). Hueckel and Borsetto (1990) proposed a parabolic yield surface expression in the T-p' plane based on the evolution of preconsolidation stress with temperature which required the determination of multiple material parameters. At stress states below the yield limit, thermal stains will be elastic. If the yield limit is approached either by mechanical or thermal loading, plastic thermal strains will be generated, and the yield surface will move to the right due to thermal hardening resulting in a larger elastic zone.

Other studies have proposed different thermal yielding curves to capture trends observed in experimental data. For example, Cui et al. (2000) proposed a simplified relationship for the yield surface where an exponential expression was used as follows:

$$p_c'(T) = p_c'(T_0)\exp(-\alpha_0 \Delta T) \quad (4.1)$$

where $p_c'(T_0)$ is the apparent preconsolidation stress at room temperature, $p_c'(T)$ is the preconsolidation stress at temperature T, and α_0 is a material parameter. To better account for the

effects of overconsolidation ratio (OCR) on volume change at high temperatures, Cui et al. (2000) introduced a second yield limit within the framework of Hueckel and Borsetto (1990). Specifically, the contractive behavior observed in overconsolidated clays at higher temperature was captured by this model.

An isotropic thermo-plastic yield limit was introduced by Laloui and Cekerevac (2003) with a logarithmic yield surface expression as follows:

$$p_c'(T) = p_c'(T_0)\left[1 - \gamma log\left(\frac{T}{T_0}\right)\right] \quad (4.2)$$

where γ is a material parameter. Abuel-Naga et al. (2007a) adopted the same relationship as that proposed by Laloui and Cekerevac (2003) in Equation (4.2) for the loading yield limit, but used a similar approach to Cui et al. (2000) with two different yield limits referred to as the thermal and loading yield limit respectively.

An issue encountered in application of the different thermo-mechanical models listed above is that normally consolidated clays will all have the same thermal volume change regardless of the initial effective stress state, a finding that contradicts experimental studies on the thermal volume change of soft clays (Samarakoon et al. 2018, 2022) as well as the trends in thermally induced excess pore water pressures of normally consolidated soil with different initial effective stresses (Abuel-Naga et al. 2007b; Uchaipichat and Khalili 2009). The isotropic yield mechanism proposed by Laloui and Cekerevac (2003) is shown in Figure 4.2(a) in the T-p' plane along with a thermal loading path for a normally consolidated clay in red. When a normally consolidated clay (initially on the yield curve) is subjected to an increase in temperature from T_0 to T_1 at constant mean effective stress, the yield curve will shift to the right. As a result of this thermal hardening phenomenon, the clay will undergo a contractive thermo-plastic volumetric change. This is represented in the e-ln p' plane by a shift in the normally consolidated line to the

left at temperature T_1 as shown in Figure 4.2(b). Regardless of the initial mean effective stress of the normally consolidated clay, the same thermal volume change will be predicted by the model.

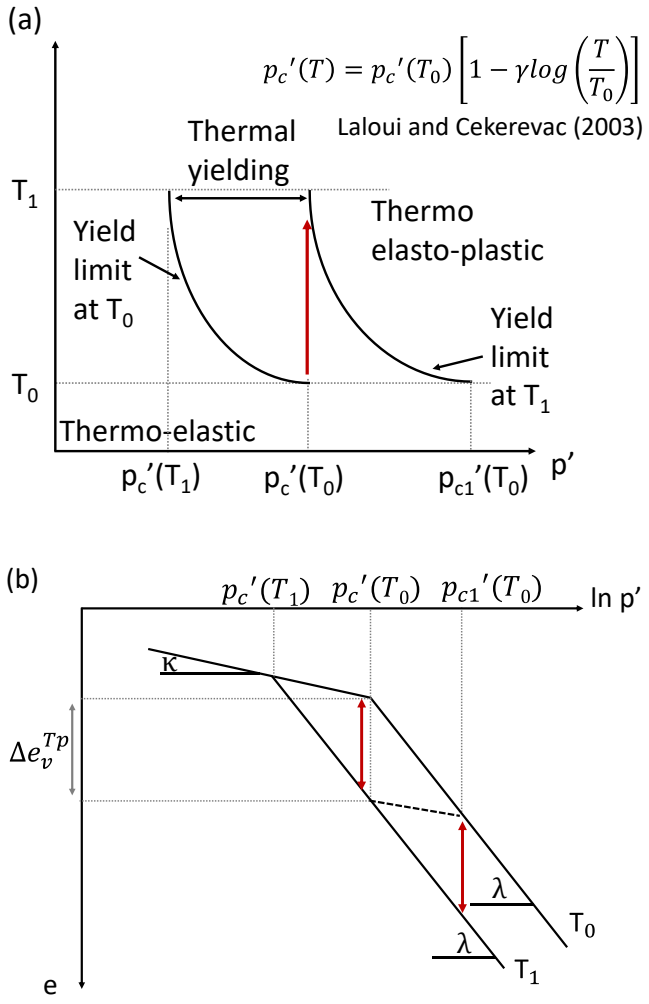

Figure 4.2. Thermo-mechanical behavior of normally consolidated clays as predicted by the model of Laloui and Cekerevac (2003): (a) Thermal yield limit in T-p' plane; (b) Thermal volume change in e vs. ln p' plane

The reason for this shortcoming of available thermo-mechanical constitutive models in being able to capture the observed thermal volume change data from the literature perhaps lies in

the approach by which the effect of temperature on the yield curve is defined, where the yield curve is defined by mechanically loading overconsolidated clays after heating to different temperatures and identifying the apparent preconsolidation stress (Eriksson 1989, Boudali et al. 1994, Sultan et al. 2002). These studies found that the slopes of the recompression curve before reaching yielding as well as the compression curve after reaching normally consolidated conditions were independent of temperature. Only a few studies have characterized the thermal volume change of soft clays under multiple mean effective stresses (Abuel-Naga et al. 2007a; Samarakoon et al. 2018, 2022). Given that the volume change predictions for normally consolidated soils were made based on these observations, the existing models have an inherent issue in predicting the same amount of volume change for normally consolidated clays, irrespective of the effective stress state (Figure 4.2(b)).

4.3 Proposed Framework for Thermal Volume Change of Normally Consolidated Clay

Based on the experimental evidence of thermal volume change of saturated normally consolidated clay in Samarakoon et al. (2022), a new thermo-elasto-plastic mechanism is required to accurately represent the thermal behavior of saturated clay at different initial mean effectives stresses. Volumetric strain can be generated due to mechanical and/or thermal loading. At stress states below the yield stress the strains will be elastic whereas plastic strains will be obtained at stress states at the yield limit. Based on the experimental observations, a new framework is proposed to obtain plastic volume changes under thermal loading at different initial isotropic stress states.

4.3.1 Thermo-elastic Strains

Although the focus of this study was on the plastic volume changes of saturated normally consolidated clay subjected to thermal loading, the thermo-elastic relationships are presented for the completion of the proposed model. The thermo-elastic strain (ε_v^{Te}) generated by thermal loading is obtained by the following relationship.

$$d\varepsilon_v^{Te} = \alpha dT \tag{4.3}$$

where α is the drained volumetric thermal expansion coefficient of clay and T is the temperature. α can be determined using thermal volume change results of highly overconsolidated clays or from heating cooling cycles applied to normally consolidated clays with a slow cooling rate. Cui et al. (2000) considered α to be a constant parameter whereas other researchers defined the coefficient α as a function of temperature and the effective stress (Laloui 2001; Abuel-Naga et al. 2007a). The elastic strains generated due to mechanical loading is obtained as follows.

$$d\varepsilon_v^e = \frac{\kappa}{1+e_0}\frac{dp\prime}{p\prime} \tag{4.4}$$

where κ is the slope of the recompression line, p' is the mean effective stress and e_0 is the initial void ratio.

4.3.2 Thermo-plastic Strains

When the stress state reaches a yield limit, thermo-plastic strains are developed. As described in section 4.1, the yield limit can be reached by mechanical loading or thermal loading at constant effective stress. The yield limit for isotropic conditions can be expressed as follows:

$$f = p' - p_c' = 0 \tag{4.5}$$

where p_c' is the apparent preconsolidation stress. Several relationships are found in literature representing the thermal evolution of the preconsolidation stress (Hueckel and Borsetto 1990;

Cui et al. 2000; Laloui and Cekerevac 2003). Based on the experimental evidence, an extension to Equation (4.2) is proposed where the parameter γ is a function of the mean preconsolidation stress $p_c'(T_0)$, as follows:

$$\gamma\left(p_c'(T_0)\right) = \frac{a}{p_c'(T_0)} + b \tag{4.6}$$

where $p_c'(T_0)$ is the apparent preconsolidation stress at room temperature, which must be greater than zero, and a and b are constants depending on the material with $a < 0$ and $b > 0$, such that γ increases with increasing mean preconsolidation stress for normally consolidated clays. For $\gamma > 0$, the condition $p_c'(T_0) > -a/b$ must be satisfied. The reason for proposing that γ is a function of mean preconsolidation stress is that all overconsolidated soils corresponding to a given preconsolidation stress will have the same value of γ, which is consistent with the way that previous thermo-mechanical models were developed. The variation in apparent thermal preconsolidation stress with temperature at different initial mean effective stresses, having different γ values is shown in Figure 4.3. Laloui & Cekerevac (2003) also reported different γ values for experimental data from Moritz (1995) for Swedish clay at different depths. Substituting Equation (4.6) into Equation (4.2) will yield the following relationship:

$$p_c'(T) = p_c'(T_0)\left[1 - b \times log\left(\frac{T}{T_0}\right)\right] - a \times log\left(\frac{T}{T_0}\right) \tag{4.7}$$

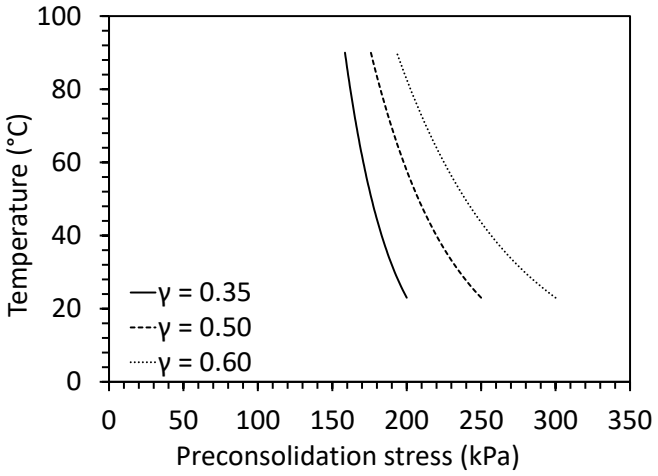

Figure 4.3. Shapes of the yield curves showing variation in thermal preconsolidation stress with temperature at different initial mean effective stresses for normally consolidated clays

For a normally consolidated clay, its current stress state will be equal to the preconsolidation stress and hence will be on the yield limit. When the temperature is increased at constant effective stress, the clay will be subjected to thermal yielding to maintain the current stress state and a plastic thermal volume change will occur. Thermally induced plastic volumetric strain, ε_v^{Tp} is related to the change in preconsolidation stress with temperature, as follows:

$$d\varepsilon_v^{Tp} = \frac{\lambda-\kappa}{1+e_0} ln\left(\frac{p_c'(T_0)}{p_c'(T)}\right) \tag{4.8}$$

where $p_c'(T)$ is the preconsolidation stress at temperature T obtained from Equation (4.7). λ is the slope of the VCL. As the parameter γ changes with the preconsolidation stress, the thermal volume change at different mean effective stresses obtained from Equation (4.8) will change as for a normally consolidated clay. This is an improvement to the existing thermo-mechanical constitutive models where the same amount of thermal volume change is predicted for normally consolidated clays irrespective of their mean effective stress.

The proposed thermo-mechanical framework is shown in Figure 4.4(a) and (b) respectively. Figure 4.4(a) shows the thermal volume change in the e vs. ln p' plane. Path ABC shows the compression curve at room temperature T_0. Path DEF is obtained by increasing the temperature of normally consolidated clay from T_0 to T_1. $p_{c1}'(T_1)$ is the preconsolidation stress at temperature T_1. As a result of drained heating at $p_{c1}'(T_0)$, a thermo-plastic volume change of Δe_v^{Tp} will occur, which can be obtained using Equation (4.8). If the clay was subjected to heating at a higher mean effective stress (i.e. $p_{c2}'(T_0)$), the yield stress will now move to point J along the NCL, and the corresponding apparent thermal preconsolidation stress will be at point H. At this stress state, a higher thermo-plastic volume change, denoted by the distance JK will be obtained. Paths DEF and HKI are both obtained at temperature T_1, where path DEF is associated with the apparent thermal preconsolidation stress corresponding to preconsolidation stress at room temperature, $p_{c1}'(T_0)$ and path HKI is associated with the apparent thermal preconsolidation stress corresponding to preconsolidation stress at room temperature, $p_{c2}'(T_0)$. In the existing thermo-mechanical models, the NCL shifts to the left as the temperature is increased. Based on the proposed model, the shift in the NCL is not only a function of temperature but also the mean effective stress for normally consolidated clays.

The corresponding thermo-mechanical paths in the T-p' plane are shown in Figure 4.4(b). The specimen is subjected to mechanical loading from path A to B. From B to E, the specimen is heated under drained conditions where the temperature increases from T_0 to T_1. Curve BD shows the yield limit and the preconsolidation stress is reduced to $p_{c1}'(T_1)$ at temperature T_1. For heating at a higher mean effective stress, the path will follow ABJ for mechanical loading and JK for drained heating. The corresponding thermal preconsolidation stress will now be at point H following the curve JH. For normally consolidated clays subjected to drained heating, the yield

curve will shift to the right due to thermal hardening. Once the specimen is cooled back to room temperature, the clay specimen will have a new preconsolidation stress which will be greater than the preconsolidation stress prior to heating. The yield limit after cooling is also shown in Figure 4.4(b). This preconsolidation stress after a heating cooling cycle can be obtained from Equation (4.7).

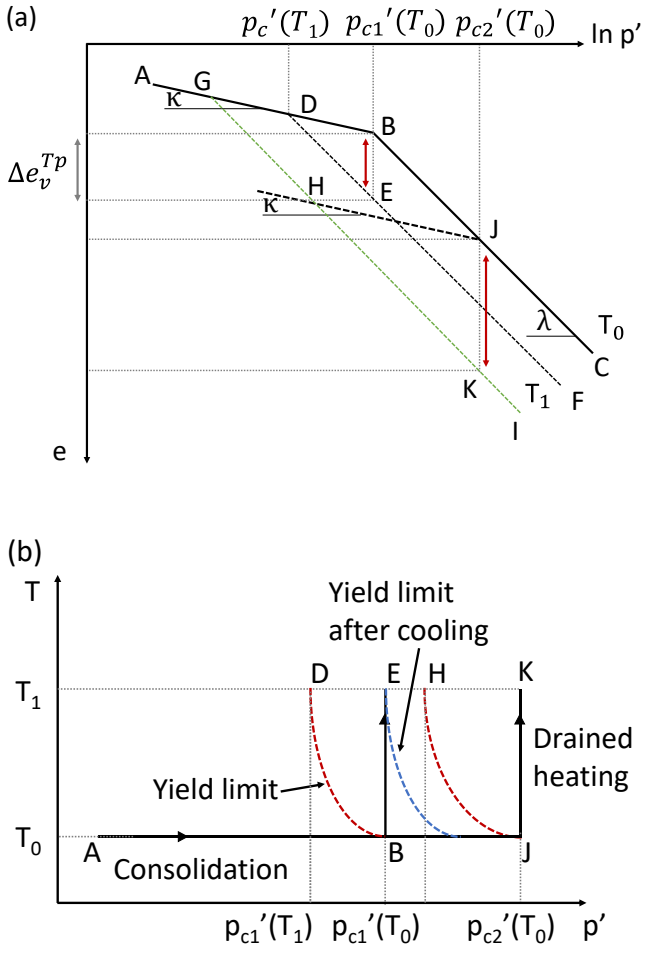

Figure 4.4. New thermo-mechanical framework: (a) Thermal volume change in e vs. ln p' plane; (b) Thermo-mechanical paths in T-p' plane

4.4 Model Calibration

To calibrate the proposed model, the experimental results from Samarakoon et al. (2022) are considered in this study. Samarakoon et al. (2022) conducted thermal triaxial tests on saturated normally consolidated kaolinite specimens at four different mean effective stresses. The specimens were first mechanically consolidated under isotropic conditions to a normally consolidated state and then subjected to drained heating where the temperature was increased to 60 °C. Finally, the specimens were sheared under undrained conditions at the elevated temperature. Normally consolidated specimens at mean effective stresses 230, 260, 290 and 320 kPa were considered. Contrary to the existing thermo-mechanical predictions, the thermal volume change obtained at each mean effective stress was different and showed an increasing trend as the mean effective stress increased. The new experimental evidence from tests conducted on normally consolidated clays reveals a limitation in the existing thermo-mechanical constitutive models when predicting thermal volume change in normally consolidated clays subjected to drained heating.

In addition to the slopes of the compression curve (κ and λ) for a given clay, the proposed model requires determination of variation in the parameter γ at different mean effective stresses through parameters a and b. At least two drained heating tests conducted on normally consolidated clay specimens at different initial mean effective stresses are required to obtain these parameters. Three tests may provide better accuracy when determining the required model parameters. Using the thermal volume change results at each mean effective stress for a given temperature, the thermal preconsolidation stress, $p_c'(T)$ corresponding to each mean effective stress can be obtained using Equation (4.8). Using the $p_c'(T)$ values at each stress state, the γ parameter corresponding to each mean effective stress can be obtained using Equation (4.2).

Finally, Equation (4.6) can be used to determine the parameters *a* and *b*. Alternatively, Equation (4.7) can also be used to obtain the parameters *a* and *b* directly after determining $p_c'(T)$ values. The obtained γ values at each mean preconsolidation stress and the fitting of Equation (4.6) to the experimental data of Samarakoon et al. (2002) are shown in Figure 4.5. The model parameters obtained for kaolinite are summarized in Table 4.1.

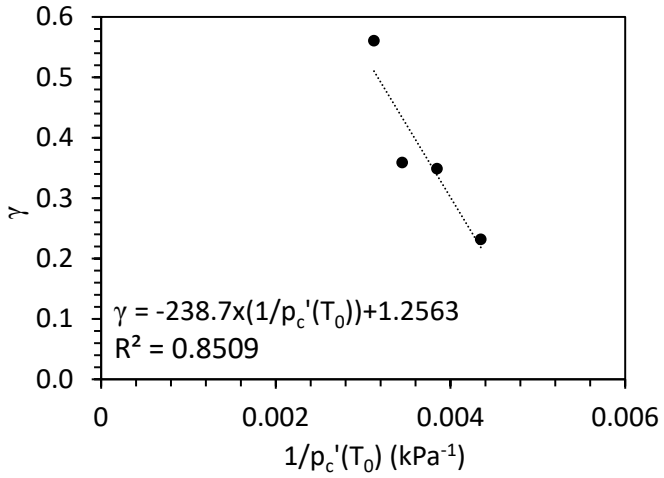

Figure 4.5. Parameter $\boldsymbol{\gamma}$ as a function of mean preconsolidation stress for normally consolidated kaolinite (Data: Samarakoon et al. 2022)

Table 4.1. Model parameters for Georgia kaolinite clay

Parameter	Value
Slope of VCL (λ)	0.09
Slope of RCL (κ)	0.02
a	-238.7
b	1.2563

Back-predictions of the experimental data of Samarakoon et al. (2022) are shown in Figure 4.6. In general, good agreement can be observed between the predictions and the experimental data and the increasing trend in thermal volumetric strain with increasing mean

effective stress of normally consolidated clays is captured by the proposed model. The thermal volume change at the lower mean effective stresses is predicted well by the model whereas the thermal volume change at the higher mean effective stress value of 320 kPa is slightly underpredicted. The thermal volumetric strain value obtained at 290 kPa seems lower in comparison and could be due to an experimental variability in the initial conditions of the sedimented clay specimens.

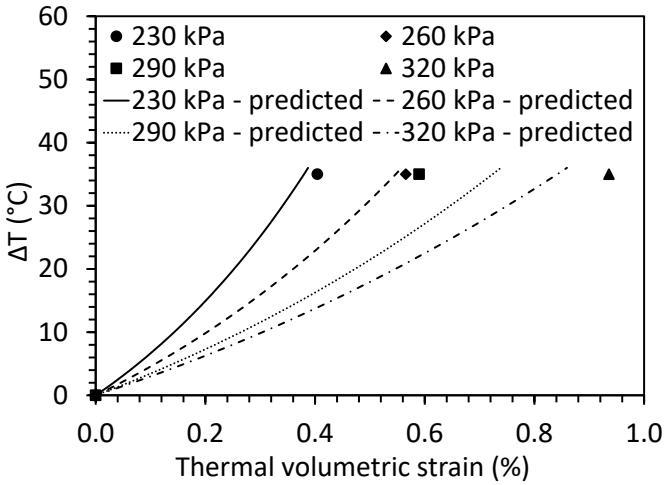

Figure 4.6. Thermal volumetric strain of normally consolidated kaolinite at different initial mean effective stresses (Data: Samarakoon et al. 2022)

The established model can capture the effect of initial mean effective stress on the thermal volume change of normally consolidated clay where the thermal volumetric strain increases with increasing mean effective stress. This is an improvement to the existing thermo-mechanical constitutive models where the same amount of volume change is predicted for normally consolidated clay irrespective of its initial stress state. Further studies on multiple soil types considering a wider range of stress states will assist in strengthening the established relationships for soil parameters. Better predictions of thermal volume change in normally

consolidated clays are important specifically in applications such as using in-situ heating for soil improvement. When the thermal volume changes at different mean effective stresses indicative of different depths can be accurately predicted, soil improvement can be strategically applied over different depths. This can also assist with designing efficient in-situ heating arrangements for soil improvement.

4.5 Application – Thermal Drain Analysis

The proposed constitutive model was applied in a numerical model developed to simulate a thermal vertical drain embedded in a soft clay layer inside a large-scale oedometer. The numerical model simulates the coupled phenomena of heat transfer, fluid flow and volume change in soft clay surrounding a thermal vertical drain. The theoretical framework, formulation of the numerical model, comparison with experimental results along with a parametric analysis on the performance of a thermal drain is described in the following sections.

4.5.1 Soil Domain Geometry

To simulate the behavior of a clay layer around a thermal drain, a finite soil domain representing a large-scale oedometer experiment by Artidteang et al. (2011) was considered in this study. The thermal drain is inserted at the center of a cylindrical specimen of height h and radius r and a surcharge is applied at the top of the specimen. A schematic diagram of the thermal drain arrangement in a finite soil domain is shown in Figure 4.7. This geometry was selected as it was used to validate the numerical model using experimental results of Artidteang et al. (2011). Although this geometry does not represent the boundary conditions expected in a

field deployment of thermal drains, it permits the effects of temperature and applied surcharge on the transient thermal consolidation process.

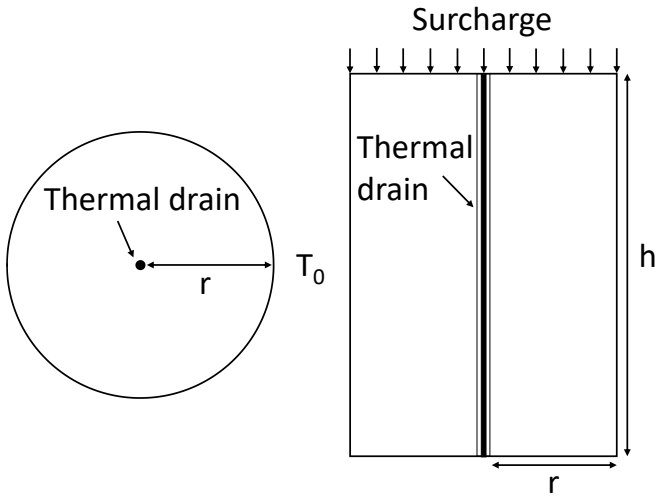

Figure 4.7. Schematic diagram of the thermal drain arrangement in a finite soil domain

4.5.2 Theoretical Framework

4.5.2.1 Heat Transfer

When a thermal drain is being used, the temperature of the surrounding soil will increase. Assuming that heat transfer through the soil medium will occur through conduction only, it can be modeled using Fourier's law and energy conservation principles. The thermal drain was considered as a line heat source where the vertical distribution of temperature was assumed to be uniform. The governing equation for conductive radial heat transfer through soil based on Fourier's law and conservation of energy will be simplified as follows in cylindrical coordinates.

$$\frac{\rho_t C}{\lambda_T}\frac{\partial T}{\partial t} = \frac{\partial^2 T}{\partial r^2} + \frac{1}{r}\frac{\partial T}{\partial r} \tag{4.9}$$

where ρ_t is the total density of soil, C is the specific heat capacity of the soil, λ_T is the thermal conductivity of the soil, and r is the radial distance. The thermal conductivity of the clay will be impacted by the volume changes occurring in the clay, where more heat conduction can occur through the soil particles as the void space reduces. The change in thermal conductivity with porosity was considered using a parallel model as follows (Dong et al. 2015):

$$\lambda_T = n\lambda_f + (1 - n)\lambda_s \quad (4.10)$$

where n is the porosity, λ_f is the thermal conductivity of the pore water and λ_s is the thermal conductivity of the soil particles.

4.5.2.2 Fluid Flow

An increase in temperature will impact the fluid flow through the porous media by thermally induced excess pore water pressures and increased hydraulic conductivity. Thermally induced excess pore water pressure is generated because of the differences in the coefficients of thermal expansion of soil particles and the pore fluid. The soil will undergo volumetric contraction as the excess pore water pressures are dissipated. Furthermore, an increase in temperature will decrease the density and viscosity of the pore fluid which will result in an increase in hydraulic conductivity. The relationship between hydraulic conductivity (k) with fluid and soil properties can be understood using the definition of the intrinsic permeability, K in Equation (4.11).

$$K = \frac{k\eta_w}{\rho_w g} \quad (4.11)$$

where η_w is the dynamic viscosity of the fluid, ρ_w is the fluid density and g is the coefficient of gravity. Abuel-Naga et al. (2006) observed an increase in hydraulic conductivity with an increase in temperature for Bangkok clay. However, the intrinsic permeability was found to be

independent of temperature. The density of water will vary with temperature according to the following relationship:

$$\frac{\partial \rho_w}{\partial t} = -\rho_w \alpha_w \frac{\partial T}{\partial t} \tag{4.12}$$

where α_w is the volumetric coefficient of thermal expansion of water. The fluid viscosity can be expressed as a function of temperature following the empirical relationship given by Hillel (1980) in Equation (4.13).

$$\eta_w(T) = -0.00046575 \ln(T) + 0.00239138 \tag{4.13}$$

Fluid flow through the porous media can be expressed using principles of mass conservation. The governing equation in cylindrical coordinates will be reduced as shown for the geometry considered as follows:

$$\frac{\partial(\mathrm{n}\rho_\mathrm{w})}{\partial \mathrm{t}} = -\frac{1}{\mathrm{r}}\frac{\partial(\mathrm{r}\rho_\mathrm{w}\mathrm{v})}{\partial \mathrm{r}} \tag{4.14}$$

where v is the fluid velocity. Fluid velocity for a porous medium can be expressed using Darcy's law as follows:

$$\mathrm{v} = -\frac{\mathrm{K}}{\eta_\mathrm{w}}\frac{\partial \mathrm{U}}{\partial \mathrm{r}} \tag{4.15}$$

where U is the pore water pressure. By substituting Equation (4.15) into Equation (4.14) and using the product rule, the following equation is obtained:

$$\mathrm{n}\frac{\partial \rho_\mathrm{w}}{\partial \mathrm{t}} + \rho_\mathrm{w}\frac{\partial \mathrm{n}}{\partial \mathrm{t}} = \frac{\mathrm{K}}{\eta_\mathrm{w}}\left(\rho_\mathrm{w}\frac{\partial^2 \mathrm{U}}{\partial \mathrm{r}^2} + \frac{\rho_\mathrm{w}}{\mathrm{r}}\frac{\partial \mathrm{U}}{\partial \mathrm{r}} + \frac{\partial \mathrm{U}}{\partial \mathrm{r}}\frac{\partial \rho_\mathrm{w}}{\partial \mathrm{r}}\right) \tag{4.16}$$

The effects of temperature on density and viscosity can be incorporated by substituting Equations (4.12) and (4.13) into Equation (4.16). Considering the spatial variation of fluid density to be negligible, a general equation for non-isothermal fluid flow through porous media is obtained as follows:

$$-\mathrm{n}\alpha_\mathrm{w}\frac{\partial \mathrm{T}}{\partial \mathrm{t}} + \frac{\partial \mathrm{n}}{\partial \mathrm{t}} = \frac{\mathrm{K}}{\eta_\mathrm{w}}\left(\frac{\partial^2 \mathrm{U}}{\partial \mathrm{r}^2} + \frac{1}{\mathrm{r}}\frac{\partial \mathrm{U}}{\partial \mathrm{r}}\right) \tag{4.17}$$

4.5.2.3 Volume Change

The volume change in a thermal drain application will consist of mechanical and thermal components. The mechanical volume change due to application of a surficial surcharge can be obtained using compressibility relationships for a normally consolidated clay, given as follows:

$$\partial e^{p} = \lambda \frac{\partial p_v'}{p_v'} \tag{4.18}$$

where p_v' is the vertical effective stress. The thermo-plastic volume changes are obtained using the proposed constitutive relationship using Equations (4.7) and (4.8). For a simultaneous application of a surcharge and heat, the total stress will remain constant. The change in effective stress resulting from a change in the pore water pressure can be obtained by subtracting the pore water pressure from the total stress, p as follows:

$$p' = p - U \tag{4.19}$$

4.5.3 Boundary and Initial Conditions

The boundary conditions evaluated in this study are representative of a large-scale oedometer which was used for the validation of the numerical model. Heat transfer and fluid flow were considered to be axisymmetric about the axis of the drain for the numerical simulation. The variation of temperature in the vertical direction was assumed to be uniform thereby simplifying the geometry to a radial drainage problem. The thermal drain is treated as a line heat source where an elevated temperature will be applied. A constant temperature boundary condition was imposed at the thermal drain whereas a convective temperature boundary condition was maintained at the outer edges of the clay layer to represent the edges of a container in the laboratory. This outer boundary can be represented based on the experimental set-up. For example, a constant temperature boundary condition or a function accounting for daily

temperature fluctuations can be used when the outer boundary is maintained at ambient temperature. On the other hand, a convective boundary condition can be used to account for heat loss or zero heat flux to model thermal insulation at the boundary. A similar approach can also be used to model the surface temperatures.

Although not require, thermal drains are typically combined with an application of a surcharge on top of the saturated clay layer. The clay layer was assumed to be normally consolidated under the surcharge stress. The outer edge of the oedometer permits zero radial strain. However, a variation in void ratio within the clay layer with radius is expected due to heating from the central thermal drain. The surcharge is applied in stress-control conditions so settlements in the clay layer can be nonuniform as a function of the radius from the thermal drain. Drainage was only permitted at the location of the thermal drain (i.e., no vertical drainage from the top and bottom of the cylinder or radial drainage from the outer boundary). Accordingly, a constant hydrostatic pressure boundary was also applied at the drain location and the fluid velocity at the outer edge of the clay layer was taken as zero (i.e., no flow) representative of a large-scale oedometer. In a field application where multiple drains are used, the influence of other drains in the vicinity will have to be considered. For instance, multiple drain locations will be at constant temperature and hydrostatic pressure boundary conditions. Although not within the scope of this study, a more complex analysis with multiple drains will aid in determining the optimum spacing arrangements for thermal drains. The initial temperature in the soil domain was taken as equal to ambient temperature and the initial pore water pressure was determined based on the hydrostatic conditions and the applied surcharge. The initial porosity was determined based on the clay.

4.5.4 Numerical Formulation

The coupled phenomena were simulated using the finite difference method. Both steady state as well as transient variations in temperature, pore water pressure and settlement were solved for using the numerical model. The soil layer along a radius was spatially discretized into elements of equal size. A central difference scheme was used in the spatial domain and a forward difference scheme was used in the time domain. The numerical formulation was implemented and solved using Matlab.

4.5.5 Comparison with Experimental Data

The thermo-hydro-mechanical behavior of a saturated normally consolidated clay layer surrounding a thermal drain was simulated using the numerical model and compared with experimental data from literature. Artidteang et al. (2011) investigated the performance of a single thermal drain in soft Bangkok clay using a large-scale oedometer similar to the arrangement shown in Figure 4.7. The clay layer was of diameter of 0.45 m and height of 0.7 m. The tests conducted using a conventional drain and a thermal drain were considered for the comparison in this study. In both tests, the clay specimens were first allowed to reach 90% consolidation under a surcharge of 50 kPa. For the specimen with a conventional drain, an additional surcharge of 50 kPa was applied whereas for the specimen with a thermal drain, a 50 kPa surcharge and heat up to 90 °C was applied simultaneously. To simulate this set-up, an axisymmetric domain with a length of 0.225 m was considered and divided into elements of size 0.0225 m. A constant temperature of 90 °C was applied at the thermal drain and a convective boundary was imposed at the outer edge of the oedometer. The initial temperature was taken as

25 °C and the initial porosity was assumed to be 0.6. The hydrostatic pressures were determined considering a mid-depth of the soil specimen.

Based on the trends observed in experimental data of Samarakoon et al. (2022) and data from Abuel-Naga et al. (2007a) a relationship for the change in parameter γ with the mean preconsolidation stress was obtained as shown in Figure 4.8. The material parameters for Bangkok clay used in the numerical model were estimated based on data from Artidteang et al. (2011) and Abuel-Naga et al. (2007a) and are summarized in Table 4.2. The predicted time series of temperature along with the corresponding data from Artidteang et al. (2011) are shown in Figure 4.9. Close agreement is observed between the experimental results and the numerical simulation, specifically at locations further away from the thermal drain (RMSD = 2.65 for r = 200mm). The temperature is slightly underestimated at locations closer to the drain (RMSD = 9.99 for r = 25mm). Convective heat transfer not being considered and the assumed values of certain material properties may have resulted in the differences observed. Figure 4.10 shows the comparison between simulated results for settlement of the clay specimen and the experimental data. The settlements obtained for the tests conducted with the conventional drain at room temperature as well as with a thermal drain with heating up to 90 °C are presented and were obtained at a radial distance of 112.5 mm. The simulated results closely match the experimental data where the increase in both the rate and magnitude of settlement obtained from a thermal drain is captured (RMSD = 16.1 for conventional drain and RMSD = 18.1 for thermal drain). The experimental data and the predicted results for the excess pore water pressure generated when using a thermal drain is shown in Figure 4.11. Although a difference in the magnitude of the maximum excess pore water pressure is observed, the numerical model captures the trend in dissipation of excess pore water pressure well (RMSD = 24.4).

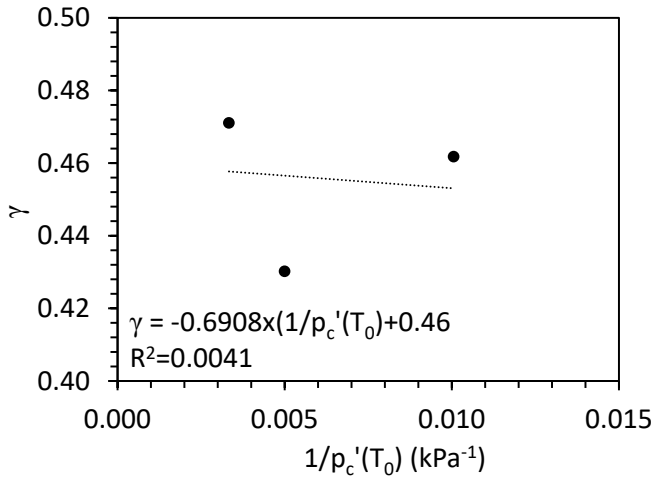

Figure 4.8. Calibrated parameter $\boldsymbol{\gamma}$ as a function of mean preconsolidation stress for normally consolidated Bangkok clay (Data: Abuel-Naga et al. 2007)

Table 4.2. Material parameters for Bangkok clay (Artidteang et al. 2011; Abuel-Naga et al. 2007)

Parameter	**Value**
Total unit weight (kN/m^3)	14.7
Initial porosity	0.6
λ (slope of VCL)	0.59
κ (slope of RCL)	0.1
γ (soil parameter)	$-0.69p_c'(T_0) + 0.46$
Thermal conductivity of soil particles (W/m/°C)	1.9
Thermal conductivity of pore water (W/m/°C)	0.6
Specific heat capacity (J/kg/°C)	1500
Intrinsic permeability (m^2)	$1.0\text{x}10^{-16}$

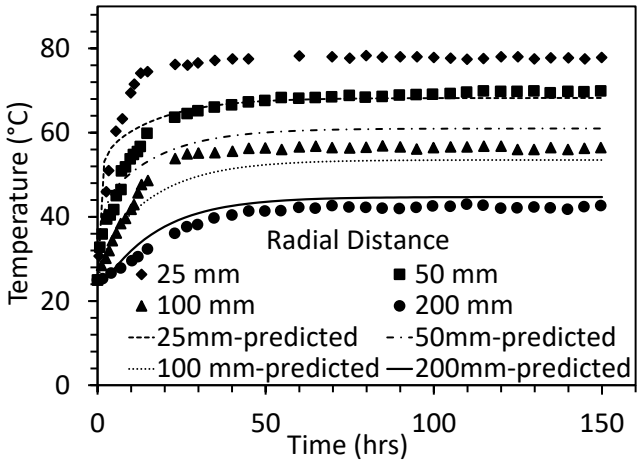

Figure 4.9. Comparison of results for time series of temperature with data from Artidteang et al. (2011)

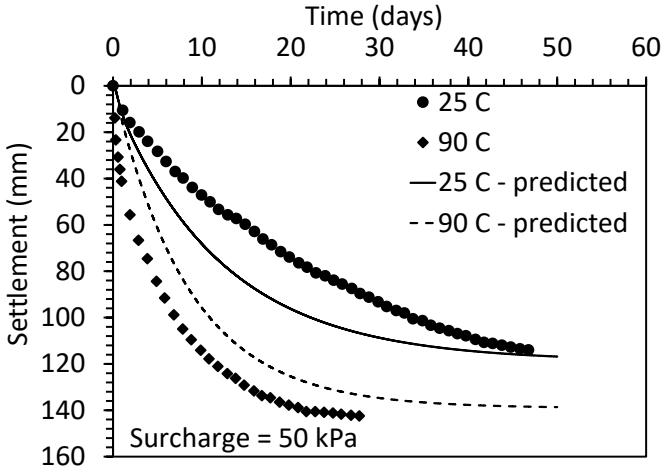

Figure 4.10. Comparison of predicted results for settlement with data from Artidteang et al. (2011)

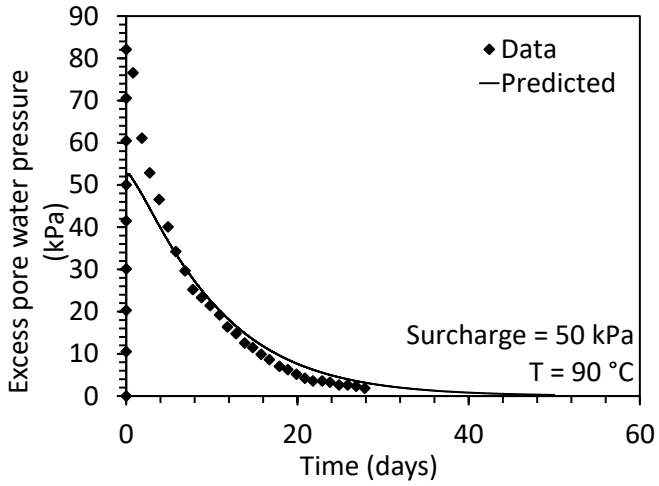

Figure 4.11. Comparison of predicted results for excess pore water pressure generated with data from Artidteang et al. (2011)

4.5.6 Parametric Analysis of Thermal Drain Performance in Normally Consolidated Clay

The validated numerical model was used to simulate the clay behavior surrounding a thermal drain, considering different variables of interest. Specifically, the impact on consolidation settlement due to the magnitude of applied temperature and surcharge load was investigated. A set up similar to that of Artidteang et al. (2011) with a Bangkok clay specimen of 0.7 m height and 0.45 m diameter was considered in the numerical simulation. Consolidation settlements obtained with a thermal drain operating at different temperatures under a surcharge of 100 kPa are shown in Figure 4.12. An increase in the magnitude as well as the rate of settlement is observed as the temperature of the thermal drain is increased, conforming with the observations made in literature. Figure 4.13 shows a comparison of the settlements obtained when using a conventional drain and a thermal drain operated at 90 °C, combined with a surcharge of 10, 25, 50 and 100 kPa respectively. An increase in the magnitude of settlement can be observed when using a thermal drain which will allow the required amount of surcharge to achieve a desired level of consolidation to be reduced. For instance, almost the same amount of

consolidation settlement obtained using a conventional drain with 25 kPa surcharge can be obtained with a thermal drain operating at 90 °C combined with only 10 kPa surcharge.

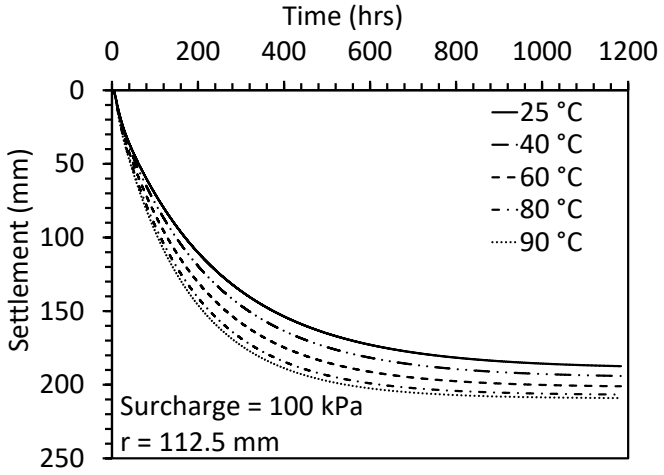

Figure 4.12. Effect of temperature on consolidation settlement for a thermal drain combined with 100 kPa surcharge

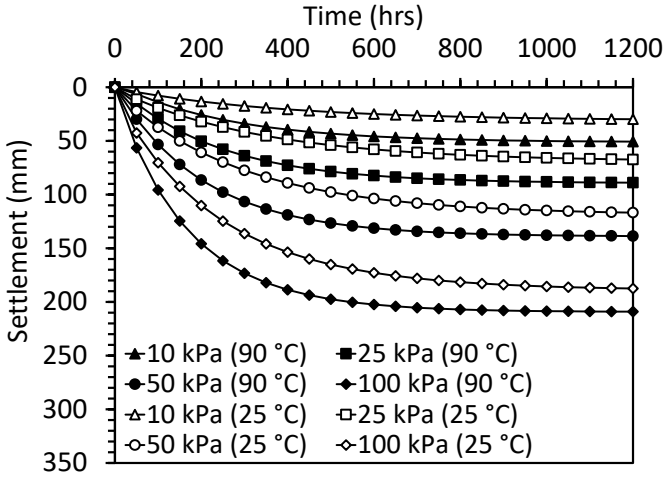

Figure 4.13. Comparison of consolidation settlements obtained at different applied surcharge stresses

The maximum settlement obtained at each surcharge value is summarized in Figure 4.14(a). As it can be seen from the figure, the contribution of thermal volume change on the total settlement is more significant at lower surcharge values. The increase in the maximum settlement obtained when using a thermal drain is shown in Figure 4.14(b). This increase can be attributed to the thermo-mechanical volume changes in the clay as a result of increasing the temperature. As described by the proposed constitutive model, the thermo-mechanical volume change can be observed to increase as the surcharge increases for normally consolidated Bangkok clay. The relationship obtained for Bangkok clay shows a small increase in parameter γ with the mean preconsolidation stress. As a result, the increase observed in thermo-mechanical volume change with surcharge is not significant. On the other hand, this increase may be more pronounced for other clay types such as kaolinite where the rate of increase in parameter γ with mean preconsolidation stress is more considerable.

The settlement obtained at different depths was also investigated using the numerical model simulating a large oedometer set-up. A comparison of settlements obtained when using a thermal drain operating at 90 °C and a conventional drain under a surcharge of 25 kPa are shown in Figure 4.15. Consolidation settlement at depths 0.15, 0.25 and 0.35 m were considered. Similar to the previous observations, an increase in the magnitude as well as the rate of settlement is observed when a thermal drain is used. Furthermore, the increase in the magnitude of settlement can be seen to increase with depth. Based on the above analysis, the surcharge required during preconsolidation can be reduced when using a thermal drain. In addition, there are significant savings with respect to time for consolidation. An optimum combination of temperature and surcharge can be determined based on factors such as soil geometry, soil properties and initial conditions, structural load, financial and time constraints. As the thermal

improvement of the clay can also be expected to depend on the depth, the temperature increments can be strategically targeted with depth. The numerical analysis in this study was conducted using a single thermal drain. In a field application, however, the use of multiple thermal drains will have to be considered. Although not within the scope of this study, this analysis can be extended to investigate the performance of multiple thermal drains by considering the intersection of thermal and hydraulic influence zones surrounding each thermal drain. Furthermore, future studies on the cost savings associated with using the thermal drains after ground improvement to provide heat exchange or heat storage may help further justify the use of this technology.

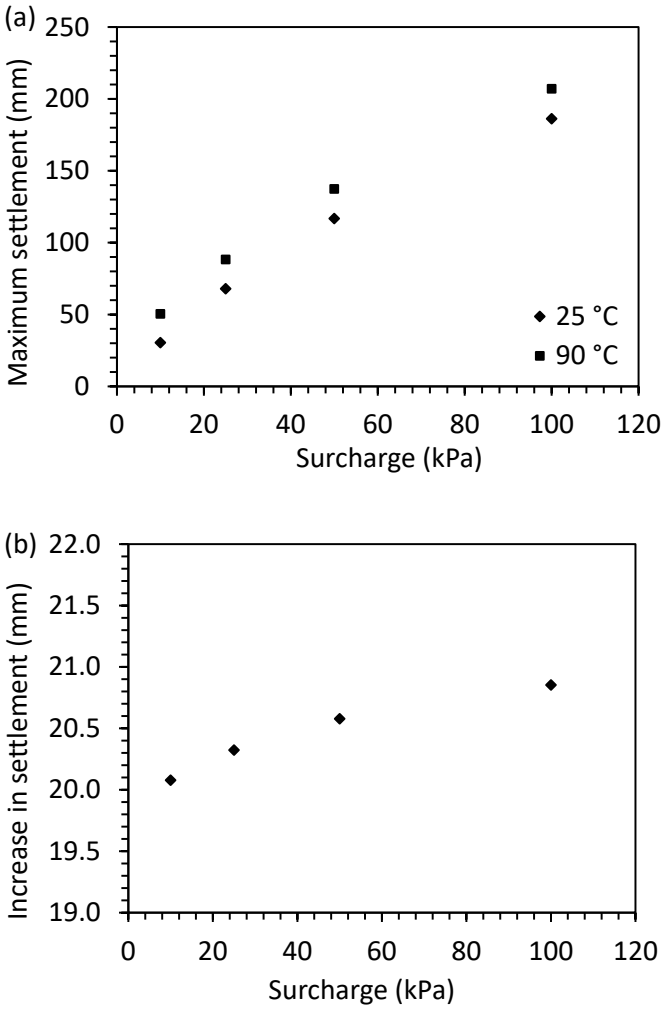

Figure 4.14. (a) Effect of temperature and surcharge stress on the maximum settlement; (b) Increase in maximum settlement obtained when using a thermal drain at different surcharge levels

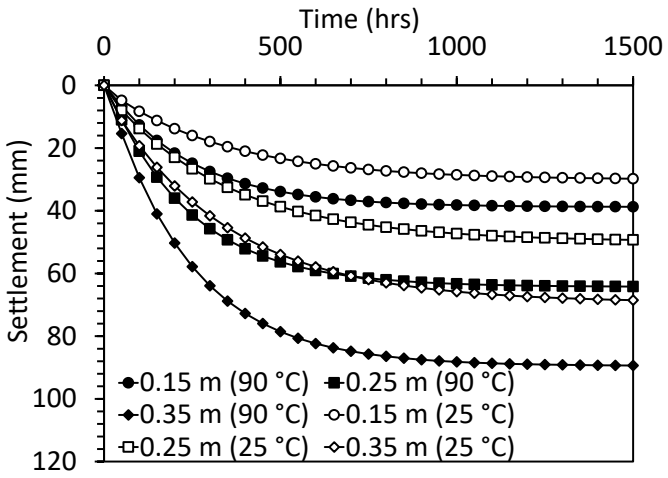

Figure 4.15. Comparison of consolidation settlements obtained at different depths

4.6 Conclusion

A new constitutive thermo-mechanical framework for predicting thermal volume change of soft clays is presented in this study. The proposed model can capture the increase in thermal volume change with increasing mean effective stress observed in experimental studies for normally consolidated clays. The model was applied in a numerical simulation of a thermal drain embedded in a soft clay deposit where coupled interactions of heat flow, fluid flow and volume change were considered. The simulated results were validated with experimental data available in literature. A parametric analysis conducted considering the effects of temperature and the surcharge applied shows that the use of a thermal drain has the potential to reduce the required amount of surcharge and significantly increase the rate of consolidation in comparison to a conventional vertical drain. The results demonstrate that the use of thermal drains can be a promising method of ground improvement while also having the potential to be used as heat exchangers subsequently, permitting sustainable and cost-effective energy usage for the building.

Further analysis can be carried out considering different clay types and to determine optimal drain arrangements in field applications.

ACKNOWLEDGEMENTS

Chapter 4 of this dissertation is based on a manuscript submitted to the Journal Computers and Geotechnics titled "Simulation of thermal drains using a new constitutive model for thermal volume change of normally consolidated clays", with authors, Radhavi Abeysiridara Samarakoon and John S. McCartney. The dissertation author is the first author of this paper.

5 Role of Initial Effective Stress on the Thermal Volume Change of Normally Consolidated Clay

5.1 Introduction

Improving soft soil deposits for construction is a crucial task for geotechnical engineers to avoid problems such as excessive settlements, bearing capacity failures and liquefaction. The use of in-situ heating as a method of soil improvement has been investigated by several researchers in recent studies (Abuel-Naga et al. 2006; Pothiraksanon et al. 2010). This technique uses geothermal heat exchangers embedded in a soft clay deposit to conduct heat to the surrounding soil where they can also be combined with vertical drains during the preconsolidation stage to expedite the consolidation process. Furthermore, the heat exchangers can be used as an underground heat storage system for buildings after the soil improvement process. These subsurface geothermal heat exchangers can be arranged in vertical or horizontal configurations depending on the extent of soil improvement required. When assessing the feasibility of thermal soil improvement techniques, it is important to study the thermo-mechanical performance of soft clays at different initial mean effective stresses indicative of different depths in a soil deposit.

It has been observed by many researchers that drained heating of normally consolidated soils lead to plastic volumetric contraction and an increase in undrained shear strength (Houston et al. 1985; Kuntiwattanakul et al. 1995; Samarakoon et al. 2018). Subsequent cooling of the soil is expected to lead to elastic contraction. Mechanical loading after a heating cooling cycle will result in an apparent overconsolidation state as a result of the thermal hardening effect experienced by the soil (Plum and Esrig 1969; Laloui and Cekerevac 2003; Abuel-Naga et al.

2007). The soil regains a normally consolidated state with further loading where it yields at a higher mean effective stress than before.

Several constitutive models have been developed to predict the thermo-mechanical behaviour of soft clays (Cui et al. 2000; Laloui and Cekerevac 2003; Abuel-Naga et al. 2007). Most of these models assume that the thermal volume change of normally consolidated clays during drained heating is independent of the initial mean effective stress. However, these models were defined based on tests carried out on initially overconsolidated specimens thermo-mechanically loaded to a normally consolidated state. Isothermal compression tests carried out at elevated temperatures resulted in compression curves with slopes similar to that of the compression curve at room temperature but with a shift to the left. The results obtained from these tests were used to predict the thermal hardening behaviour of normally consolidated clays. In the thermo-mechanical constitutive models mentioned above, heating normally consolidated clays will lead to a shift in the preconsolidation stress, an expansion of the yield surface, and contractile volume change, as shown schematically in Figure 5.1. An interesting observation from these constitutive models is that all normally consolidated clays are expected to have the same hardening response and same thermal volume change regardless of the initial void ratio.

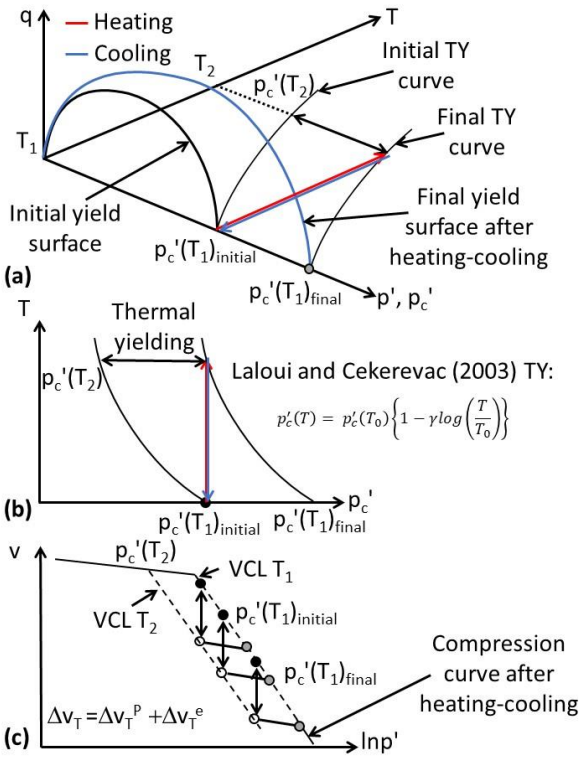

Figure 5.1. Thermal hardening of normally consolidated soils during a heating-cooling cycle: (a) Yield surface in q-p'-T space; (b) Evolution in the thermal yield (TY) curve during heating of a normally consolidated clay; (c) Thermal volume change and effects on subsequent mechanical loading of normally consolidated clay

On the other hand, subjecting normally consolidated clay specimens at different initial void ratios, indicative of different depths to drained heating at constant stress conditions may results in different thermal volume changes depending on their initial stress state. Limited experimental data available for initially normally consolidated soils under different initial mean effective stresses indicate that thermal volume change is dependent on the initial mean effective stress (Tanaka et al. 1997; Delage et al. 2004; Samarakoon et al. 2018). A study on the thermal behaviour of Boom clay specimens was conducted by Delage et al. (2004) where the specimens were first isotropically consolidated and then subjected to a drained heating cooling cycle at

constant effective stress. Figure 5.2 shows the thermal volume change results obtained for normally consolidated Boom clay specimens at two different initial mean effective stress values of 1.2 and 3.85 MPa respectively. A difference in the thermal volumetric strain for a given temperature can be observed based on the results. In this particular study a higher initial mean effective stress has resulted in a lower amount of volumetric strain whereas a higher volumetric strain was obtained at a lower initial mean effective stress. Tanaka et al. (1997) conducted a similar study on illitic clay where the specimens were first isotropically consolidated and then subjected to drained heating. The thermal volume change of normally consolidated specimens was observed to be dependent on the initial mean effective stress. Furthermore, in a previous study by the authors (Samarakoon et al. 2018), thermal volume change during drained heating of normally consolidated kaolinite specimens was observed to be dependent on the initial mean effective stress.

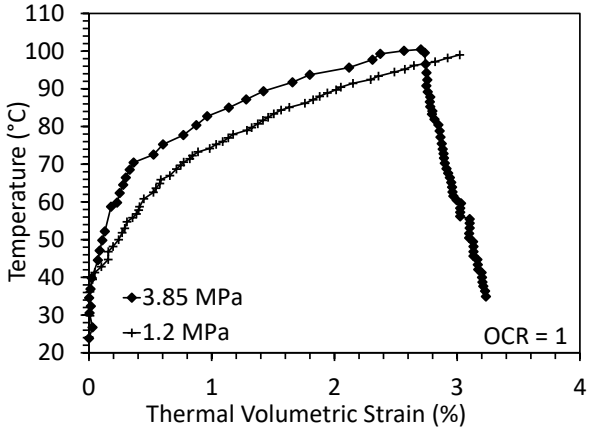

Figure 5.2. Thermal volume change of Boom clay under different initial mean effective stresses (Delage et al. 2004)

These observations from previous studies in the literature call for further investigation on the role of initial mean effective stress on the thermal consolidation of normally consolidated clays. In this regard, this study presents the results obtained from thermal triaxial tests on saturated normally consolidated clay specimens at different initial mean effective stresses to interpret the possible impacts of the initial mean effective stress (and corresponding initial void ratio), and to provide guidance on the development of future constitutive models for the thermal response of normally consolidated clays.

5.2 Material and Test Methods

5.2.1 Material

Commercial Kaolinite clay obtained from M&M Clays Inc. of McIntyre, GA was used in this study. Properties of the clay are given in Table 2.1. These properties include the compression indices obtained in an isotropic compression test at room temperature.

5.2.2 Experimental Set-up

A modified triaxial system developed by Alsherif and McCartney (2015) was used to perform the laboratory tests in this study. A schematic of the system is shown in Figure 3.4. The system comprised of a Pyrex pressure vessel capable of withstanding higher temperatures and pressures applied during testing. The temperature within the cell was controlled by circulating heated water from a temperature-controlled circulating bath through a stainless-steel U-shaped pipe placed inside the cell. Uniform mixing of cell water was achieved by using a circulation pump able to accommodate high temperatures and pressures. The cell fluid temperature was measured using a thermocouple and a temperature recorder having an accuracy of 0.5 °C. The

cell pressure was applied using a flow pump and the back-pressure was controlled using a pressure panel. A pore water pressure transducer was used to monitor the changes in pore water pressure during heating and cooling.

In addition to monitoring drainage from the specimen during heating and cooling, two high resolution cameras (Nikon D7500, AF-P DX NIKKOR 70-300mm f/4.5-6.3G ED lens) were used to capture images of the specimen to measure changes in volume using an approach like that of Uchaipichat et al. (2011). The images were captured from two planes of the specimen which are perpendicular to each other at different time intervals throughout the test. The total specimen volume was assumed to consist of discrete volumes associated with a series of stacked disks where the height of a single disk was one vertical pixel and the diameter was the number of horizontal pixels. The average volume obtained by the two image planes was taken as the specimen volume at a given time.

5.2.3 Procedure

The clay specimens were prepared by mixing clay powder with deionized water in a mixer to form a slurry with a water content of 130%. The slurry was then poured into a steel hollow cylinder of diameter 88.9 mm. Porous stones and filter paper were placed at the top and bottom of the slurry. The slurry was first consolidated using a compression frame at a constant rate of 0.04mm/min for 48 hours. Then it was subjected to constant vertical stresses of 26, 52, 103 and 181 kPa in 24 hour-long increments. The sedimented clay layer was then extracted and trimmed to a smaller cylindrical specimen with a diameter of 72.4 mm, suitable for testing in the thermal triaxial cell.

Once placed in the thermal triaxial cell, the specimen was back-pressure saturated by applying cell pressure and back-pressure in stages until the Skempton's pore water pressure parameter B value was at least 0.95. The specimen was then isotropically consolidated to a desired mean effective stress. A total of three kaolinite specimens were tested in this study which were isotropically consolidated to mean effective stress values of 150, 200 and 250 kPa respectively. The specimens were at normally consolidated conditions at these stress states. After the consolidation stage, each specimen was subjected to a drained heating cooling cycle where the drainage valves at the top and the bottom of the specimen were kept open. During heating, the temperature was increased from 23 °C to 57 °C in 5 increments and each increment was maintained until the volume change stabilized. Then the specimens were cooled back to room temperature in a similar manner. Following a heating cooling cycle, the specimens were isotropically loaded in increments up to a desired mean effective stress.

5.3 Experimental Results and Discussion

As described in the experimental procedures, the saturated normally consolidated kaolinite specimens at different initial mean effective stresses were subjected to a drained heating cooling cycle. Typical volume change results during heating showed volumetric contraction whereas volumetric expansion was observed during cooling. The changes in void ratio during heating and cooling along with the corresponding temperature profile for the clay specimens with initial mean effective stresses of 150, 200, and 250 kPa are shown in Figures 5.3, 5.4, and 5.5, respectively.

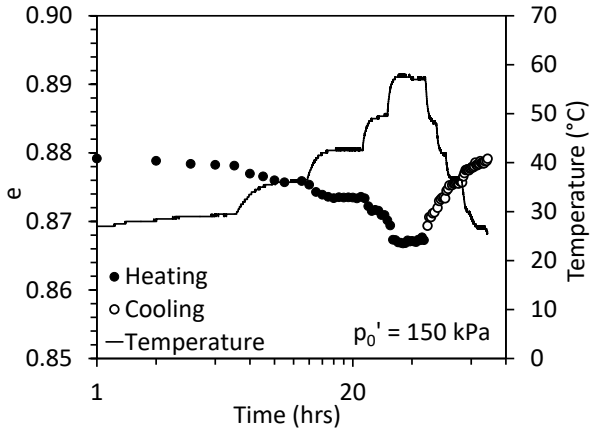

Figure 5.3. Volume change during drained heating and cooling for the test at a mean effective stress of 150 kPa

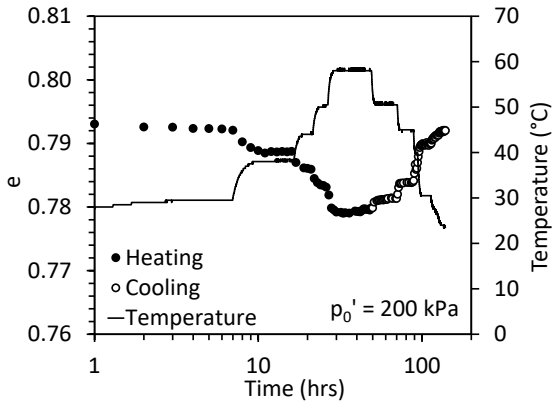

Figure 5.4. Volume change during drained heating and cooling for the test at a mean effective stress of 200 kPa

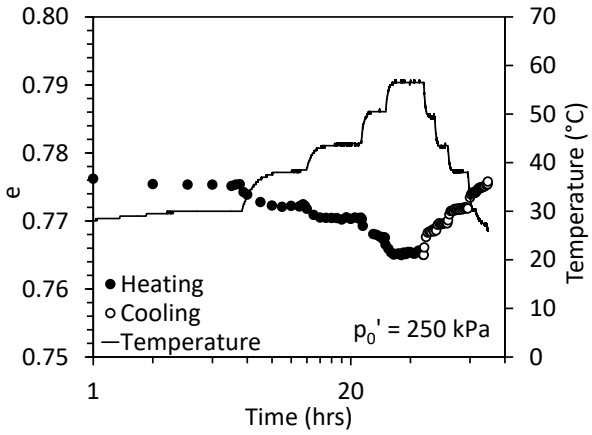

Figure 5.5. Volume change during drained heating and cooling for the test at a mean effective stress of 250 kPa

In all three tests, contraction was observed during drained heating. An interesting observation is that during cooling the thermal contraction was nearly recoverable. Although expansion during cooling has been observed in several experimental studies (Plum and Esrig 1969; Hueckel and Baldi 1990; Tanaka et al. 1997), most constitutive models assume that soils will contract elastically during cooling. The formulation in the constitutive models is based on several studies that observed elastic contraction during cooling (Baldi et al. 1991; Sultan et al. 2002; Abuel-Naga et al. 2006; Samarakoon et al. 2018). Care was taken in the current study to ensure that the volume changes during cooling were drained.

The change in thermal volumetric strain with temperature for the specimen at 200 kPa initial mean effective stress is shown in Figure 5.6. Similar observations were made for the specimens at the other two initial stress levels. Although the contraction during heating agrees with the observations in literature from previous studies, the increase in void ratio during cooling contradicts with the general trend observed in the literature (Baldi et al. 1991; Sultan et al. 2002; Delage et al. 2004; Abuel-Naga et al. 2006; Samarakoon et al. 2018). However, there exists

several studies (Plum and Esrig 1969; Hueckel and Baldi 1990; Tanaka et al. 1997) which observed thermal expansion during drained cooling.

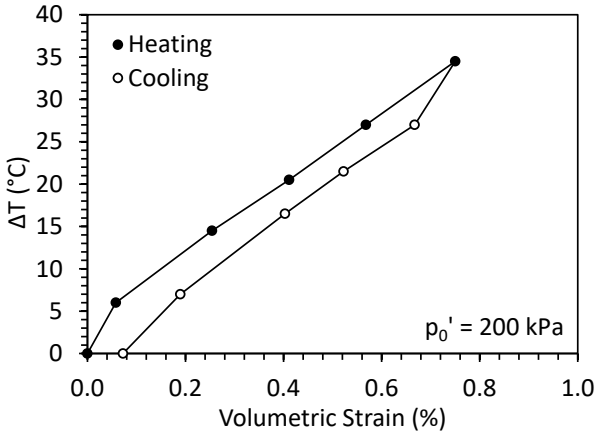

Figure 5.6. Change in thermal volumetric strain with temperature

The compression curve for the specimen initially subjected to a mean effective stress of 200 kPa is shown in Figure 5.7 in the e vs ln (p') plane. The specimen was first mechanically loaded to a mean effective stress of 200 kPa where it is at a normally consolidated state. Then, the void ratio of the specimen can be seen to decrease during heating and increase again after cooling at the same mean effective stress level. Mechanical loading of the specimen after a heating cooling cycle showed overconsolidated behaviour, although the specimen was initially at a normally consolidated state. The slope of the compression curve, immediately after a heating cooling cycle is observed to be similar to that of the recompression index (κ) of the clay. The specimen regains a normally consolidated state at a higher mean effective stress, upon further loading. The slope in this section of the compression curve is similar to that of the compression index (λ). This is in accordance with the thermal hardening phenomena described in literature where a soil specimen undergoes a hardening effect due to a change in temperature. The yield

surface expands after a heating cooling cycle as illustrated in Figure 5.1 and as a result, a higher effective stress is required for the specimen to regain plastic deformation.

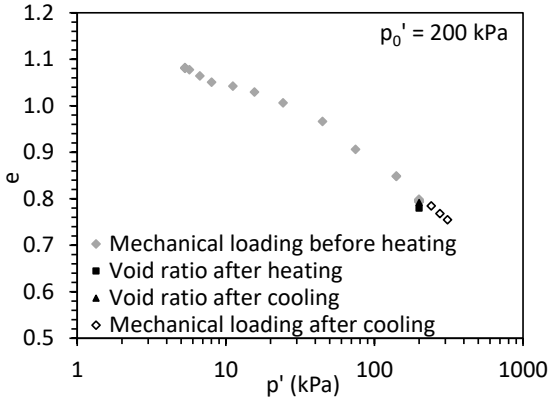

Figure 5.7. Compression curve during thermo-mechanical loading for the normally consolidated clay consolidated to 200 kPa

The thermal volumetric strains obtained at different initial mean effective stress levels were compared to investigate the effect of initial mean effective stress on the thermal volumetric strain. A comparison of the results obtained for the initial stress levels considered in this study is shown in Figure 5.8. The thermal volumetric strain observed as a result of drained heating up to 60 °C was 0.6%, 0.75% and 0.83% for specimens at initial mean effective stresses of 150, 200 and 250 kPa respectively. These values are in agreement with the typical strain values observed in the literature for normally consolidated clays. Thermal volumetric strains reported in the literature are in the range of 0.25-1% for illite (Plum and Esrig 1969), Boom clay (Baldi et al. 1988; Delage et al. 2004), Pontida clay (Hueckel and Baldi 1990) and kaolin (Cekerevac and Laloui 2004) heated up to 60 °C with the exception of Bangkok clay (Abuel-Naga et al. 2006) where a 3.25% thermal volumetric strain was observed. An interesting observation in this study is that the thermal volumetric strain obtained during heating is observed to increase as the initial

mean effective stress of the specimen increases. During cooling, volumetric expansion is observed at all stress levels. For the test at 150 kPa initial mean effective stress, the volumetric strain obtained during heating was completely recovered during cooling, resulting in zero volume change. On the other hand, net contractive volumetric strains were observed for the tests at 200 and 250 kPa initial mean effective stress. While the thermal response of the normally consolidated specimen at 150 kPa seems almost elastic, net plastic volumetric strain was observed for the specimens at 200 and 250 kPa initial mean effective stresses after being subjected to a heating cooling cycle. It was interesting to notice that this net plastic volumetric contraction also showed an increasing trend with increasing initial mean effective stress. However, further investigation will be required to arrive at a definitive conclusion with respect to trends in thermal volumetric strain with initial mean effective stress.

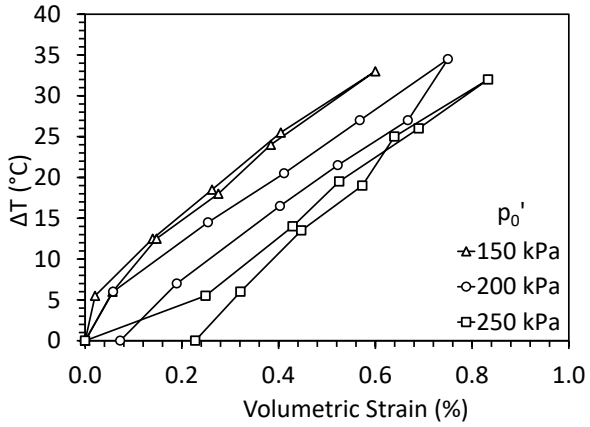

Figure 5.8. Comparison of thermal volumetric strain of normally consolidated clays at different initial mean effective stresses

The void ratio values prior to a heating cooling cycle, after heating, and after cooling for specimens at each initial mean effective stress level are summarized in Figure 5.9. Similar to the

observations drawn from Figure 5.8, the contractive behaviour during drained heating and the expansive behaviour during drained cooling is observed from the results. However, these results are in contrast with the previous observations made by the authors (Samarakoon et al. 2018), where a higher change in void ratio was observed at lower initial mean effective stresses. The authors attribute these inconsistencies to the differences in the experimental procedures followed. For a given mean effective stress, Samarakoon et al. (2018) obtained void ratio values from three separate tests conducted on specimens at room temperature, subjected to heating and a heating cooling cycle respectively. The void ratio for each test, was calculated at the end of the test, using specimen water content measurements.

Furthermore, the clay specimens in Samarakoon et al. (2018) were subjected to relatively fast rates of heating in contrast to the incremental step heating used in this experimental study. During the slurry preparation stage, the clay specimens were consolidated in a larger diameter cylinder where it was quartered at the end of the sedimentation process to obtain 4 separate triaxial test specimens. On the other hand, in the current test set-up each triaxial specimen is prepared individually starting from the sedimentation process and the volume change is measured during a single test throughout the heating cooling cycle. The differences in the experimental methods may have led to the inconsistencies in the results observed.

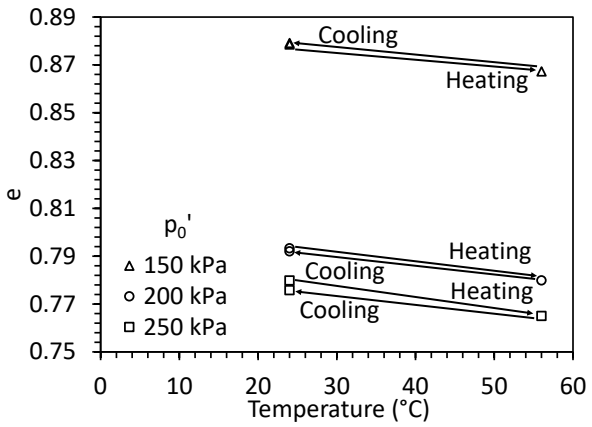

Figure 5.9. Void ratio of kaolinite specimens at each stage of the heating cooling cycle

The above results indicate that the thermal volumetric strain response of normally consolidated kaolinite specimens is dependent on the initial mean effective stress. Thermal volumetric strains obtained during heating seem to follow a trend where the volumetric strain increases with increasing mean effective stress. After a heating cooling cycle, the thermal behaviour observed in normally consolidated kaolinite specimens seem to transition from elastic deformation recoverable upon cooling to net plastic contraction as the initial mean effective stress increased. These observations contradict the available thermo-elasto-plastic models where the magnitude of volumetric strain for normally consolidated soils after drained heating is predicted to be the same, irrespective of the initial mean effective stress.

On the other hand, some field tests (Bergenstahl et al. 1994), laboratory tests (Uchaipichat and Khalili 2009; Ghaaowd et al. 2017) and poromechanics theories (Campanella and Mitchell 1968) suggest that higher excess pore water pressures will be generated in soils with higher initial mean effective stresses during undrained heating. It can be reasoned that thermal excess pore water pressure generation will be linked with thermal volume change. However, the excess pore water pressure generation under partially drained or drained conditions

can be small or negligible. Further studies on a broader range of soil types and stress levels will be required to better understand the trends of thermal volume change and improve the existing models incorporating the effect of initial stress on volumetric strain during a heating cooling cycle.

5.4 Conclusion

The results from an experimental study investigating the effect of initial mean effective stress on the thermal volume change of normally consolidated clay were presented in this study. Kaolinite specimens at three different initial mean effective stresses were subjected to an incremental heating cooling cycle. The experimental results show contractive volumetric strain during heating where the thermal volumetric strain increased with increasing initial mean effective stress. An expansive trend was observed during cooling and the net volume change after a heating cooling cycle changed from expansion to contraction as the initial mean effective stress increased.

Although not considered in existing constitutive models, the effect of initial mean effective stress on the thermal volume change of normally consolidated clays is a critical factor to be considered when configuring geothermal heat exchangers in a thermal soil improvement application. Further investigation on different soil types and stress states will assist in developing constitutive models used to assess the feasibility of geothermal heat exchangers for improving soft soil deposits.

ACKNOWLEDGEMENTS

Chapter 5 of this dissertation is based on material published by 2nd International Conference on Energy Geotechnics (ICEGT-2020) in E3S Web of Conferences titled “Role of initial effective stress on the thermal consolidation of normally consolidated clays”, with authors, Radhavi Abeysiridara Samarakoon and John S. McCartney. The dissertation author is the first author of this paper.

6 Use of Bender Elements to Evaluate Linkages between Thermal Volume Changes and Shear Modulus Hardening in Drained and Undrained Thermal Triaxial Tests

6.1 Introduction

The impact of temperature on the stress-strain characteristics of clay is important to understand in many geotechnical engineering applications including the use of in-situ heating for soil improvement. Several researchers have investigated the effect of temperature on soil behavior including volume change, shear strength, stiffness, and hydraulic conductivity. For normally consolidated clays, drained heating results in plastic contractive volumetric strains whereas undrained heating results in elastic expansion (Hueckel and Baldi 1990; Cekerevac and Laloui 2004; Abuel-Naga et al. 2007a). The thermal volumetric strains obtained during drained heating leads to an increase in undrained shear strength (Houston et al. 1985; Kuntiwattanakul et al. 1995; Abuel-Naga et al. 2006; Samarakoon et al. 2018, 2022). A limited number of studies have been conducted on the effect of temperature on the elastic moduli of soil and the elastic moduli are assumed to be independent of temperature in most thermo-mechanical constitutive models. Cekerevac and Laloui (2004) and Abuel-Naga et al. (2007) investigated the effects of temperature on the elastic secant modulus of Kaolin clay and Bangkok clay, respectively, using triaxial tests. In both studies, the elastic secant modulus was found to increase with increasing temperature. The thermal volume changes occurring in soil may result in thermally induced changes in the elastic moduli of soil. However, further investigation is required to better understand the effects of temperature on the small-stain elastic moduli of clay. This study focuses on the effect of a heating-cooling cycle on the volume change and small strain shear modulus of normally consolidated clay using drained and undrained thermal triaxial tests. The

small strain shear modulus was calculated using the shear wave velocity measured using bender elements.

Bender elements are piezoelectric bending actuators which can convert electrical energy to mechanical energy and vice versa. The transmitting element is excited with a small voltage where it generates a bending motion to induce a vertically propagating shear wave (or s-wave) in a soil layer. The vibration propagating through the soil is detected by the receiver element that outputs a voltage signal. The transmitted and the received waveforms can be used to obtain the shear wave velocity. The shear wave velocity (V_s) is calculated using the time required for the wave motion to travel from the transmitter to the receiver and the tip-to-tip distance between benders.

$$V_s = \frac{tip-to-tip\ distance}{travel\ time} \tag{6.1}$$

The small strain shear modulus (G_{max}) can be obtained using the following relationship where ρ is the soil density.

$$G_{max} = \rho V_s^{\,2} \tag{6.2}$$

Typical transmitted and received shear wave signals from a pair of bender elements in a triaxial cell are shown in Figure 6.1. Compression waves (or p-waves) can be determined in a similar manner to those from bender elements but a piezoelectric actuator is used to impart a vertically propagating compressive pulse on a soil layer. The compression wave velocity is typically not measured in saturated soils as the pore water has a higher compressive wave velocity than the soil skeleton.

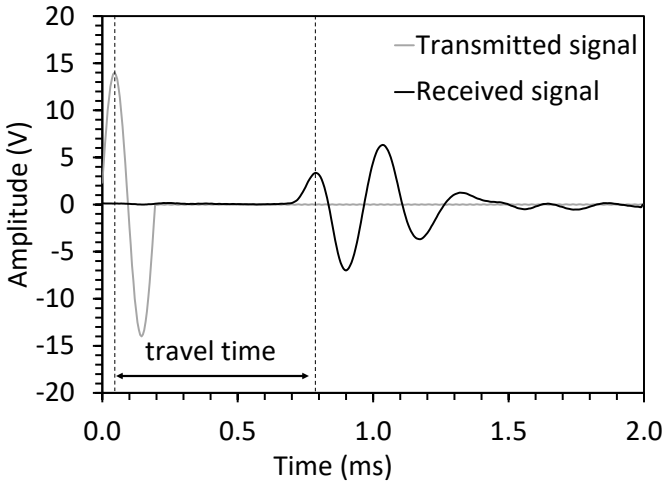

Figure 6.1. Typical shear wave signals obtained from bender elements in a thermal triaxial cell

6.2 Material and Test Methods

6.2.1 Material

This study was conducted on Kaolinite clay obtained from M&M Clays Inc. of McIntyre, GA. The properties of the clay are summarized in Table 2.1, including the compression indices obtained from an isotropic compression test at room temperature.

6.2.2 Experimental Set-up

A triaxial cell with a cell pressure capacity of 4 MPa and internal instrumentation obtained from GDS Instruments of Hook, UK was modified to perform temperature-controlled tests. The internal instrumentation includes linearly variable differential transformers (LVDTs) to measure the axial and radial displacements of the specimen, as well as piezoelectric elements embedded in the top and bottom caps to measure the compressional and shear wave velocities of the specimen. A pore water pressure transducer was used to monitor the changes in pore water pressure at the bottom of the specimen. Temperature control was achieved by circulating the cell

fluid through a closed-loop copper heat exchanger that was embedded within a Julabo heat pump (model DYNEO DD-600F). The cell fluid was circulated using a high-pressure, high-temperature circulating pump used in solar thermal panel applications (model S5 from US Solar Pumps). The closed-loop heat exchanger was connected to the top and bottom of the cell to mix the cell fluid and ensure uniform temperatures within the cell. The cell fluid temperature was measured using a thermocouple inserted at the top of the cell. The cell pressure and the back-pressure were controlled using a pressure panel. The thermal triaxial system is shown in Figure 6.2.

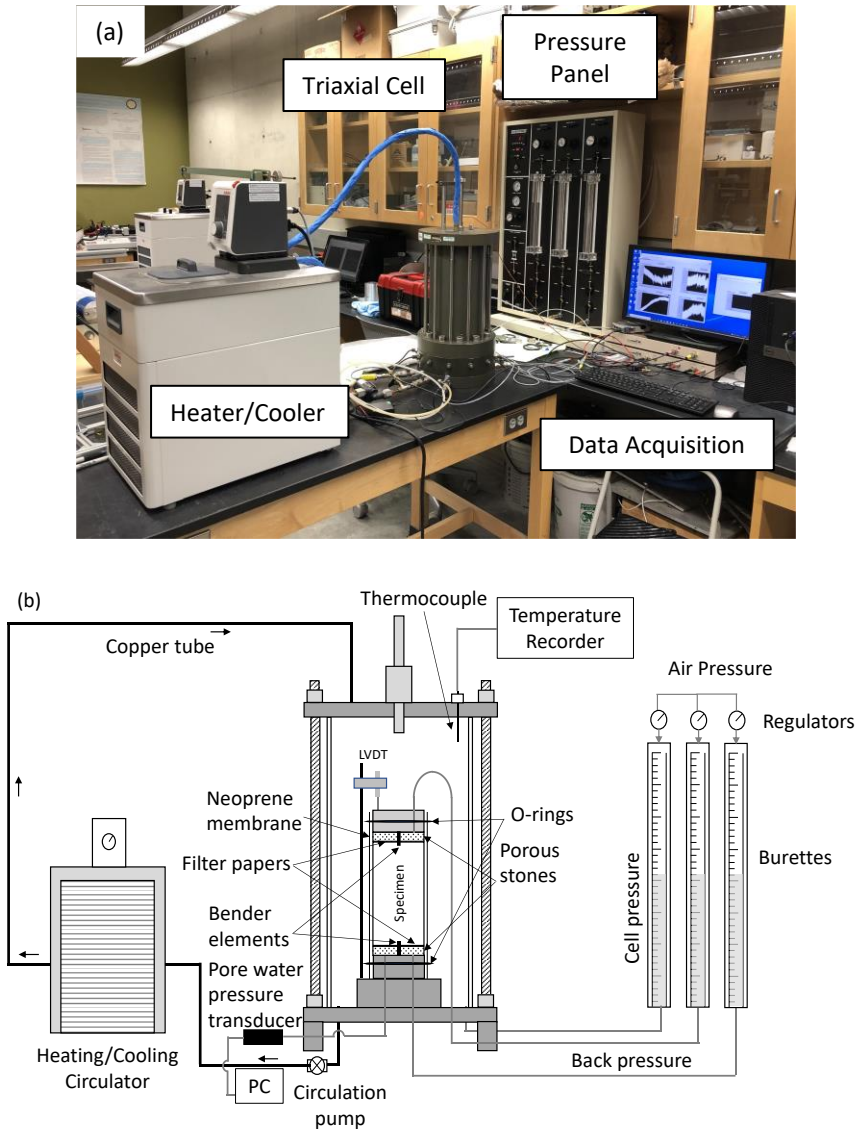

Figure 6.2. Thermal triaxial system with bender elements: (a) Picture of assembled cell prior to installation of insulation around the cell; (b) Schematic of the triaxial set-up showing the internal instrumentation and the circulation system

It is important to characterize the thermal deflections of the triaxial system during a temperature application. Machine deflections due to temperature were obtained by using a dummy Aluminum specimen ($\alpha = 2.3 \times 10^{-5}$ m/m°C) of height 71.2 mm and diameter 71.11 mm. The machine deflections were evaluated by subtracting the known elastic thermal deflections of

the Aluminum specimen from the measured LVDT readings. A heating cooling cycle was applied where the temperature was changed incrementally. The maximum temperature applied was similar to that used in the test program. The machine deflection for the thermal triaxial system is shown in Figure 6.3.

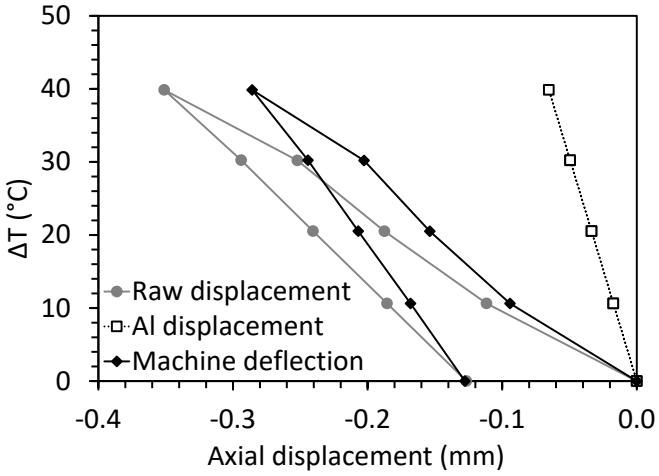

Figure 6.3. Machine deflection of the thermal triaxial system

6.2.3 Procedure

The clay specimens were prepared by mixing clay powder with deionized water in a commercial planetary mixer to form a slurry with a gravimetric water content of 115%. The slurry was then poured into a steel hollow cylinder of diameter 88.9 mm with porous stones and filter paper placed at the top and bottom. The slurry was first consolidated using a compression frame at a constant rate of 0.04mm/min for 48 hours. Then it was subjected to constant vertical stresses of 26, 52, 103 and 181 kPa in 24 hour-long increments. The sedimented clay layer was extracted and trimmed to a smaller cylindrical specimen with a diameter of 72.4 mm.

Once placed atop the bottom pedestal of the thermal triaxial cell, the specimen was encased within a neoflex membrane obtained from Karol Warner. The neoflex membrane is a pure latex membrane coated with a layer of neoprene that can be used to temperatures up to 120 °C. After assembly of the internal instrumentation and filling of the cell and heat exchange system with water, the specimen was back-pressure saturated by applying cell pressure and back-pressure in stages until the Skempton's pore water pressure parameter B value was at least 0.95. The specimen was then isotropically consolidated in stages to a mean effective stress of 250 kPa, which corresponds to normally consolidated conditions. After mechanical consolidation, the specimen was subjected to a heating-cooling cycle, then compressed further to high stresses to measure any changes in mean preconsolidation stress.

Two kaolinite specimens were tested in this study: one subjected to a drained heating-cooling cycle and the other subjected to an undrained heating-cooling cycle that included drainage stages after reaching a stable temperature after heating and after cooling, respectively. The purpose of performing these tests is to evaluate the impact of drainage conditions on the thermal volume change of the soil, and also to evaluate the coupling between thermal pressurization of pore water, pore water dissipation, and volume change in the specimens. In the undrained heating-cooling test, the pore water pressure was measured at the base of the specimen and drainage was allowed only from the top of the specimen to track dissipation of thermally induced excess pore water pressure. For the specimen with drained heating, the temperature was increased from 23 °C to 63 °C at a rate of 0.3 °C/hr that was sufficient to prevent the generation of thermally-induced excess pore water pressure within the specimen. After specimen temperature and the displacement stabilized, the specimen was cooled back to room temperature at the same rate. The temperature was increased rapidly at a rate of 22 °C/hr to 63 °C from room

temperature for the specimen subjected to an undrained heating cooling cycle. The temperature was maintained until the thermally induced excess pore water pressure stabilized and then the top drain valve was opened to permit the specimen to drain. Then the specimen was subjected to undrained cooling at the same rate as heating followed by drainage in a similar manner. Following a heating-cooling cycle, the specimens were isotropically loaded in increments up to a mean effective stress of 393 kPa. The thermo-mechanical paths for the drained and undrained tests performed on different specimens are shown in Figure 6.4.

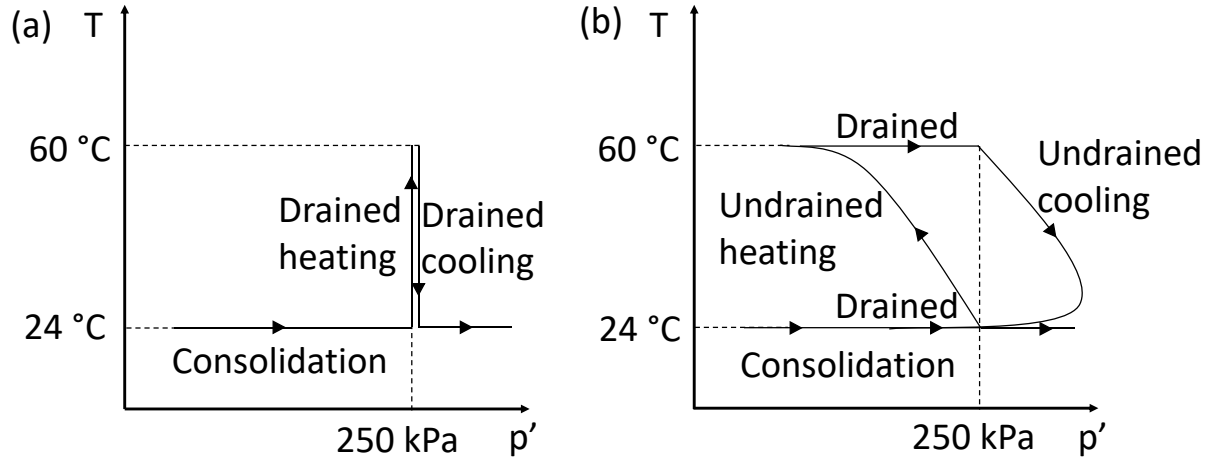

Figure 6.4. Thermo-mechanical paths: (a) Drained heating-cooling cycle; (b) Undrained heating-cooling cycle with drainage after reaching thermal equilibrium during heating and cooling

6.3 Experimental Results

6.3.1 Typical Time Series Results

The change in axial strain during the heating-cooling cycle for the two specimens are shown in Figure 6.5 where compressive strains are positive. Figure 6.5(a) shows the results during drained heating and cooling. The axial strain is observed to increase as the temperature

increases and a slight decrease is observed during drained cooling. During undrained heating however, expansion is observed as seen in Figure 6.5(b). Once the specimen is allowed to drain at the elevated temperature, the expansion is recovered, and a net contraction is observed. During undrained cooling the specimen is subjected to further contraction where a part of it is recovered during drainage after cooling. The corresponding results for excess pore water pressure are shown in Figure 6.6. The excess pore water pressure generated during a drained heating-cooling cycle is negligible as observed in Figure 6.6(a). During undrained heating thermally induced excess pore water pressure is generated and after the specimen is allowed to drain, these pore water pressures are dissipated. During undrained cooling excess pore water pressures are negative and regains its equilibrium value after the specimen is allowed to drain as seen in Figure 6.6(b). The axial strain along with the corresponding excess pore water pressure during an undrained heating-cooling cycle are shown in Figure 6.7.

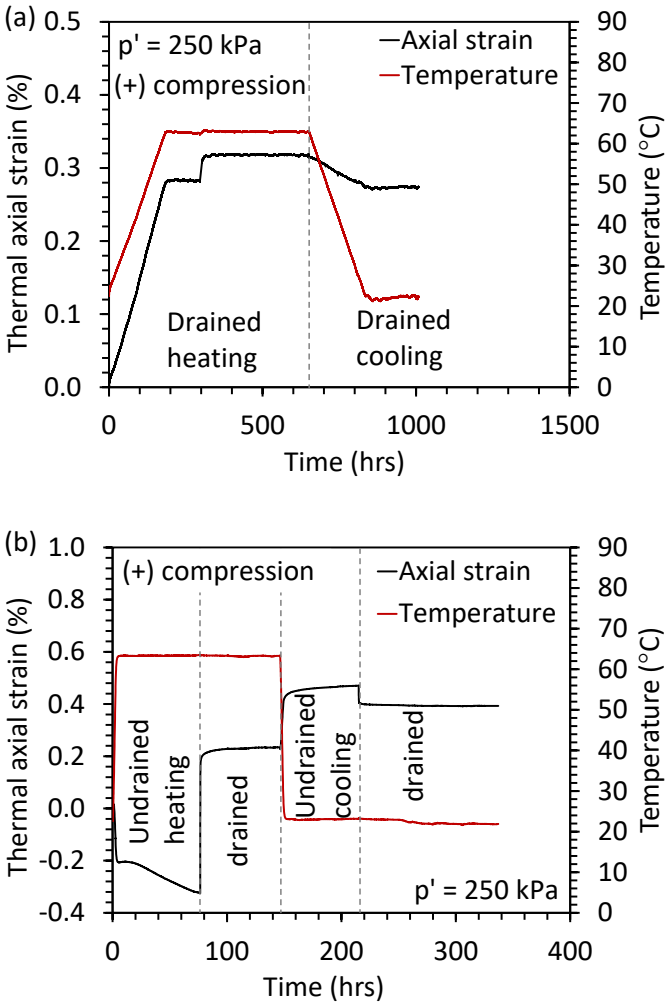

Figure 6.5. Change in axial strain during heating and cooling: (a) Drained heating-cooling cycle; (b) Undrained heating-cooling cycle

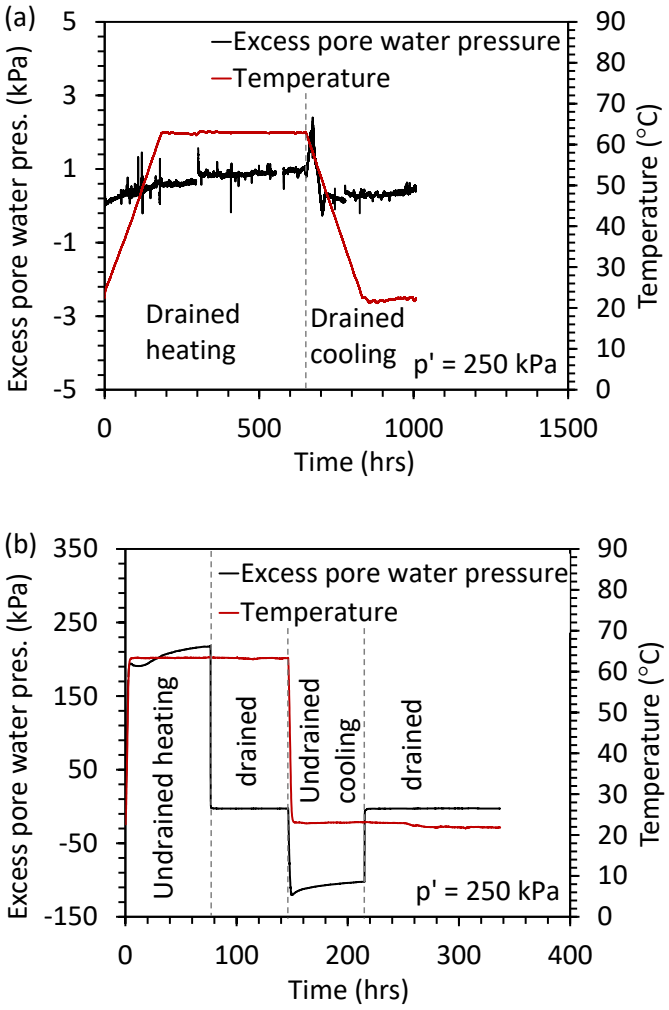

Figure 6.6. Excess pore water pressure during heating and cooling: (a) Drained heating-cooling cycle; (b) Undrained heating-cooling cycle

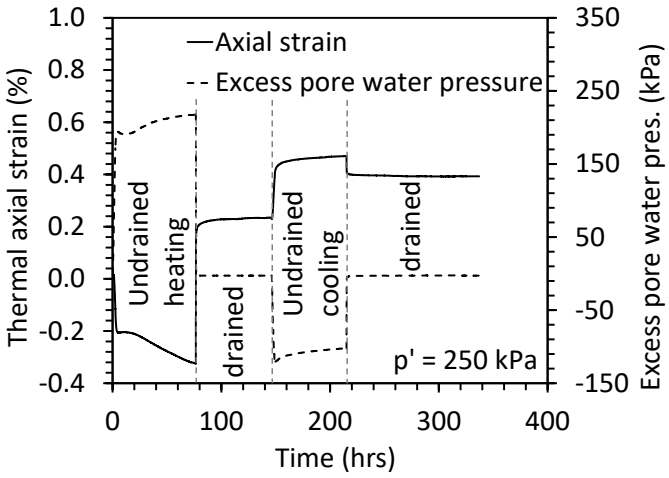

Figure 6.7. Change in thermal axial strain and excess pore water pressure with time

6.3.2 Shear Wave Velocity Measurements

The results obtained for shear wave velocity for the drained and undrained tests are shown in Figure 6.8. For the specimen subjected to a drained heating-cooling cycle, the shear wave velocity can be observed to increase with temperature and remained almost constant during cooling. This increase can be attributed to the plastic thermal strains observed in the clay specimen. Figure 6.8(b) shows the results for shear wave velocity for the specimen subjected to an undrained heating-cooling cycle. During undrained heating the shear wave velocity is observed to decrease with temperature. However, during drainage at elevated temperature, the shear wave velocity is observed to increase. A slight increase in velocity is observed during undrained cooling which again is reduced during drainage after cooling. A net increase of about 12 m/s is observed after a heating-cooling cycle. The differences in the initial shear wave velocity of the two specimens are attributed to the differences in the initial conditions.

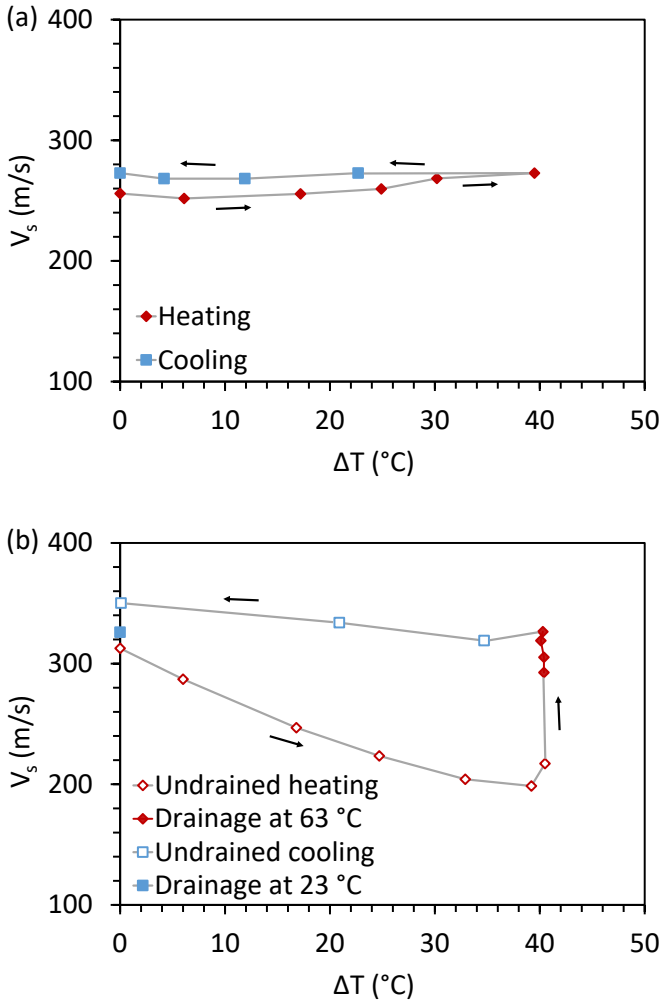

Figure 6.8. Change in shear wave velocity with temperature: (a) Drained heating-cooling cycle; (b) Undrained heating-cooling cycle

6.4 Analysis

6.4.1 Thermal Strains

The change in thermal axial strain with temperature is shown in Figure 6.9. Compressive strains observed during drained heating and the elastic expansion during cooling agree with the observations made in literature for normally consolidated clays. The specimen subjected to an undrained heating-cooling cycle also observed a net contraction, which was slightly greater than

that obtained from a drained heating-cooling cycle. The dissipation of thermally induced excess pore water pressure during undrained heating and cooling may have contributed to the increase in the axial displacement observed. The compression curve and the corresponding time series results of axial strain for the specimen subjected to a drained heating-cooling cycle is shown in Figure 6.10. As seen in Figure 6.10(b), overconsolidated behavior can be observed as the specimen is subjected to mechanical loading after a heating-cooling cycle, although the specimen was at a normally consolidated state prior to heating. The specimen regains a normally consolidated state at a higher stress state upon further loading. This conforms the thermal hardening behavior observed in literature where the yield surface expands after a heating-cooling cycle. The compression curve and time series results for the specimen subjected to an undrained heating-cooling cycle is shown in Figure 6.11. An interesting observation made is the elastic expansion during undrained heating, which follows a slope similar to that of the recompression line. Similar observations were made by Ghaaowd et al. (2017) during undrained heating of kaolinite specimens. Upon further mechanical loading after cooling the observed results were similar to that of the specimen subjected to drained heating and cooling where overconsolidated behavior is observed immediately after cooling. The compression curve in terms of volumetric strain for the two specimens is shown in Figure 6.12 where the volumetric strain was calculated using the axial strain results. Although radial strains are expected to be higher than axial strains as a result of the specimen preparation process (Samarakoon et al. 2022), a simplified approach assuming isotropic conditions was used to obtain the volumetric strain. Measurements of radial and axial strains at initial and stress conditions used in this study will facilitate better estimates of volumetric strains.

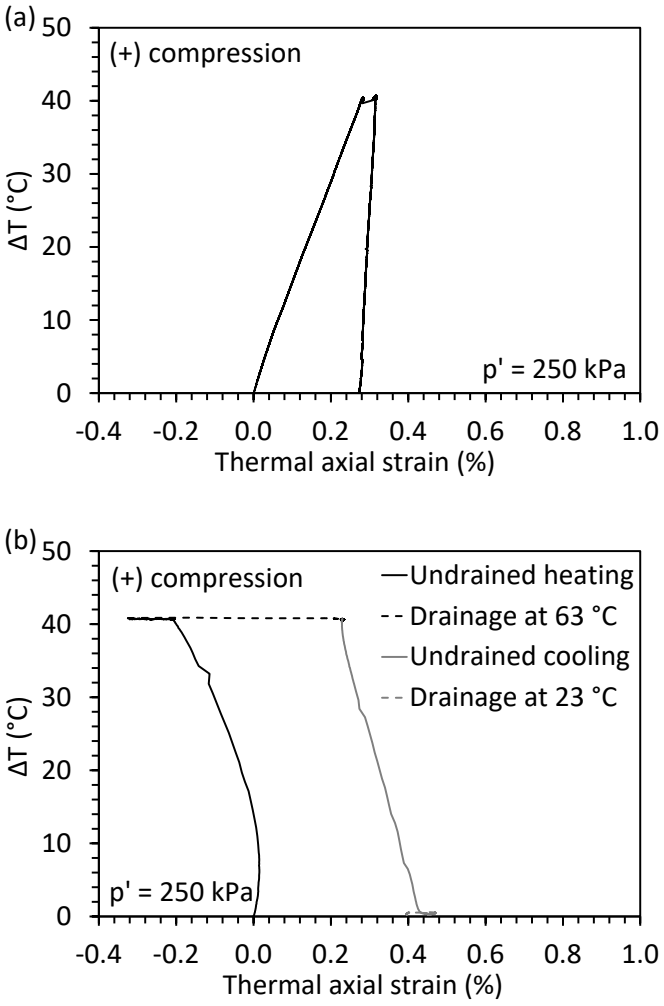

Figure 6.9. Change in thermal axial strain with temperature: (a) Drained heating-cooling cycle; (b) Undrained heating-cooling cycle

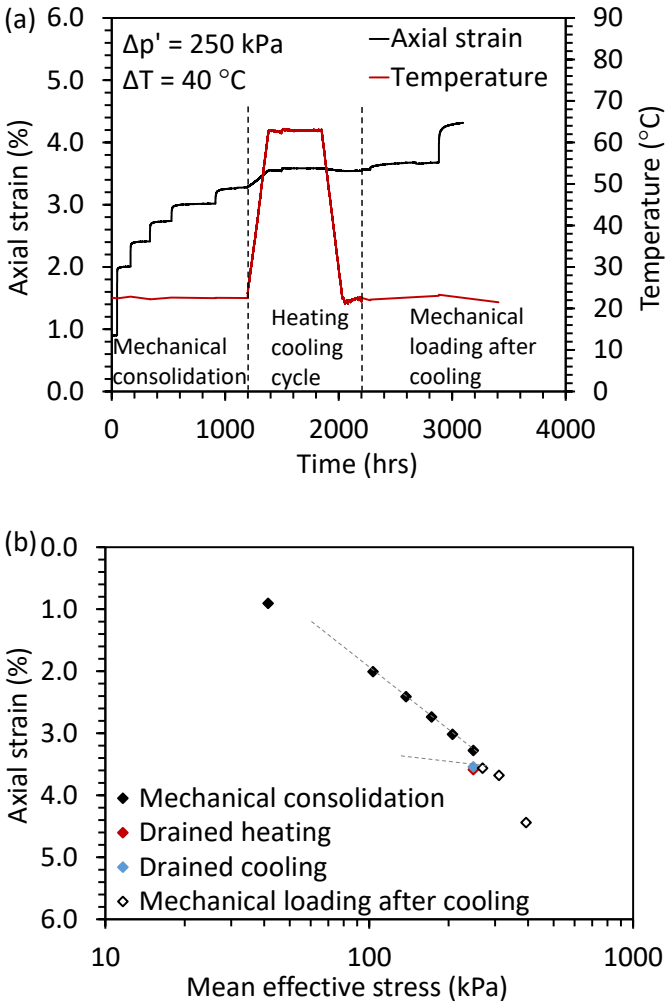

Figure 6.10. Thermo-mechanical response of kaolinite subjected to a drained heating-cooling cycle: (a) Change in axial strain with time; (b) Compression curve

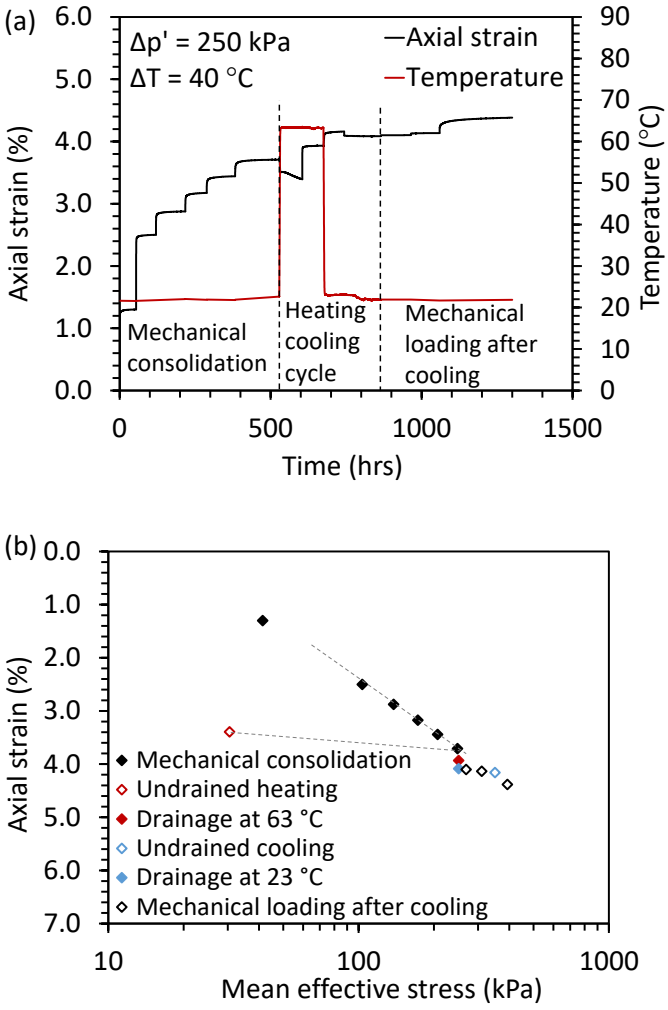

Figure 6.11. Thermo-mechanical response of kaolinite subjected to an undrained heating-cooling cycle:

(a) Change in axial strain with time; (b) Compression curve

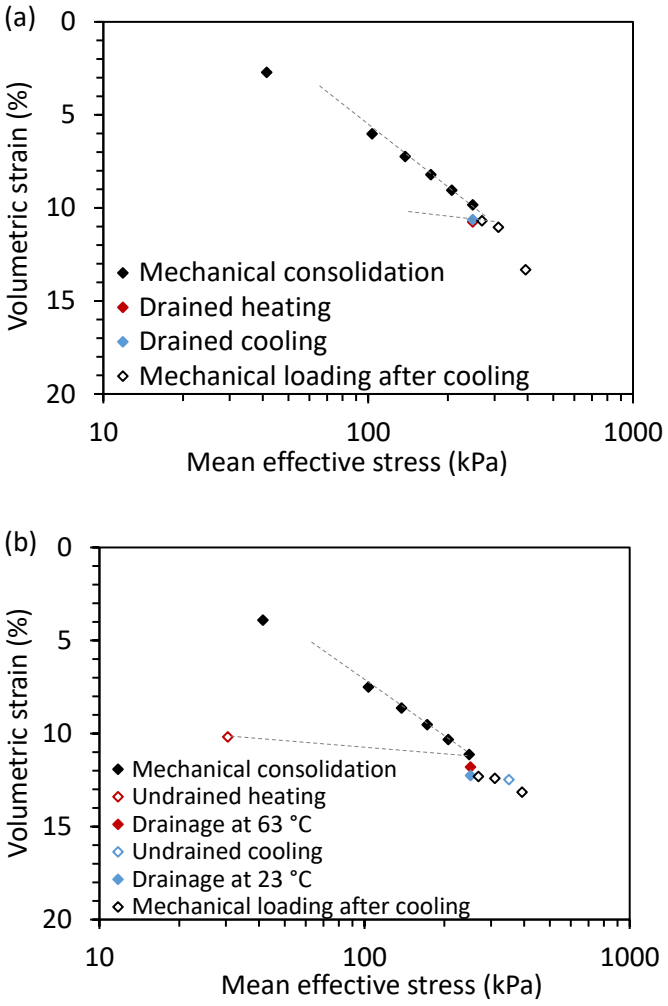

Figure 6.12. Compression curve: (a) Drained heating-cooling cycle; (b) Undrained heating-cooling cycle

6.4.2 Small Strain Shear Modulus Estimates

The calculated small strain shear modulus (G_{max}) for the two specimens tested are shown in Figure 6.13. Similar to the shear wave velocity, the shear strain modulus can also be observed to increase during heating and no significant change is observed after cooling. This increase can be attributed to the plastic thermal strains observed in the clay specimen. Samarakoon et al. (2022) also observed an increase in undrained shear strength in specimens subjected to drained heating. Figure 6.13(b) shows the small strain shear modulus for the specimen subjected to an

undrained heating-cooling cycle. Trends similar to that of shear wave velocity is observed where the small strain shear modulus decreases with temperature during undrained heating and increases during drainage at elevated temperature. An increase in the modulus is observed during undrained cooling which again is reduced during drainage after cooling.

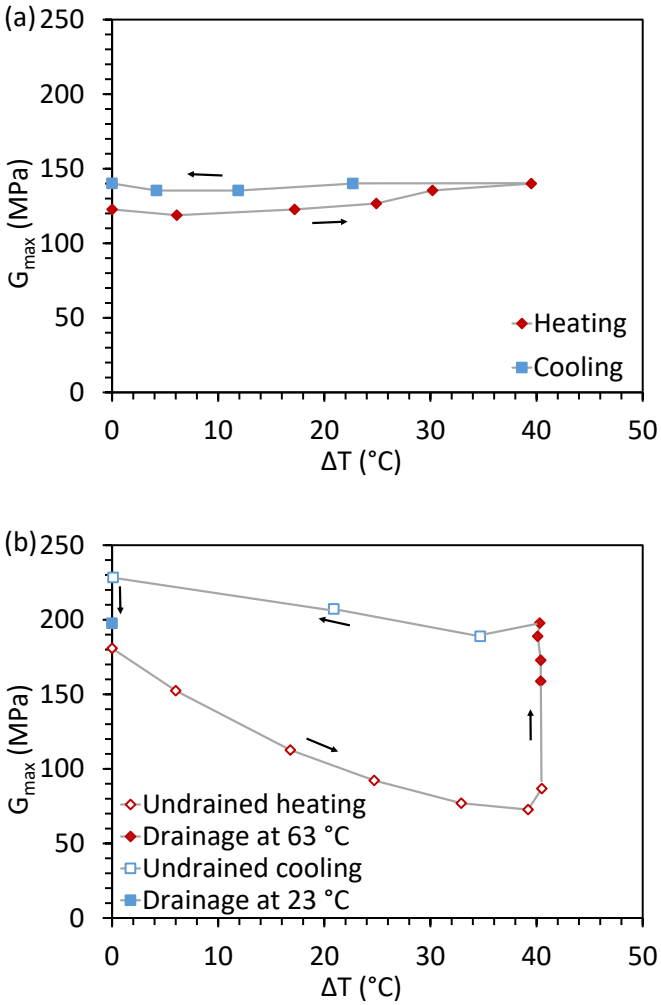

Figure 6.13. Change in small strain shear modulus with temperature: (a) Drained heating-cooling cycle; (b) Undrained heating-cooling cycle

6.5 Conclusion

This study presents the results of an experimental investigation where the linkages between thermal volume change and small strain shear modulus hardening was evaluated. Two normally consolidated kaolinite specimens were subjected to drained and undrained heating-cooling cycles respectively. In both specimens, net contractive thermal strains were observed as a result of being subjected to a heating-cooling cycle with slightly higher strains obtained for the specimen subjected to an undrained heating-cooling cycle. Upon further mechanical loading after cooling, both specimens exhibited overconsolidated behavior, even though the specimens were at a normally consolidated state prior to heating. The shear wave velocity was observed to increase with temperature during drained heating and remained constant during drained cooling. On the other hand, shear wave velocity was observed to decrease during undrained heating followed by an increase during drainage at elevated temperature. During undrained cooling, a slight increase in velocity was observed with a subsequent reduction during drainage after cooling. The change in small strain shear modulus was also observed to follow a similar trend to that of shear wave velocity for the kaolinite specimens. A net increase in shear wave velocity as well as small strain shear modulus was observed in both specimens after a heating-cooling cycle which can be attributed to the contractive thermal volume changes observed in normally consolidated clay.

ACKNOWLEDGEMENTS

Chapter 6 of this dissertation is based on material from a manuscript in preparation for publication, tentatively titled “Use of bender elements to evaluate linkages between thermal volume changes and shear modulus hardening in drained and undrained thermal triaxial tests”,

with authors, Radhavi Abeysiridara Samarakoon, Isaac L. Kreitzer and John S. McCartney. The dissertation author is the first author of this paper.

REFERENCES

Abuel-Naga, H.M., Bergado, D.T., Chaiprakaikeow, S. (2006). "Innovative thermal technique for enhancing the performance of prefabricated vertical drain during the preloading process." *Geotextiles and Geomembranes*. 24, 359-370.

Abuel-Naga, H.M., Bergado, D.T., Bouazza, A., Ramana, G.V. (2007a). "Volume change behaviour of saturated clays under drained heating conditions: experimental results and constitutive modeling." *Canadian Geotechnical Journal*. 44, 942-956.

Abuel-Naga, H.M., Bergado, D.T., Bouazza, A. (2007b). "Thermally induced volume change and excess pore water pressure of soft Bangkok clay." *Engineering Geology*. 89, 144-154.

Abuel-Naga, H.M., Bergado, D.T., Bouazza, A., Pender, M. (2009). "Thermomechanical model for saturated clays." *Géotechnique*. 59(3), 273-278.

Alsherif, N. A., McCartney, J. S. (2015). "Nonisothermal behavior of compacted silt at low degrees of saturation." *Géotechnique*. 65(9), 703-716. DOI: 10.1680/geot./14 P 049.

Artidteang, S., Bergado, D.T., Saowapakpiboon, J., Teerachaikulpanich, N., Kumar, A. (2011). "Enhancement of efficiency of prefabricated vertical drains using surcharge, vacuum and heat preloading." *Geosynthetics International.* 18(1), 35-47.

Baldi, G., Hueckel, T., Pellegrini, R. (1988). "Thermal volume changes of the mineral-water system in low-porosity clay soils." *Canadian Geotechnical Journal*. 25, 807-825.

Baldi, G., Hueckel, T., Peano, A., Pellegrini, R. (1991). "Developments in modelling of thermo-hydro-geomechanical behaviour of Boom clay and clay-based buffer materials." *Commission of the European Communities, Nuclear Science and Technology,* EUR 13365.

Bergenstahl, L., Gabrielsson, A., Mulabdic, M. (1994). "Changes in soft clay caused by increase in temperature." *Proc. 13th International Conference on Soil Mechanics and Foundation Engineering*. New Delhi, India. Jan 5-10. 1637-1641.

Boudali, M., Leroueil, S., Srinivasa Murthy, B. R. (1994). "Viscous behavior of natural clays." *Proc. 13th Int. Conf. on Soil Mechanics and Foundation Engineering*. New Delhi, India.

Brandl, H. (2006). "Energy foundations and other thermo-active ground structures." *Géotechnique*. 56(2), 81-122.

Campanella, R.G., Mitchell, J.K. (1968). "Influence of temperature variations on soil behavior." *Journal of the Soil Mechanics and Foundation Division. ASCE*. 94(3), 709-734.

Cekerevac, C., Laloui, L. (2004). "Experimental study of thermal effects on the mechanical behaviour of a clay." *International Journal for Numerical and Analytical Methods in Geomechanics*. 28, 209-228.

Coccia, C.J.R., McCartney, J.S. (2012). "A thermo-hydro-mechanical true triaxial cell for evaluation of the impact of anisotropy on thermally-induced volume changes in soils." *ASTM Geotechnical Testing Journal*. 35(2), 227-237.

Cui, Y. J., Sultan, N., Delage, P. (2000). "A thermomechanical model for clays." *Canadian Geotechnical Journal* 37(3), 607–620.

Delage, P., Cui, Y.J., Sultan, N. (2004). "On the thermal behaviour of Boom clay." *Proceedings of the Eurosafe Conference.* Berlin, Germany. 1–8.

Dong, Y., McCartney, J.S., Lu, N. (2015). "Critical review of thermal conductivity models for unsaturated soils." *Geotechnical and Geological Engineering.* 33, 207-221.

Eriksson, L. G. (1989). "Temperature effects on consolidation properties of sulphide clays." *Proc. 12th Int. Conf. on Soil Mechanics and Foundation Engineering*. Rio de Janeiro, Brazil.

Finn, F. N. (1951). "The effects of temperature on the consolidation characteristics of remolded clay." *Symposium on Consolidation Testing of Soils*. ASTM STP 126, 65–72.

Gens, A., Olivella, S. (2001). "Clay barriers in radioactive waste disposal." *Revue Française de Génie Civil*. 5(6), 845-856.

Ghaaowd, I., Takai, A., Katsumi, T., McCarntey, J.S. (2017). "Pore water pressure prediction for undrained heating of soils." *Environmental Geotechnics*. 4(2), 70-78.

Ghaaowd, I., McCartney, J.S. (2021). "Centrifuge modeling methodology for energy pile pullout from saturated soft clay." *ASTM Geotechnical Testing Journal*. 45(2), 332-354.

Ghaaowd, I., McCartney, J.S., Saboya, Jr., F. (2022). "Centrifuge modeling of temperature effects on the pullout capacity of torpedo piles in soft clay." *Soils and Rocks. Special Issue on Energy Piles*. 45(1), e2022000822.

Ghabezloo, S., Sulem, J. (2009). "Stress dependent thermal pressurization of a fluid-saturated rock." *Rock Mechanics and Rock Engineering*. 42(1), 1-24.

Hillel, D. (1980). *Fundamentals of Soil Physics.* Academic Press. New York, NY, USA.

Hormdee, D., Kaikeerati, N., Jirawattana, P. (2014). "Application of image processing for volume measurement in multistage triaxial tests." *Advanced Materials Research.* Trans Tech Publications Ltd. 931-932, 501-505.

Houston, S.L., Houston, W.N., Williams, N.D. (1985). "Thermo-mechanical behavior of seafloor sediments." *Journal of Geotechnical Engineering. ASCE*. 111(12), 1249-1263.

Hueckel, T., Baldi, M. (1990). "Thermoplasticity of saturated clays: Experimental constitutive study." *Journal of Geotechnical Engineering*. 116(12), 1778-1796.

Hueckel, T., Borsetto, M. (1990). "Thermoplasticity of saturated soils and shales: constitutive equations." *Journal of Geotechnical Engineering*. 116(12), 1765–1777.

Hueckel, T., Pellegrini, R. (1992). "Effective stress and water pressure in saturated clays during heating-cooling cycles." *Canadian Geotechnical Journal* 29, 1095-1102.

Hueckel, T., Pellegrini, R. (1996). "A note on thermomechanical anisotropy of clays." *Engineering Geology*. 41, 171–180.

Kuntiwattanakul, P., Towhata, I., Ohishi, K., Seko, I. (1995). "Temperature effects on undrained shear characteristics of clay." *Soils and Foundation*. 35(1), 147-162.

Laloui, L. (2001). "Thermo-mechanical behaviour of soils." *Revue Française de Génie Civil*. 5(6), 809-843.

Laloui, L., Cekerevac, C. (2003). "Thermo-plasticity of clays: an isotropic yield mechanism." *Computers and Geotechnics*. 30(8), 649–660.

Macari, E. J., Parker, L. K., Costes, N. C. (1997). "Measurement of volume changes in triaxial tests using digital imaging techniques." *Geotechnical Testing Journal.* 20(1), 103-109.

Moritz, L. (1995). "Geotechnical properties of clay at elevated temperatures." *Report No 47 Swedish Geotechnical Institute*.

Pothiraksanon, C., Bergado, D.T., Abuel-Naga, H.M. (2010). "Full-scale embankment consolidation test using prefabricated vertical thermal drains." *Soils and Foundations*. 50(5), 599-608.

Plum, R. L., Esrig, M. I. (1969). "Some temperature effects on soil compressibility and pore water pressure." *Highway Research Board,* Washington DC, Report 103, 231–242.

Salager, S., Laloui, L. Nuth, M. (2012). "Efficiency of thermal vertical drains for the consolidation of soils." *2nd International Conference on Transportation Geotechnics*. Hokaido, Japan. 1-10.

Samarakoon, R.A., Ghaaowd, I., McCartney, J. S. (2018). "Impact of drained heating and cooling on undrained shear strength of normally consolidated clay." *Proc. 2nd International Symposium on Energy Geotechnics*. Lausanne. A. Ferrari, L. Laloui, eds., Vienna. 243-249.

Samarakoon, R.A., McCartney, J.S. (2020a). “Analysis of thermal drains in soft clay.” G*eoAmericas 2020: 4th PanAm Conference on Geosynthetics*. Rio de Janeiro, Brazil. Oct 26-31. 1-9.

Samarakoon, R.A., McCartney, J.S. (2020b). “Role of initial effective stress on the thermal consolidation of normally consolidated clays.” *Proc. 2nd International Conference on Energy Geotechnics (ICEGT-2020)*. E3S Web of Conferences, Les Ulis, France. 205, 09001.

Samarakoon, R.A., McCartney, J.S. (2021). “Performance of prefabricated thermal drains in soft clay.” *Geosynthetics Conference 2021*. Kansas City, MO, USA. Feb 21-24. Nicks, J. and Beauregard, M., eds. IFAI, Roseville, MI. 1-12.

Samarakoon, R.A., Kreitzer, I.L., McCartney, J.S. (2022). “Impact of initial effective stress on the thermo-mechanical behavior of normally consolidated clay.” *Geomechanics for Energy and the Environment* [In Review].

Shanina, M., McCartney, J.S. (2017). “Influence of anisotropic stress states on the thermal volume change of unsaturated silt.” *Soils and Foundations*. 57(2), 252-266.

Sultan, N., Delage, P., Cui, Y. J. (2002). “Temperature effects on the volume change behavior of boom clay.” *Engineering Geology*. 64, 135-145.

Takai, A., Ghaaowd, I., Katsumi, T., McCartney, J. S. (2016). “Impact of drainage conditions on the thermal volume change of soft clay.” G*eoChicago 2016: Sustainability, Energy and the Geoenvironment*. Chicago. Aug. 14-18. 32-41.

Tanaka, N., Graham, J. Crilly, T. (1997). “Engineering behaviour of reconstituted Illitic clay at different temperatures.” *Engineering Geology*. 47(4), 339-350.

Tidfors, M., Sällfors, G. (1989). “Temperature effect on preconsolidation pressure.” *Geotechnical Testing Journal*. 12(1), 93–97.

Towhata, I., Kuntiwattanakul, P., Seko, I., Ohishi, K. (1993). “Volume change of clays induced by heating as observed in consolidation tests.” *Soils and Foundations*. 33(4), 170–183.

Uchaipichat, A., Khalili, N. (2009). “Experimental investigation of thermo-hydro-mechanical behaviour of an unsaturated silt.” *Géotechnique*. 59(4), 339–353.

Uchaipichat, A., Khalili, N., Zargarbashi, S. (2011). “A temperature controlled triaxial apparatus for testing unsaturated soils.” *Geotechnical Testing Journal*. 34(5), 1-9.